

University of Mississippi

eGrove

Electronic Theses and Dissertations

Graduate School

1-1-2020

Approaches To Alleviate The Vigabatrin Induced Retinal Toxicity

Anitha Police

Follow this and additional works at: <https://egrove.olemiss.edu/etd>

Recommended Citation

Police, Anitha, "Approaches To Alleviate The Vigabatrin Induced Retinal Toxicity" (2020). *Electronic Theses and Dissertations*. 1842.

<https://egrove.olemiss.edu/etd/1842>

This Dissertation is brought to you for free and open access by the Graduate School at eGrove. It has been accepted for inclusion in Electronic Theses and Dissertations by an authorized administrator of eGrove. For more information, please contact egrove@olemiss.edu.

APPROACHES TO ALLEVIATE THE VIGABATRIN INDUCED RETINAL TOXICITY

A Dissertation

submitted in partial fulfillment of requirements

for the Doctor of Philosophy degree in pharmaceutical sciences in the Department of

Pharmaceutics and drug delivery

The University of Mississippi

By

Anitha Police

May 2020

Copyright Anitha Police 2020

ALL RIGHTS RESERVE

ABSTRACT

Safety of therapeutics is one of the primary concerns during the treatment of any ailments. Most of the toxic effects of drugs occurs due to accumulation of drug in organs, which is dependent on the dosage of the drug. The ideal therapy should minimize the risk of causing adverse events at the same time elicit intended therapeutic effects. Vigabatrin (VGB) is an antiepileptic drug used primarily in the treatment of infantile spasms and it acts by inhibiting gamma amino butyric acid (GABA) transaminase thereby increasing inhibitory neurotransmitter GABA levels. At therapeutic doses, VGB accumulates in retina leading to peripheral visual field defects and retinal degeneration. To alleviate retinal toxicity of VGB, different approaches have been explored to decrease the ocular accumulation of VGB and to protect retina from deleterious effects of VGB.

Intranasal administration approach was investigated to deliver VGB directly to brain via olfactory region. The *in vivo* acute, sub-acute and pharmacodynamic studies were performed in Sprague Dawley rats by administering VGB through intraperitoneal and intranasal routes. The mechanism of VGB transport across blood retinal barrier was studied using retinal epithelial cells (ARPE-19) cells. The *in vitro* and *in vivo* studies were performed to evaluate the mechanism involved in retinal uptake of VGB and identify approach to decrease VGB retinal uptake. The effects of VGB on retinal neuronal (R28) and ARPE-19 cells were studied. The cytoprotective effect of silymarin and taurine on VGB induced retinal toxicity was investigated.

The subacute intranasal administration decreased retinal VGB levels and histological changes compared to intraperitoneal administration. Intranasal pharmacodynamic study

demonstrated smaller dose produced significant antiepileptic activity with prolonged duration of VGB action. The ARPE19 cellular transport studies showed Na⁺/Cl⁻ dependent transporter, TauT was involved in retinal VGB uptake. Further, *in vitro* cell uptake and *in vivo* SD rat studies demonstrated TauT inhibitors decreased VGB retinal uptake, thus confirming role of TauT in retinal uptake of VGB. The *in vitro* cell toxicity studies demonstrated, VGB treatment produced cell death in ARPE19 and R28 cells are due to apoptosis and necrosis, respectively. Further, studies demonstrated antioxidants silymarin and taurine constituents decreased VGB induced cell toxicity. The study results demonstrate intranasal administration of VGB along with a safe TauT inhibitor and an antioxidant as a supplement would be beneficial to prevent the VGB induced retinal toxicity.

DEDICATION

Dedicated to my parents and siblings

LIST OF ABBREVIATIONS

ANOVA	Analysis of Variance
ARPE-19	Adult Retinal Pigment Epithelium
BRB	Blood Retinal Barrier
CE	Complexation efficiency
DCFDA	2,7- dichlorodihydrofluorescein diacetate
DMEM	Dulbecco's Modified Eagle Medium
DPBS	Dulbecco's Phosphate-Buffered Saline
FBS	Fetal Bovine Serum
GABA	Gamma-aminobutyric acid
GES	Guanidinoethyl Sulfonate
HPLC	High Performance Liquid Chromatography
IS	Internal Standard

JC-1	5,5',6,6'-tetrachloro-1,1',3,3'-tetraethylbenzimidazolylcarbocyanine iodide
LLOQ	Lower Limit of Quantification
MBCP	Multiblock Copolymer
MTT	3-(4,5-dimethylthiazol-2-yl)-2,5-diphenyltetrazolium bromide
NDA	2, 3- Naphthalene di carboxaldehyde
PTZ	Pentylentetrazol
RPE	Retinal Pigment Epithelium
SD	Standard Deviation
SLC	Solute Carrier Transporter
TauT	Taurine Transporter
VGB	Vigabatrin

ACKNOWLEDGEMENTS

I would like to express my deep and sincere gratitude to my advisor, Dr. S. Narasimha Murthy for his support, guidance, and encouragement throughout my research work. His motivation and support at all the time during my research helped me learn many aspects required to achieve my research goals. I would like to take this opportunity to express my sincere thanks to my dissertation committee members, Dr. Michael A. Repka, Dr. Mahavir B Chougule, and Dr. NP Dhammika Nanayakkara for accepting my request, and providing valuable suggestions during my prospectus that I believe have improved my overall work. It was kind of Ms. Deborah for helping me with all the departmental procedures and making sure that the things necessary for the projects are provided on time.

I owe a great thanks to Vijay and Srinivas for their valuable suggestions and helping me completion of various projects successfully. I would like to acknowledge my senior lab members Dr. Avadhesh, Dr. Abhijeet and Dr. Murali for assisting me to learn research basics in our lab and their continuing support throughout my projects. I also thank my group members Purnendu, Dr. Srinath Rangappa, Dr. Srinatha Anegundha, Marey, Apoorva, Supriya, Tasnim, Maha, Abhishek and all graduate students of pharmaceuticals and drug delivery department for their support in various projects.

I would like to acknowledge the help of Dr. Seongbong Jo, Dr. Majumdar, Dr. Mika Jeakabsons and Dr. H. N. Shivakumar (Institute for Drug Delivery and Biomedical Research, Bangalore, India) their assistance and support to conduct my various projects successfully.

I would like to thank Sushmitha, Neeraja, Apoorva, Disha, Akshaya, Nagi Reddy, Vimal, Tahir, Tabish, Adal, Kuldeep, Abhisheak, Sandeep, Raman, Karthik, Narender, Prasad, Suresh, Dr. RK, Dr. Vish, Rama Aunty, Rithu and Swapna for making Oxford life lovable and cherishing.

Above all, I owe my thanks to my loving brother (P Veera Reedy), Sister (Praveena), father (P Neelakanta Reddy), mother (Uma devi), for their unconditional support, encouragement and for all their sacrifices and for believing in me. I would like to thank all my family and friends for their support.

TABLE OF CONTENTS

Abstract	ii
Dedication	iv
List of abbreviations	v
Acknowledgements	vii
List of Tables	xii
List of Figures	xiii
Chapter 1	1
Introduction.....	1
Chapter 2	3
Intranasal Drug Delivery to Alleviate the Vigabatrin Induced Retinal Toxicity.....	3
1. Introduction.....	3
2. Materials and Methods.....	5
2.1 Chemicals and reagents	5
2.2 Instrumentation and chromatographic conditions.....	5
2.3 Standard solutions	6
2.4 Sample preparation	6
2.5 Optimization of NDA Derivatization.....	7
2.6 Method validation	7
2.6.1 LLOQ determination	8

2.6.2	Specificity and selectivity.....	8
2.6.3	Calibration curve	9
2.6.4	Precision and accuracy	9
2.6.5	Recovery	10
2.6.6	Stability experiments	10
2.6.7	Dilution effect.....	11
2.7	Vigabatrin thermosensitive gel	11
2.7.1	Preparation of Chitosan Hydrogel	11
2.7.2	Preparation of MBCP Hydrogel	12
2.8	Permeation of VGB across bovine olfactory mucosa	12
2.8.1	Preparation of Bovine Olfactory Mucosa	12
2.8.2	Permeation study	12
2.9	<i>In-vivo</i> study studies.....	13
2.9.1	Retina, brain, and plasma exposure studies	14
2.9.1.1	Acute study.....	14
2.9.1.2	Chronic study	14
2.9.2	Antiepileptic activity of Vigabatrin intranasal dose	15
2.9.2.1	Induction of Seizure	16
2.9.2.2	PTZ effect on intraperitoneal and intranasal administration of VGB	16
2.10	Statistical analysis	17
3.	Results and Discussion	17

3.1	Liquid chromatography	17
3.2	Optimization of NDA Derivatization.....	18
3.3	Method validation	19
3.3.1	Specificity & selectivity	19
3.3.2	Recovery	22
3.3.3	Calibration curve	24
3.3.4	Precision and accuracy	24
3.3.5	Stability.....	27
3.3.6	Dilution effect.....	30
3.4	Vigabatrin thermosensitive gel	30
3.5	Permeation of VGB across bovine olfactory mucosa	30
3.6	<i>In-vivo</i> study.....	31
3.6.1	Retina, brain and plasma exposure studies	32
3.6.1.1	Acute Study	32
3.6.1.2	Chronic Study.....	34
3.7	Vigabatrin antiepileptic activity on intranasal administration	38
4.	Conclusion	40
Chapter 3	41
	Role of Taurine Transporter in the Retinal Uptake of Vigabatrin	41
1.	Introduction.....	41
2.	Materials and Methods.....	43

2.1	ARPE-19 Cell culture	43
2.2	ARPE-19 cell uptake studies.....	44
2.3	Effect of osmolarity and pH on uptake of VGB	44
2.4	Effect of Guanidinoethyl sulfonate on uptake of VGB.....	45
2.5	Competitive inhibition of cellular uptake of TauT substrates in ARPE-19 cells.....	45
2.6	Animal Studies.....	46
2.7	Sample preparation	46
2.8	HPLC analysis.....	47
2.9	Statistical analysis	47
3.	Results.....	48
3.1	ARPE-19 cell uptake studies.....	48
3.2	Involvement of TauT in VGB uptake by ARPE-19 cells	50
3.2.1	Effect of osmolarity and pH on uptake of VGB	50
3.2.2	Effect of Guanidinoethyl sulfonate on uptake of VGB	52
3.2.3	Competitive inhibition of cellular uptake of TauT substrates in ARPE-19 cells	52
3.3	Animal studies.....	55
4.	Discussion.....	56
5.	Conclusion	58
	Chapter 4	59
	Cytoprotective Effects of Silymarin on Antiepileptic Drug Induced Retinal Toxicity	59
	1. Introduction.....	59

2. Materials and Methods.....	60
2.1 Retinal Cell culture	61
2.1.1 ARPE-19 cell culture.....	61
2.1.2 R28 cell culture.....	61
2.2 Cell Viability Assay	62
2.3 Nuclear condensation and DNA fragmentation assay	62
2.4 Mitochondrial membrane potential assay	64
2.5 Detection of Reactive oxygen species generation.....	64
2.6 Cytoprotective effect.....	65
2.7 Statistical Analysis.....	66
3. Results and Discussion	66
3.1 Cell Viability Assay	66
3.2 Nuclear condensation and DNA fragmentation assay	69
3.3 Mitochondrial membrane potential assay	75
3.4 Detection of Reactive oxygen species generation.....	77
3.5 Cytoprotective effect.....	81
4. Conclusion	85
Bibliography	86
VITA.....	98

LIST OF TABLES

Chapter-2

Table 1. The recovery of taurine, GABA and vigabatrin at different concentration levels from different biological matrices and water (n=6)	23
Table 2. The Intra-day precision determination of taurine, GABA and vigabatrin (n=6)	25
Table 3. The Inter-day precision determination of Taurine, GABA and Vigabatrin (n=18)	26
Table 4. The stability data of taurine, GABA and vigabatrin at HQC concentration in biological matrices (n=6).....	28
Table 5. The stability data of derivatized product of taurine, GABA and vigabatrin at LQC and HQC concentration (n=6)	29

Chapter-4

Table 1. Effect of silymarin and taurine on changes in ratio of J-aggregates to J-monomers in ARPE-19 cells produced by vigabatrin and gabapentin (mean \pm SD) n=6	77
------------------------------------------------------------------------------------------------------------------------------------------------------------------------------------	----

LIST OF FIGURES

Chapter-2

Figure 1. The HPLC Chromatograms of blank (a), blank with IS (b), low limit of quantification (c) and high-quality control (d).....	20
Figure 2. The HPLC Chromatograms of blank (a), human plasma blank with IS (b), human plasma with high quality control (c)	20
Figure 3. The HPLC Chromatograms of blank (a), blank rat plasma (b) and in vivo plasma sample at 2hr after VGB administration (c).....	21
Figure 4. The HPLC Chromatograms of blank (a), blank rat brain (b) and in vivo rat brain sample at 2hr after VGB administration (c).....	21
Figure 5. The HPLC Chromatograms of blank (a), blank rat retina (b) and in vivo rat retina sample at 2hr after VGB administration (c).....	22
Figure 6. Permeation of vigabatrin across bovine olfactory mucosa on application of 20% of VGB solution, 20% of VGB in MBCP, 0.1% chitosan, 0.25% chitosan and 0.5% chitosan gel (mean \pm SD) n=3.....	31
Figure 7. The concentrations of taurine, GABA and vigabatrin in rat plasma, retina and brain at 2 h after single intraperitoneal and intranasal dose of vigabatrin in <i>Sprague-Dawley</i> rats (mean \pm SD) n=5.....	33

Figure 8. The concentrations of taurine, GABA and vigabatrin in rat plasma, retina and brain at 2 h after 28th day intraperitoneal and intranasal (chronic) dose of vigabatrin in *Sprague-Dawley* rats (mean \pm SD) n=536

Figure 9. The microscopical image of retinal histology stained with H&E of control (A), intranasal (B) and intraperitoneal (C) group of *Sprague-Dawley* rats37

Figure 10. The antiepileptic activity; onset of seizures and severity score of convulsions on intraperitoneal and intranasal dose of VGB.....39

Chapter-3

Figure 1. The ARPE-19 cell uptake of (A) VGB, (B) GABA and (C) Taurine at different concentrations (mean \pm SD) n=649

Figure 2. The effect of osmolarity and pH on uptake of (A, C) VGB and (B, D) taurine by ARPE-19 cells. (* p < 0.05, ** p < 0.01, and *** p < 0.001) (mean \pm SD) n=6.....51

Figure 3. The effect of GES on uptake of VGB, GABA and taurine by ARPE-19 cells (mean \pm SD) n=6.....52

Figure 4. Competitive uptake inhibition (Lineweaver-Burk plot) of VGB, GABA and taurine in ARPE-19 cells. Effect of VGB on uptake of (A) GABA and (B) taurine. Effect of GABA on uptake of (C) VGB and (D) taurine. Effect of Taurine on uptake of (E) VGB and (F) GABA by ARPE-19 cells (mean \pm SD) n=654

Figure 5. The effect of chronic administration of taurine and GES on retinal exposure of VGB on single dose of VGB 400 mg/kg body weight. (* p < 0.05, ** p < 0.01, and *** p < 0.001) (mean ± SD) n=655

Chapter-4

Figure 1. Effect of varying concentrations of vigabatrin(A), gabapentin(A), tiagabine(B), topiramate(C) and hydrogen peroxide(D) exposure on viability of R28 cells (mean ± SD) n=6 67

Figure 2. Effect of varying concentrations of vigabatrin(A), gabapentin(A), tiagabine(B), topiramate(C) and hydrogen peroxide(D) exposure on viability of ARPE-19 cells (mean ± SD) n=668

Figure 3. Representative DAPI and bright field fluorescence images show morphological changes of ARPE-19 cells detected with staining of Hoechst 33258. The images of cells untreated (A&B), treated with 25 mM vigabatrin (C&D) and 50 mM Gabapentin (E&F) for 24 h and imaged by fluorescence microscope (magnification 10X)71

Figure 4. Representative DAPI and bright field fluorescence images show morphological changes of R28 cells detected with staining of Hoechst 33258. The images of cells untreated (A&B), treated with 25 mM vigabatrin (C&D) and 15 mM Gabapentin (E&F) for 24 h and imaged by fluorescence microscope (magnification 10X)72

Figure 5. Representative DAPI and GFP fluorescence images show morphological changes of ARPE-19 cells detected by staining with Dead end TUNEL system and Hoechst 33258. The

images of untreated cells (A1-A3), treated with vigabatrin (B1-B3) and Gabapentin (C1-C3) for 24 h and imaged by fluorescence microscope (magnification10X)..... 73

Figure 6. Representative DAPI and GFP fluorescence images show morphological changes of R28 cells detected by staining with Dead end TUNEL system and Hoechst 33258. The images of untreated cells (A1-A3), treated with vigabatrin (B1-B3) and Gabapentin (C1-C3) for 24 h and imaged by fluorescence microscope (magnification10X) 74

Figure 7. Concentration dependent effect of vigabatrin and gabapentin on ratio of J-aggregates to J-monomers in ARPE-19 cells (mean \pm SD) n=6..... 76

Figure 8. Concentration dependent effect of vigabatrin and gabapentin on ratio of J-aggregates to J-monomers in R28 cells (mean \pm SD) n=6..... 76

Figure 9. Effect of taxifolin (100 μ M), silychrsitin (100 μ M), silydianin (100 μ M), silybin (100 μ M), isosilybin (100 μ M) and taurine (10 mM) on ROS generated by gabapentin (25 mM), vigabatrin (50 mM) and hydrogen peroxide (0.3 mM) exposure in ARPE-19 cells (mean \pm SD) n=6 79

Figure 10. Effect of taxifolin (100 μ M), silychrsitin (100 μ M), silydianin (100 μ M), silybin (100 μ M), isosilybin (100 μ M) and taurine (10 mM) on ROS generated by gabapentin (15 mM), vigabatrin (25 mM) and hydrogen peroxide (0.3 mM) exposure in R28 cells (mean \pm SD) n=6. 80

Figure 11. The cytoprotective effect of different concentrations of silymarin (A, B and C) and taurine (D) on vigabatrin, gabapentin and hydrogen peroxide produced R28 cellular toxicity (mean \pm SD) n=6 83

Figure 12. The cytoprotective effect of different concentrations of silymarin (A, B and C) and taurine (D) on vigabatrin, gabapentin and hydrogen peroxide produced ARPE19 cellular toxicity (mean \pm SD) n=6 **83**

CHAPTER 1

Introduction

Infantile spasm is an epileptic disorder in infancy and early childhood, commonly occurs between 3 to 12 months of age. The symptoms of spasms involve a series of transient jerking movements of arms and legs, which last for few seconds or occurs in clusters¹. The etiology of infantile spasm involves complex mechanisms occurring in prenatal, perinatal or postnatal stages. The major causes are central nervous system malformations, brain tumors, metabolic or genetic syndromes. More than 70 percent of infantile spasms cases are associated with tuberous sclerosis complex (TSC) syndrome². TSC syndrome affects many parts of body leading to multiple hamartoma formation in skin, brain, kidney, heart and lungs. Infantile spasms diagnosed using electroencephalogram (EEG) usually shows specific pattern called hypsarrhythmia³. Early diagnosis and treatment in infants reduce risk of development into complex seizures.

Vigabatrin (VGB) an antiepileptic drug, acts by inhibiting Gamma-aminobutyric acid (GABA) transaminase. It is used as first line treatment for infantile spasm and the drug of choice for infantile spasm with tuberous sclerosis complex syndrome¹⁻³ and adjuvant drug in the treatment of refractory complex partial seizures. In European Union and other countries VGB has been used since 1990 and in August 2009 USA approved VGB for potential benefit of the drug outweighing risk of causing permanent concentric visual field defects. VGB treatment is known to cause peripheral visual field defects and retinal damage in 10-40% of the patients³.

In humans, VGB on oral administration of therapeutic dose, is rapidly absorbed with T_{max} of 1.5 h and 60-70% bioavailability. VGB does not bind to plasma proteins and extensively distributed in the body on oral administration. Over 80% of orally administered VGB is excreted through urine unmetabolized⁴. Only 10% of absorbed VGB enters the brain and responsible for its therapeutic activity. The various studies carried out in animal models have proven that chronic administration of VGB in rats leads to ocular toxicity by VGB accumulation in retina, ^{5,6} which increases GABA concentrations much higher in retina compared to brain^{7,8}. The high GABA levels in ocular tissues sensitizes photoreceptors for light leading to retinal degeneration. In vitro studies have revealed increased GABA levels inhibit retinal uptake of taurine by competitively inhibiting taurine transporters at retinal pigmental epithelium⁹. Taurine is an antioxidant which plays a major role in neuroprotective activities and preclinical studies have reported that taurine deficiency causes retinal degeneration^{10–12}. VGB treatment in rodent models decreased taurine plasma and retinal levels and taurine supplementation evidenced a marked decrease in VGB induced ocular toxicity^{13,14}. In VGB clinical studies plasma taurine level is considered as biomarker for study of the structure and function of the retina in patients with refractory complex partial seizures^{15,16}. Further preclinical studies are required to elucidate mechanisms of VGB induced taurine deficiency and phototoxicity. There is a need to evaluate different approaches to alleviate the retinal toxicity of this potential drug.

CHAPTER 2

Intranasal Drug Delivery to Alleviate the Vigabatrin Induced Retinal Toxicity

1. Introduction

On intranasal drug delivery, low molecular weight drugs are directly transported to brain through olfactory mucosa¹⁷⁻¹⁹. Intranasal drug delivery pathway bypasses blood brain barrier and blood-cerebrospinal fluid barriers. The main advantage of intranasal route is ease of administration, patient complaint, low dose requirement, reduces the systemic drug exposure and associated drug toxicity. The nose to brain delivery of VGB would be a potential approach to deliver the drug to brain and decrease the systemic exposure, thus associated VGB retinal toxicity.

The accurate estimation of VGB, GABA and taurine concentrations in plasma, brain, and retina after different routes of administration, gives an insight into the drug efficiency and toxicity level. A simple, sensitive, and reproducible analytical method is also essential to investigate novel approaches for alleviating retinal toxicity of VGB in animal models. The estimation of biogenic amines (GABA and taurine) and VGB in the biological matrices is challenging because they consist of other endogenous amines, which would compromise the selectivity of the analytical method. The analysis of these components requires optimization of chromatographic method with suitable mobile phase composition of appropriate pH and specific column to maintain adequate resolution by preventing interference of other endogenous amines. Also, these analytes are small aliphatic molecules and not electroactive nor possess chromophore or fluorophore.

Hence, for detection of these compounds through simple analytical technique, it is necessary to derivatize the analytes for introducing chromophore or fluorophore. The derivatized product should be sensitive and stable for analysis using HPLC. There are previously reported analytical methods using derivatization techniques with various reagents for quantification of VGB^{4,20-24}, taurine²⁵ and GABA²⁶⁻³² in various biological matrices. Also, some analytical methods include simultaneous estimation of VGB along with GABA^{33,34} and taurine along with GABA^{35,36} in different biological matrices. These currently available methods have low detection limits^{20,22,26}, long run times^{20,29,34}, complex derivatization procedures^{4,23,24,26,30,31} and instable derivatized products^{20,22,27,28,34,36}. To date, there is no reported analytical technique for simultaneous estimation of VGB, taurine and GABA. In this study, 2, 3- Naphthalene di carboxaldehyde (NDA) derivatization method was optimized to increase sensitivity and stability of derivatized product.

In the present study, a simple, cost effective, highly sensitive and reproducible HPLC method was developed and validated for simultaneous estimation of VGB, GABA and taurine in human plasma, rat plasma, brain, and retina. The developed HPLC method was applied for investigation of VGB modulatory effects on GABA and taurine levels in plasma, brain, and retina of rats after intraperitoneal and intranasal administration. The effect of chitosan and multiblock copolymer on VGB *ex-vivo* permeation across bovine olfactory mucosa was assessed. The levels of VGB, GABA and taurine in plasma, brain, and retina on acute and chronic dose of VGB (intraperitoneal and intranasal) in *Sprague Dawley* rats were evaluated. The retinal histology examination of rats administered with chronic intraperitoneal and intranasal dose of VGB was performed. The antiepileptic activity on intranasal dose of VGB in pentylenetetrazol induced rat seizure model was investigated.

2. Materials and Methods

2.1 Chemicals and reagents

VGB was obtained from Santa Cruz Biotechnology, Inc. USA. GABA, Chitosan medium molecular weight, pentylenetetrazol, paraformaldehyde, and NDA were purchased from Sigma Aldrich Inc. USA and taurine standards were purchased from Spectrum chemicals USA. Human plasma was purchased from Innovative Research Inc. Emsure[®] Potassium cyanide for analysis was purchased from EMD Millipore USA. Euthasol[®] (pentobarbital sodium and phenytoin sodium) Solution was procured from Virbac USA. HPLC grade solvents acetonitrile, methanol, dibasic potassium phosphate, glacial acetic acid, O-phosphoric acid, sucrose, and Milli Q water are of research grade used without further purification.

2.2 Instrumentation and chromatographic conditions

The chromatographic analysis was performed using Waters HPLC system equipped with Waters 2475 fluorescence detector and Waters 1525 binary pump system operational with an auto-sampler. Initially the feasibility of different columns (phenyl and C-18), and solvents acetonitrile and methanol with buffers such as sodium and potassium dihydrogen phosphate (varying pH 3 to 8) along with altered flow rates (in the range of 0.80–1.50 mL/min) was used to achieve an effective chromatographic resolution of VGB, GABA and taurine. The mobile phase was passed through the 0.45 μ m Millipore filter membrane and degassed prior to use. The optimum wavelength of excitation and emission for analyzing eluent was determined by excitation and emission scan function in detector.

2.3 Standard solutions

The 2 mg/mL of VGB, GABA and taurine primary stock solutions were prepared by dissolving accurately weighed standards in Milli Q water. Working standard solutions were prepared from the primary stock solutions by subsequent dilutions in Milli Q water. Primary standards were stored at -20 °C and working standards were prepared regularly and stored at 4 °C until derivatization and analysis.

2.4 Sample preparation

The brain and retina were isolated from the euthanized male Sprague Dawley rats (7-8 weeks) and immediately snap frozen in dry ice. These tissue samples along with plasma samples collected from the study and blank animals were stored in -70 ± 5 °C until analysis. The brain and retinal tissue samples were weighed individually; brain was transferred into 15 mL tarson tubes and retina to 1.5 mL of micro centrifuge tubes. These tissues were homogenized in two-fold volume of freshly prepared ice-cold Phosphate Buffered Saline pH 7.4 using ultrasound probe sonicator. Aliquots of 100 μ L of rat brain homogenate/ rat retinal homogenate/ rat plasma/ human plasma was precipitated with 1000 μ L of ice-cold acetonitrile, and vortexed for 2 min and centrifuged at 13000 rpm at 4 °C. The aliquots of supernatants were used for derivatization of amino acids.

2.5 Optimization of NDA Derivatization

Several analytical studies use O-phthalaldehyde (OPA) as precolumn derivatizing agent for generating both electroactive and fluorescent active derivatization products of amino acids (primary amines)^{20,22,28,29,34,36-38}. Researchers have reported on instability of the derivatized products formed by OPA reagents³⁹. Other agents for derivatizing compounds with primary amine include dansyl chloride,^{23,24} 2-hydroxy naphthaldehyde,^{30,31} fluorescamine,²¹ 2,4-dinitrofluorodinitro benzene²⁶ and NDA³¹⁻³³. NDA forms relatively stable, sensitive and fluorescent active 1-cyanobenz (f) isoindole derivatives with primary amines in the presence of cyanide ions in alkaline conditions^{40,41}. Also, the stable NDA derivatives are more convenient for the sample handling during HPLC analysis and for HPLC system devoid of online pre-column derivatization. In this study, samples extracted were derivatized using NDA in presence of cyanide ions for introducing fluorophore to analytes and internal standard. The derivatization method was optimized by assessing effect of different concentration of NDA (0.5 to 10 mM), and KCN (0.5 to 10 mM) in different pH (5 to 9.2) of reaction mixture and different reaction time on sensitivity and stability of formed isoindole derivative. After the reaction time, reaction mixture was quenched with 20 μ L of 1% glacial acetic acid in water, vortex mixed and 10 μ l of this mixture was injected on to HPLC for analysis of derivatized product.

2.6 Method validation

At present there is no existing regulatory guidelines for estimation of endogenous compound, hence a 'fit-for-purpose' approach is suggested to demonstrate the efficiency of the method. The RP-HPLC method was validated to meet the acceptance criteria of USFDA industrial guidance for the bioanalytical method validation using surrogate matrix, as biological matrices

devoid of GABA and Taurine are not readily available. Milli Q water was used as surrogate matrix and used for validating the HPLC method for simultaneous estimation of VGB, GABA and taurine in human plasma, rat plasma, brain and retina samples using gabapentin as internal standard (IS).

2.6.1 LLOQ determination

The lower limit of quantification (LLOQ) were calculated based on the standard deviation of the response and the slope obtained by plotting calibration curves of each analytes (ICH guideline)⁴². LLOQ were calculated as $10\alpha/S$, where α is the standard deviation of y-intercept and S is the slope of straight line.

2.6.2 Specificity and selectivity

The samples of the human plasma, rat plasma, brain, and retina from five different lots were analyzed for evaluating the specificity of the method developed to study the possible interferences at the retention time of VGB and IS. The specificity for VGB, GABA, taurine and IS was evaluated by analyzing the 6 injections of Milli Q water to identify the potential interferences at the retention time of these molecules. The study acceptance criterion was that at least 80% of total lots must have a peak area less than 5 times of the lower limit of quantification (LLOQ) peak area in that matrix.

2.6.3 Calibration curve

The peak-area ratio of VGB, GABA and taurine to that of IS against the actual concentration of calibration standards in Milli Q water were used for plotting calibration curves. The concentrations for standard analytes used were 64.6, 129, 258, 646, 1292, 2583, 5166 and 6458 ng/mL for VGB; 51.5, 103, 206, 515, 1030, 2060, 4120 and 5150 ng/mL for GABA and 62.5, 125, 250, 625, 1250, 2500, 5000 and 6250 ng/mL for taurine. The linear regression analysis was performed with weighting factor of $1/X^2$, the acceptance criteria for calibration curve should have a correlation coefficient (r^2) of 0.99 or better. The acceptance criteria for each back-calculated standard concentration were $\pm 15\%$ deviation from the actual concentration except at LLOQ, which was set at $\pm 20\%$.

2.6.4 Precision and accuracy

The precision and accuracy (intra and inter day) were determined using six replicates at 4 different levels LLOQ, low, middle, and high-quality control (LQC, MQC and HQC) for each analyte in three different runs. The quality control (QC) concentration values for VGB were 64.6, 194, 3229, and 5812 ng/mL of LLOQ, LQC, MQC, and HQC, respectively. The QC values for GABA were 51.5, 155, 2575 and 4635 ng/mL of LLOQ, LQC, MQC, and HQC, respectively. The QC values for taurine were 62.5, 188, 3125 and 5625 ng/mL of LLOQ, LQC, MQC, and HQC, respectively. The acceptance criteria for accuracy are $\pm 15\%$ of the actual concentrations except for LLOQ where it is $\pm 20\%$ of actual concentrations. For all quality control samples, a precision of 15% relative standard deviation (RSD), except for LLOQ it should not exceed 20% of RSD.

2.6.5 Recovery

The extraction recovery of VGB, GABA, taurine and IS was determined by comparing the peak-area ratios of the analytes from LQC, MQC, and HQC levels spiked in human plasma, rat plasma, brain and retinal homogenate (n = 6) with the responses of analytes of LQC, MQC and HQC concentrations in Milli Q water. The recovery of the GABA and taurine was calculated by mean background correction and for VGB and IS recovery was calculated with no background correction.

2.6.6 Stability experiments

The stability of analytes was evaluated in biological matrix (human plasma, rat plasma, rat brain and retina homogenate) by spiking high QC levels and the samples were evaluated for 8-h bench top (on ice bath), freeze-thaw (12-h time duration between each of 3 freeze and thaw cycle, the samples stored at -70 ± 5 °C between cycles) and 60-days long term stability (at -70 ± 5 °C). The stability of GABA and taurine in biological matrix was calculated by correction for mean background response (six replicates), which was performed as reported by Richardson et al⁴³. The stability samples were processed as described in ‘Sample preparation’ section. The stability of processed sample/derivatized analytes at LQC and HQC concentrations were subjected to 8 h bench-top (at room temperature) and in-injector (auto sampler 10 °C) stability. In-injector stability of processed samples was estimated by injecting at time intervals of 24, 48 and 60 h. All Stability samples were compared with freshly prepared calibration standard. Samples were considered stable if assay values were within the acceptable limits of accuracy $\pm 15\%$ from fresh samples and precision of 15% RSD.

2.6.7 Dilution effect

Dilution integrity was assessed to ensure that the biological samples could be diluted with Milli Q water without having effect on the final concentrations. The biological samples were spiked with the known high concentrations of VGB (12915 ng/mL), GABA (10300 ng/mL) and taurine (12500 ng/mL). These samples were diluted 5 times and 10 times with Milli Q water in six replicates and analyzed. The accuracy of the back calculated samples should be in the range of 85-115 % of the actual concentrations and the precision should be within 15 % RSD.

2.7 Vigabatrin thermosensitive gel

On intranasal administration, drugs are extensively cleared due to mucociliary activity. The mucociliary clearance of a drug can be decreased by employing a mucoadhesive gel to increase retention of the drug in nasal cavity. Formulating a thermosensitive gel which are liquid at room temperature and forming gel at nasal cavity temperature would be beneficial to administer the dose and increase the drug retention at nasal cavity⁴⁴. VGB is a low molecular weight molecule with high aqueous solubility. The chitosan and multiblock copolymer (MBCP) are thermosensitive and mucoadhesive polymers. The chitosan and MBCP (synthesized in house) were used to prepare gels containing 20% of VGB.

2.7.1 Preparation of Chitosan Hydrogel

Chitosan a naturally occurring polycationic linear polysaccharide polymer, insoluble at neutral and alkaline pH conditions. At acidic pH, the chitosan solubility increases due to protonation of amino group. Chitosan with different molecular weight (low < 50 kDa, medium 50-150 kDa, high > 150 kDa) are available, the viscosity of gel increases with increase in the

molecular weight. 20% of vigabatrin was dissolved in 0.1% of glacial acetic acid and different concentration of medium molecular weight chitosan (0.1, 0.25 and 0.5%) was added at room temperature and gel formation of these solutions were observed at 32 °C.

2.7.2 Preparation of MBCP Hydrogel

MBCP polymers are novel triblock copolymers synthesized from Pluronic acid® P104 and di-(ethylene glycol) divinyl ether by employing previously published method by Garipelli et al⁴⁵. The MBCP rheological properties on gelation controls drug release and thus on intranasal administration forms a *in situ* depot. The gelation temperature of MBCP polymers are 20 to 40 °C and degrades at acidic pH. These properties of MBCP gels are ideal for intranasal administration, as the nasal mucosal temperature is ~34 °C and with a physiological pH of 5.0-6.0⁴⁵. The MBCP polymer at concentrations of 10, 15 and 20% was dispersed in water and the dissolution of MBCP was facilitated by placing at 2-8 °C. Vigabatrin was dissolved separately in water and added to the polymer dispersions to prepare final concentration of 20% and mixed thoroughly using magnetic stirrer.

2.8 Permeation of VGB across bovine olfactory mucosa

2.8.1 Preparation of Bovine Olfactory Mucosa

The bovine olfactory mucosa for permeation studies were purchased from Pel-Freez Biologicals, Arkansas. The excised bovine olfactory mucosa is good model to study the drug transport across the barrier⁴⁶. The excised tissue was supplied frozen and tissue was used for the studies within 24 h of tissue isolation. The tissue was thawed for 30 min, washed with PBS 7.4 pH and used for permeation studies.

2.8.2 Permeation Study

The vigabatrin permeation studies across the bovine olfactory mucosa was performed using vertical Franz diffusion cells. The bovine olfactory mucosa was sandwiched between donor and receiver chamber of Franz diffusion cell with an active diffusion area of 0.64 cm², and the mucosal surface was exposed to the donor chambers. To ensure the integrity of olfactory mucosa, resistance across the mucosa was measured using a wave form generator. The bovine olfactory mucosa with resistance of ≥ 2.5 K Ω .cm² was used for permeation studies. To evaluate vigabatrin permeation from solution and gel across olfactory mucosa, donor compartment was filled with 200 μ L of 20% vigabatrin solution, 200 mg of MBCP and chitosan (0.1%, 0.2% and 0.5%) gel containing 20% of VGB. The receiver chamber was filled with 5 ml of PBS pH 7.4 and constantly stirred at 600 rpm with a magnetic stir bar. The temperature was maintained at 37 °C with a circulating water bath. The 200 μ L of samples were withdrawn from receiver compartment at different time intervals (0, 0.25, 0.5, 1, 2, 3, 4, 6 and 8 h) and an equal volume of fresh receiver media was replaced. The above samples were derivatized and subjected to HPLC analysis.

2.9 *In-vivo* study

Male *Sprague-Dawley* rats of 7-8 weeks were used for *in-vivo* studies. The animals were housed in a room where temperature and humidity were controlled with 12 h light: 12 h dark cycle.

2.9.1 Retina, brain, and plasma exposure studies

The Animal study was conducted as per study protocol at University of Mississippi, School of Pharmacy, Mississippi-38677, USA approved by the institutional animal ethical committee. The dose used in intraperitoneal animals was equivalent to therapeutic human maintenance dose (3 g/day)⁴⁷, calculated using body surface area conversion factor⁴⁸.

2.9.1.1 Acute Study

Acute studies were conducted with 15 Animals and divided into three groups each containing 5 animals. The first group of animals was used as blank where they were dosed with normal saline to estimate the basal levels of taurine and GABA. The second group of animals was dosed at 400 mg/kg dose of VGB by intraperitoneal route of administration. The third group of animals was dosed at 40 mg/kg dose of VGB by intranasal route of administration. After 2h of dosing, animals were euthanized using Euthasol[®] and eyes, brain and blood was harvested. The plasma was separated from the blood, retina was isolated from the enucleated eye at 4 °C and all these biological samples were snap frozen immediately after collection and stored at -70 ± 5 °C until bioanalysis.

2.9.2.1 Chronic Study

Chronic studies were conducted with 15 Animals and divided into three groups each containing 5 animals. The first group of animals were used as blank where they were dosed with normal saline for 28 days to estimate the basal levels of taurine and GABA. The second group of animals was dosed at 400 mg/kg dose of VGB by intraperitoneal route of administration for 28 days. The third group of animals was dosed at 40 mg/kg dose of VGB by intranasal route of

administration for 28 days. On 28th day, after 2h of dosing animals were euthanized using Euthasol[®] and eyes, brain and blood was harvested. The plasma was separated from the blood, retina was isolated from the enucleated eye at 4 °C and all these biological samples were snap frozen immediately after collection and stored at -70 ± 5 °C until bioanalysis.

One eye from each animals was used for bioanalysis and other eye was used to examine the histological changes on chronic intranasal and intraperitoneal dose of VGB. The isolated rat eyes were fixed with 4% paraformaldehyde with a small puncture in the cornea and stored in 4 °C for 24 h. After specified time period, the paraformaldehyde was decanted and replaced with 30% sucrose and stored for 2 h at room temperature. The sucrose was washed with PBS after 2 h and stored at -70 °C and eye samples were shipped for AML laboratories Inc, Florida, USA in dry ice for cryosectioning. In AML lab, eyes were embeded with optimal cutting temperature (OCT) compound medium and samples were refrozen. The frozen embeded posterior part of eye were cryosectioned and sections were mounted on slides. The slides were stained with Heamotoxylin and Eosin (H&E). The slides were examined under Zeiss microscope, at 20X magnification at The Univeristy of Mississippi, USA.

2.9.2 Antiepileptic activity of Vigabatrin intranasal dose

The pharmacodynamic studies in epileptic model of SD rats were outsourced and performed at Invivo Biosciences, Bengaluru, India. The study protocol was approved by the institutional animal ethical committee of Invivo Biosciences and CPCSEA guidelines for research in small animals was followed for studies. Pharmacodynamic studies was conducted with 35 animals and divided into 7 groups each containing 5 animals. The first group was used as control, where they were dosed with normal saline subcutaneously and observed for normal behavior.

2.9.2.1 Induction of Seizure

The seizure was induced in animals by administering the pentylenetetrazol (PTZ) at dose of 100 mg/kg subcutaneously ⁴⁹ and observed for seizure intensity. The Scale for seizure intensity was observed and scoring 0, 1, 2, 3, 4, and 5 was assigned for signs of motionless, isolated myoclonic jerks, atypical minimal seizures (some movements observed), minimal seizures (clonic seizures involving head and forelimb muscles), generalized clonic seizures / tonic phase is absent / righting reflexes lost, and complete generalized tonic-clonic seizures with loss of righting reflexes generalized, respectively.

2.9.2.2 PTZ effect on intraperitoneal and intranasal administration of VGB

Prior to PTZ administration, animals were treated with vigabatrin at different time intervals and observed for signs of seizures. The second group of animals were dosed with 100 mg/kg of PTZ subcutaneously and observed for seizure intensity, these animals were used as negative control. The third group of animals were administered with 900 mg/kg intraperitoneal dose, 6 h prior to 100 mg/kg of PTZ subcutaneous dose. The fourth, fifth, sixth and seventh group of animals were administered with 40 mg/kg of intranasal dose, 0.5, 1, 2 and 4 h prior to 100 mg/kg of PTZ subcutaneous dose, respectively. After PTZ subcutaneous dose, scale for seizure intensity was observed and scored based on signs.

2.10 Statistical Analysis

The statistical significance was calculated using GraphPad prism software. The unpaired, two-tailed t-test analysis was performed for comparing the control group and treated group taurine and GABA concentrations in rat plasma, rat brain homogenate and retinal samples. The P values > 0.05 were considered as statistically significant.

3. Results and Discussion

3.1 Liquid chromatography

The resolution of VGB, GABA and taurine were poor on phenyl and C-8 column. On Zorbax Eclipse AAA C18 column adequate resolution was observed. The peak tailing was eliminated by replacing the aqueous mobile phase sodium dihydrogen phosphate with potassium phosphate dibasic. At pH 6.5 of aqueous mobile phase significantly increased the response of all three analytes. The resolution and peak shape of analyte was better on use of methanol compared to acetonitrile. Gabapentin was used as IS as it has similar physicochemical properties with VGB, GABA and taurine. It is soluble in polar solvents, retained on Zorbax Eclipse AAA column and elutes with good peak shape and intensity, which will correct the loss of analyte response due to any variation in instrument. The effective chromatographic separation was obtained using Zorbax Eclipse AAA column (150 x 4.6mm, 3.5 μ m; Agilent Technologies) maintained at 25 \pm 2 $^{\circ}$ C. The resolution of peaks was best achieved with a binary mobile phase system consisting of reservoir A (methanol) and reservoir B (10mM potassium phosphate dibasic in Milli Q water, pH 6.5 adjusted with phosphoric acid) was run on a gradient profile (0–5.0min, 60% A; 5.0–10.0min 60 to 90% A; 10.0–11.0min, 90% A; 11.0-12.0min, 90 to 60% A and 12.0–15.0min, 60% A) at a flow rate of 1 mL/min with a run time of 15 min. A good chromatographic resolution was observed

with a shorter run time compared to previously reported methods for estimation of GABA and VGB with long run times^{20,29,34}. The optimum response of VGB, GABA, taurine and IS were found at excitation and emission wavelength of 400nm and 500nm, respectively. These wavelengths were used to monitor the eluent for method development and validation studies.

3.2 Optimization of NDA Derivatization

By increasing concentration of reagents in reaction mixture, the peak area response of VGB, GABA and taurine increased. The isoindole products are formed at neutral to basic pH, the various trials carried out at different pH (6, 6.5, 7, 7.5, 8.0, 8.5 and 9) demonstrated that analyte peak response of derivatized product was maximum at pH 6.5. The analyte peak area at the concentration of 0.3 mM of potassium cyanide and 0.2 mM of NDA in dibasic potassium phosphate buffer at pH 6.5 was optimum. On further increasing concentration of reagents in the reaction mixture, the interference was increased without increase in the response of VGB, GABA and taurine. The response of derivatized product increased with reaction time from 2 min to 10 min, after 10 min there was no increase in the response of VGB, GABA and taurine. The sensitive, stable and linear (at calibration range of vigabatrin, GABA and taurine used for validation) isoindole derivative was formed with reaction mixture containing 20 µl of sample with primary amine group, 20 µl of potassium cyanide (4 mM) in water, 20 µl of NDA (2.5 mM) in methanol and 180 µl of dibasic potassium phosphate buffer (pH 6.5). This modified NDA derivatization method was used for validation studies by addition of 180 µL of dibasic potassium phosphate buffer (pH 6.5) containing IS. The NDA derivatization involves a simple procedure at normal room conditions unlike other derivatization techniques (4-chloro-7-nitrobenzofurazan⁴, fluorescamine²¹,

dansyl chloride^{23,24}, 2,4-dinitrofluoro dinitrobenzene²⁶ and 2-hydroxy naphthaldehyde^{30,31}) which involves complex procedures like incubating at higher temperatures with longer reaction times.

3.3 Method validation

3.3.1 Specificity & selectivity

The analytical run with the liquid chromatographic conditions described in section 3.1, the VGB, GABA, taurine and IS were well resolved with total run time of 15 min. There was good chromatographic specificity with no interference of biological matrices and byproducts of derivatizing agent were observed. The retention time of taurine, GABA, VGB and IS were 3.8, 4.8, 6.4 and 11.8 min, respectively. No junk peaks were observed at the retention times of analyte and IS in Milli Q water and biological matrices. Representative chromatograms for the blank (free of analytes and IS), IS spiked in matrices (Milli Q water, human plasma, rat plasma, brain and retina), Milli Q water spiked with VGB, GABA and taurine at LLOQ and HQC along with IS and *in-vivo* (rat plasma, brain and retina) samples are shown in the Figures 1, 2, 3, 4 and 5, respectively.

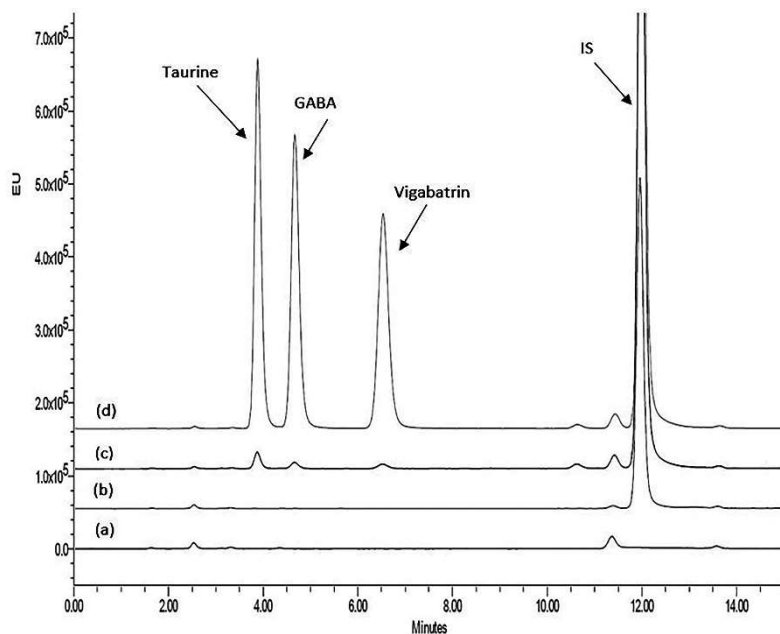


Figure.1 The HPLC Chromatograms of blank (a), blank with IS (b), low limit of quantification (c) and high-quality control (d).

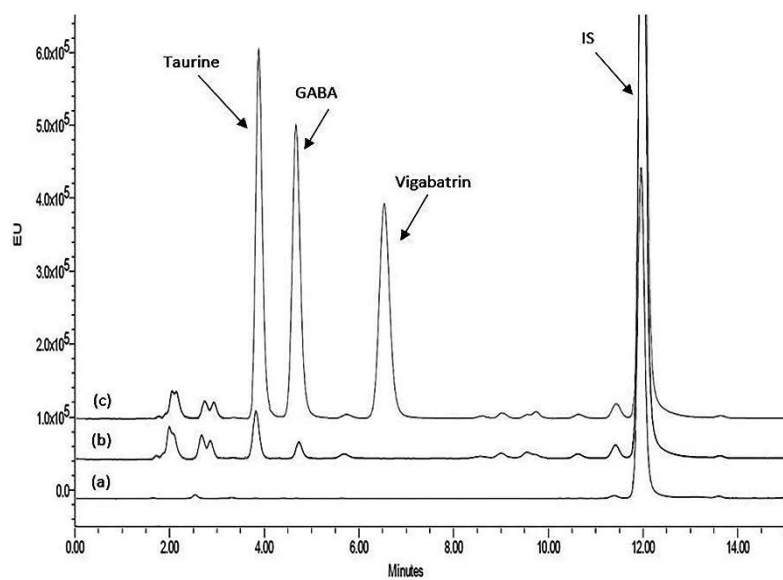


Figure.2 The HPLC Chromatograms of blank (a), human plasma blank with IS (b), human plasma with high quality control (c)

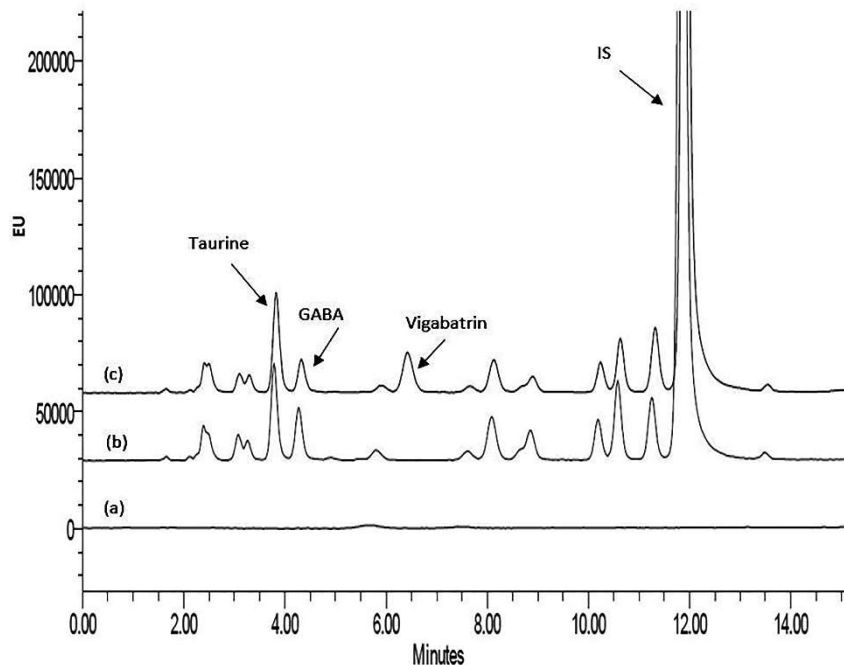


Figure.3 The HPLC Chromatograms of blank (a), blank rat plasma (b) and in vivo plasma sample at 2hr after VGB administration (c)

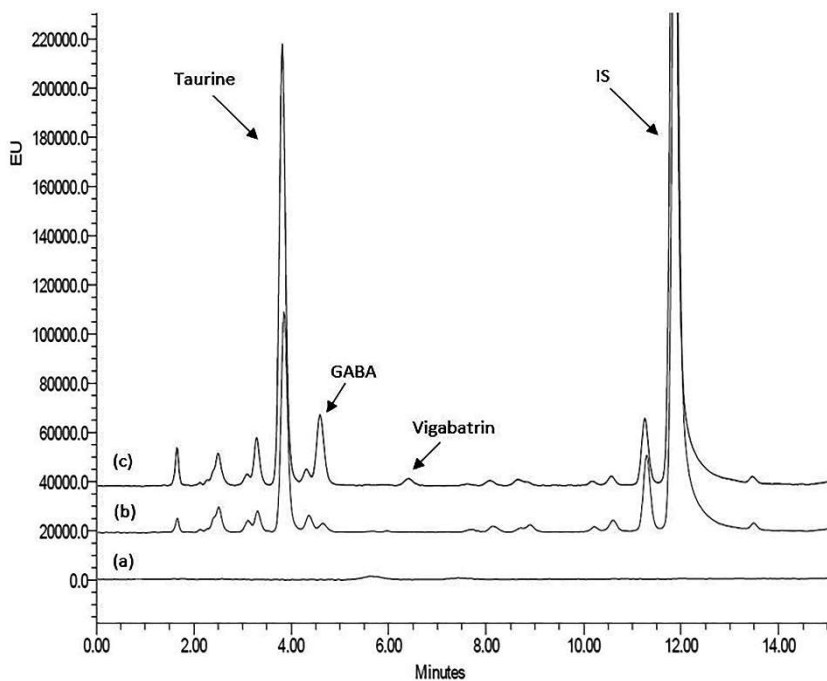


Figure.4 The HPLC Chromatograms of blank (a), blank rat brain (b) and in vivo rat brain sample at 2hr after VGB administration (c)

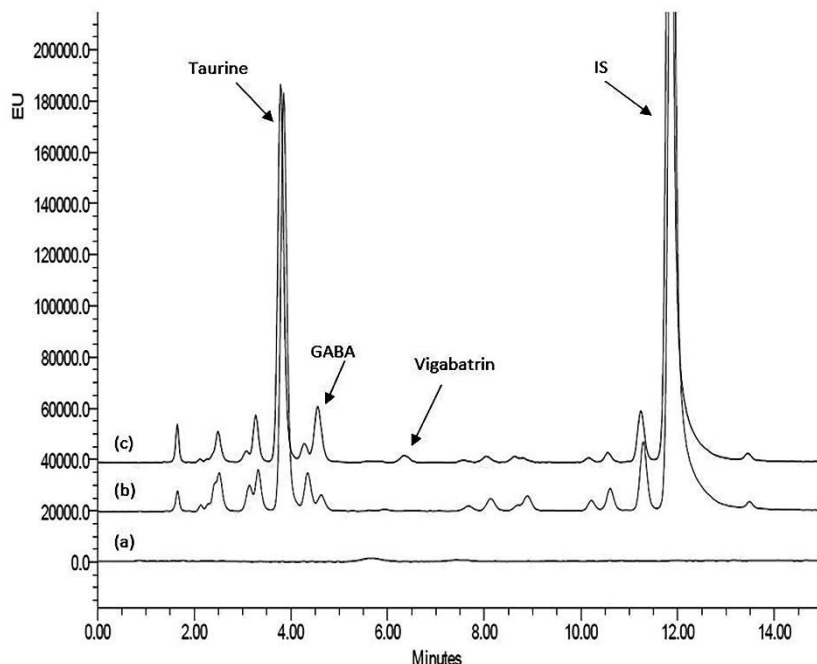


Figure.5 The HPLC Chromatograms of blank (a), blank rat retina (b) and in vivo rat retina sample at 2hr after VGB administration (c)

3.3.2 Recovery

The simple protein precipitation method was preferred over liquid-liquid and solid phase extraction method for extracting analytes as they are highly polar in nature. The protein precipitation method is simple, rapid and cost effective compared to solid phase and liquid-liquid extraction method. The extraction trials were carried out with acidified and alkalinized organic solvents (acetonitrile and methanol) for enhancing the recovery of analytes from biological samples. At different concentration level (LQC, MQC and HQC) of each analyte the recovery was evaluated, and peak area ratio was considered for the calculations. The results (Table 1) demonstrated the recovery of VGB, GABA and taurine from different matrices were concentration independent, reliable and reproducible with the use of organic solvent acetonitrile (without acidification nor alkalinization). The extracted samples were adequately clean as the biological samples were extracted with higher volume of acetonitrile in ratio of 1:10 (sample: acetonitrile).

The recovery for the IS at concentration of 2 $\mu\text{g/mL}$ in Milli Q water, human plasma, rat plasma, rat brain and rat retina were 93.7 ± 2.95 , 93.6 ± 9.20 , 92.7 ± 7.18 , 91.4 ± 5.17 and $91.4 \pm 5.17\%$, respectively.

Table 1. The recovery of taurine, GABA and vigabatrin at different concentration levels from different biological matrices and water (n=6)

Biological Matrix	Stability test	% Recovery (Mean \pm SD)		
		Taurine	GABA	Vigabatrin
Rat Plasma	LQC	87.8 ± 5.17	91.3 ± 8.14	86.7 ± 2.74
	MQC	88.3 ± 6.63	94.9 ± 5.42	93.5 ± 3.75
	HQC	91.2 ± 4.92	91.7 ± 4.19	90.7 ± 8.32
Rat Brain	LQC	86.2 ± 10.7	90.8 ± 7.17	87.3 ± 3.67
	MQC	89.8 ± 4.42	88.1 ± 2.74	86.3 ± 11.1
	HQC	93.2 ± 3.29	87.1 ± 5.28	92.4 ± 5.16
Rat Retina	LQC	89.5 ± 9.09	85.8 ± 4.30	91.2 ± 7.20
	MQC	86.2 ± 10.5	90.7 ± 9.21	86.8 ± 2.27
	HQC	90.8 ± 7.79	85.8 ± 7.14	87.2 ± 4.79
Human plasma	LQC	90.1 ± 5.97	93.2 ± 2.99	95.0 ± 6.26
	MQC	83.3 ± 8.55	87.4 ± 6.69	85.6 ± 0.82
	HQC	88.9 ± 8.17	94.1 ± 9.43	89.7 ± 7.32

3.3.3 Calibration curve

The standard calibration curve was reproducible over the specified concentration range for each analyte. A linear response was observed for the range of concentrations 64.6 to 6458 ng/ml for VGB ($r^2 > 0.994$); 51.5 to 5150 ng/ml for GABA ($r^2 > 0.999$) and 62.5 to 6250 ng/ml ($r^2 > 0.998$) for taurine. The percentage accuracy observed for the mean of back-calculated concentration of three linearity's was within 89.5–107 % for VGB, 88.7–110% for GABA and 95.3–114% for taurine. The accuracy of the back calculated concentrations of VGB, GABA and taurine linearity's were in the range of 85-115 % of the actual concentrations, which met the acceptance criteria. The linearity range was selected from the LLOQ to 100 times of LLOQ, as the concentration of the analytes in biological samples depends on the acute or chronic dose of vigabatrin in human and rats.

3.3.4 Precision & accuracy

The precision and accuracy of intra and inter-day analysis were determined by using LLOQ, LQC, MQC and HQC levels (six replicates each) on three different days (Table 2 and 3). The intra-day precisions were in the range of 0.30-5.90, 0.27-4.15, and 0.66-9.15% RSD for VGB, GABA and taurine, respectively. The inter day precisions were in the range of 1.39-5.30, 2.71-4.08, and 3.53-8.88% RSD for VGB, GABA and taurine, respectively. The accuracy of the back calculated samples of intra and inter-day were in the range of 85-115 % of the actual concentrations and the precision was well within 15 % RSD, which met the acceptance criteria.

Table 2. The Intra-day precision determination of taurine, GABA and vigabatrin (n=6).

Quality control	Run	Measured concentration (ng/mL)								
		Taurine			GABA			Vigabatrin		
		Mean ± SD	RSD	% Accuracy	Mean ± SD	RSD	% Accuracy	Mean ± SD	RSD	% Accuracy
LLOQ	1	63.3 ± 1.65	2.61	101	52.1 ± 1.26	2.48	101	66.1 ± 1.46	2.21	103
	2	67.2 ± 1.58	2.36	107	53.9 ± 1.83	3.40	105	64.6 ± 3.81	5.90	100
	3	58.8 ± 5.38	9.15	94.0	52.8 ± 1.35	2.56	103	66.2 ± 3.78	5.71	103
LQC	1	192 ± 4.56	2.37	103	144 ± 5.00	3.46	93.4	204 ± 2.34	1.15	106
	2	176 ± 9.94	5.64	94.0	141 ± 2.79	1.97	91.4	201 ± 5.16	2.57	104
	3	160 ± 8.26	5.17	85.5	140 ± 2.61	1.87	90.5	183 ± 0.73	0.40	94.0
MQC	1	3054 ± 140	4.59	97.7	2672 ± 25.0	0.94	104	3191 ± 24.2	0.76	99.0
	2	2899 ± 50.7	1.75	92.8	2444 ± 42.8	1.75	94.9	3122 ± 56.4	1.81	96.8
	3	2852 ± 18.9	0.66	91.3	2618 ± 15.9	0.61	102	3155 ± 9.32	0.30	97.8
HQC	1	5138 ± 38.2	0.74	91.3	4590 ± 12.4	0.27	99.0	5258 ± 19.9	0.38	90.6
	2	5096 ± 148	2.91	90.6	4349 ± 181	4.15	93.8	5315 ± 192	3.61	91.6
	3	4810 ± 82.4	1.71	85.5	4312 ± 52.0	1.21	93.0	5022 ± 38.2	0.76	86.5

SD: Standard Deviation; RSD: Relative Standard Deviation.

Table 3. The Inter-day precision determination of Taurine, GABA and Vigabatrin (n=18).

Quality control	Measured concentration (ng/mL)								
	Taurine			GABA			Vigabatrin		
	Mean ± SD	RSD	% Accuracy	Mean ± SD	RSD	% Accuracy	Mean ± SD	RSD	% Accuracy
LLOQ	63.0 ± 4.65	7.38	101	52.9 ± 1.57	2.96	103	65.7 ± 3.01	4.58	102
LQC	176 ± 15.6	8.88	93.9	142 ± 3.84	2.71	91.8	196 ± 10.4	5.30	101
MQC	2935 ± 119	4.07	93.9	2578 ± 105	4.08	100	3156 ± 44.0	1.39	97.9
HQC	5015 ± 177	3.53	89.1	4417 ± 162	3.66	95.3	5198 ± 168	3.22	89.5

SD: Standard Deviation; RSD: Relative Standard Deviation

3.3.5 Stability

The stability studies were performed to assess stability of VGB, GABA and taurine under probable sample handling and storage conditions. The stability of analytes in biological matrix (human plasma, rat plasma, rat brain and rat retina homogenate) was calculated by comparison of nominal concentration with observed value (after correction for basal levels). The stability results of analytes in biological matrix for 8-h bench top (ice bath), three freeze–thaw cycles (at $-70 \pm 5^{\circ}\text{C}$ between cycles) and 60-day long term stability (at $-70 \pm 5^{\circ}\text{C}$) were found to be within $\pm 15\%$ of the nominal concentrations (Table 4).

The calculated concentrations of processed samples at LQC and HQC level in 8 h bench-top and 48 h in-injector stability test were $\pm 15\%$ of actual concentrations, whereas at 60 h concentration of the processed samples were $< 15\%$ of actual concentrations (Table 5). However, the processed samples started to degrade after 48 h, which was depicted with the sample analyzed at 60 h. The optimized derivatization method produces stable derivatives of VGB, GABA and taurine compared to previous reported NDA method for GABA, which demonstrated derivatives were stable for only 16 h³².

Table 4. The stability data of taurine, GABA and vigabatrin at HQC concentration in biological matrices (n=6)

Biological Matrix	Stability test	Measured concentration (ng/mL)								
		Taurine			GABA			Vigabatrin		
		Mean \pm SD	RSD	% Accuracy	Mean \pm SD	RSD	% Accuracy	Mean \pm SD	RSD	% Accuracy
Rat Plasma	0 h	5472 \pm 270	4.93	97.3	4303 \pm 268	6.23	92.8	5852 \pm 196	3.35	101
	Bench Top	5453 \pm 180	3.30	96.9	4372 \pm 196	4.47	94.3	5776 \pm 198	3.43	99.4
	Freeze Thaw	5315 \pm 186	3.50	94.5	4324 \pm 304	7.03	93.3	5734 \pm 137	2.39	98.7
	Long Term	5468 \pm 241	4.41	97.2	4261 \pm 159	3.73	91.9	5640 \pm 79.4	1.41	97.0
Rat Brain	0 h	5266 \pm 280	5.32	93.6	4267 \pm 165	3.86	92.1	5558 \pm 172	3.09	95.6
	Bench Top	5372 \pm 232	4.33	95.5	4308 \pm 117	2.71	93.0	5572 \pm 204	3.66	95.9
	Freeze Thaw	5230 \pm 140	2.68	93.0	4388 \pm 116	2.64	94.7	5609 \pm 71.2	1.27	96.5
	Long Term	5400 \pm 75.1	1.39	96.0	4364 \pm 131	3.01	94.2	5580 \pm 154	2.76	96.0
Rat Retina	0 h	5286 \pm 160	3.04	94.0	4469 \pm 161	3.61	96.4	5522 \pm 158	2.86	95.0
	Bench Top	5297 \pm 340	6.41	94.2	4426 \pm 157	3.54	95.5	5494 \pm 155	2.82	94.5
	Freeze Thaw	5304 \pm 181	3.41	94.3	4367 \pm 163	3.72	94.2	5533 \pm 132	2.39	95.2
	Long Term	5271 \pm 201	3.81	93.7	4429 \pm 168	3.80	95.6	5507 \pm 106	1.92	94.8
Human Plasma	0 h	5284 \pm 126	2.38	93.9	4412 \pm 159	3.60	95.2	5613 \pm 178	3.61	96.6
	Bench Top	5274 \pm 186	3.53	93.8	4384 \pm 109	2.49	94.6	5587 \pm 146	2.61	96.1
	Freeze Thaw	5273 \pm 155	2.93	93.7	4375 \pm 143	3.28	94.4	5380 \pm 329	6.09	92.6
	Long Term	5211 \pm 170	3.26	92.6	3365 \pm 149	3.41	94.2	5482 \pm 194	3.53	94.3

SD: Standard Deviation; RSD: Relative Standard Deviation.

Table 5. The stability data of derivatized product of taurine, GABA and vigabatrin at LQC and HQC concentration (n=6)

Quality control	Time	Measured concentration (ng/mL)								
		Taurine			GABA			Vigabatrin		
		Mean ± SD	RSD	% Accuracy	Mean ± SD	RSD	% Accuracy	Mean ± SD	RSD	% Accuracy
LQC	0 h	182 ± 7.57	4.16	96.9	143 ± 5.50	3.86	92.1	188 ± 2.44	1.30	97.1
	Bench top (8 h)	186 ± 7.90	4.25	98.8	147 ± 8.56	5.84	94.6	184 ± 10.0	5.47	94.8
	24 h	184 ± 8.06	4.39	97.8	144 ± 3.91	2.71	93.0	185 ± 5.03	2.72	95.4
	48 h	177 ± 5.38	3.04	94.0	147 ± 3.87	2.64	94.7	189 ± 7.02	3.70	97.6
	60 h	154 ± 7.55	4.90	81.9	129 ± 9.45	7.35	83.0	165 ± 9.04	5.48	85.1
HQC	0 h	5526 ± 113	2.04	98.2	4390 ± 120	2.74	94.7	5436 ± 187	3.44	93.5
	Bench top (8 h)	5450 ± 133	2.45	96.9	4415 ± 186	4.22	95.2	5681 ± 112	1.98	97.7
	24 h	5468 ± 97.8	1.79	97.2	4443 ± 81.1	1.83	95.9	5472 ± 236	4.31	94.2
	48 h	5545 ± 140	2.52	98.6	4426 ± 98.9	2.23	95.5	5495 ± 128	2.33	94.6
	60 h	4608 ± 110	2.38	81.9	3814 ± 237	6.22	82.3	4672 ± 198	4.24	80.4

SD: Standard Deviation; RSD: Relative Standard Deviation.

3.3.6 Dilution effect

The biological samples were spiked with the known high concentrations of VGB (12915 ng/mL), GABA (10300 ng/mL) and taurine (12500 ng/mL). The biological samples spiked with higher concentrations and diluted 5 times had accuracy in range of 94.3-107, 97.1-114 and 87.1-112% for VGB, GABA and taurine respectively. The samples diluted 10 times had accuracy in range of 89.3-110, 86.1-104 and 92.1-113% for VGB, GABA and taurine respectively. The accuracy of the back calculated samples was in the range of 85-115 % of the actual concentrations and the precision was within 15 % RSD, which met the acceptance criteria. This study demonstrates that the samples with concentrations greater than the upper limit of quantitation can be diluted and analyzed to obtain accurate results.

3.4 Vigabatrin thermosensitive gel

The thermosensitive MBCP polymer is solution at 2-8 °C and forms a clear gel at room temperature. These studies have shown 15% of MBCP polymer is optimum to form a vigabatrin gel, whereas at 10% of polymer was insufficient to form a gel and with 20% MBCP polymer concentrations, it formed a very thick gel.

3.5 Permeation of VGB across bovine olfactory mucosa

The VGB permeation across bovine olfactory mucosa results are presented in Figure. 6. There was no difference in permeation of VGB from 20% solution, 0.1, 0.25 and 0.5% chitosan gels. Whereas, the permeation of VGB from MBCP gels were increased 1.2-fold compared to 20% VGB solution. The vigabatrin cumulative amount permeated across bovine olfactory mucosa was in the following order: 20% VGB solution < 0.5% chitosan gel < 0.25% chitosan gel < 0.1%

chitosan gel < MBCP gel. This study demonstrates MBCP polymers have better VGB permeation enhancing potential compared to 0.1, 0.25 and 0.5% of chitosan gel.

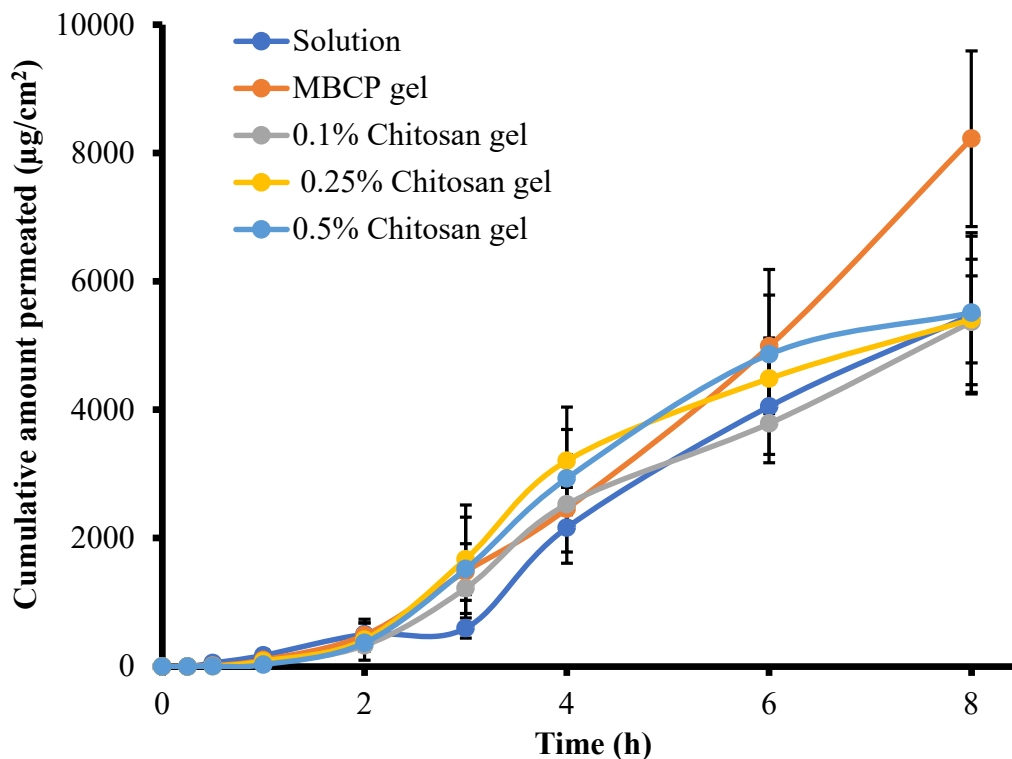


Figure.6 Permeation of vigabatrin across bovine olfactory mucosa on application of 20% of VGB solution, 20% of VGB in MBCP, 0.1% chitosan, 0.25% chitosan and 0.5% chitosan gel (mean \pm SD) n=3.

3.6 *In-vivo* study

The results obtained from the selectivity and sensitivity studies were found to be adequate for simultaneous quantification of VGB, GABA and taurine in rat plasma, brain and retina following intraperitoneal and intranasal administration of VGB. 20% VGB in MBCP gels were used for *in vivo* acute and chronic intranasal studies.

3.6.1 Retina, brain and plasma exposure studies

3.6.1.1 Acute Study

The acute study results on VGB intraperitoneal administration of 400 mg/kg, have shown higher VGB concentrations in retina ($19.2 \pm 3.65 \mu\text{g/g}$) compared to plasma ($8.19 \pm 1.28 \mu\text{g/mL}$) and brain ($1.49 \pm 0.45 \mu\text{g/g}$). The concentration of VGB in retina was ~ 2.35 and 12.9 times higher compared to plasma and brain, respectively. The GABA levels in plasma ($27.0 \pm 1.22 \mu\text{g/mL}$), brain ($73.3 \pm 33.2 \mu\text{g/g}$) and retina ($392 \pm 81.7 \mu\text{g/g}$) were increased by ~ 1.47 , 2.29 and 7.22 folds, respectively on intraperitoneal VGB treatment compared to control group. Acute intraperitoneal studies demonstrated there was no significant difference in the taurine levels in control and VGB treated animals, which indicates the decrease in taurine levels is not immediate and potentially chronic administrations might lead to taurine deficiency in retinal tissues. The concentrations of VGB, GABA and taurine observed in plasma, brain and retinal homogenate on acute study were shown in Figure 7.

The acute studies after VGB intranasal administration of 40 mg/kg, have shown VGB concentrations in brain ($0.43 \pm 0.22 \mu\text{g/g}$) and no VGB levels were found in retina and plasma. There was negligible change in taurine levels in plasma, retinal and brain on intranasal VGB treatment compared to control group. There was negligible change in GABA levels in plasma and retinal on intranasal VGB treatment compared to control group. There was 2.1-fold increase in GABA levels in brain on intranasal VGB treatment compared to control group. Acute studies have demonstrated on intranasal administration VGB was selectively delivered to brain and there were below detectable levels of VGB in brain and plasma.

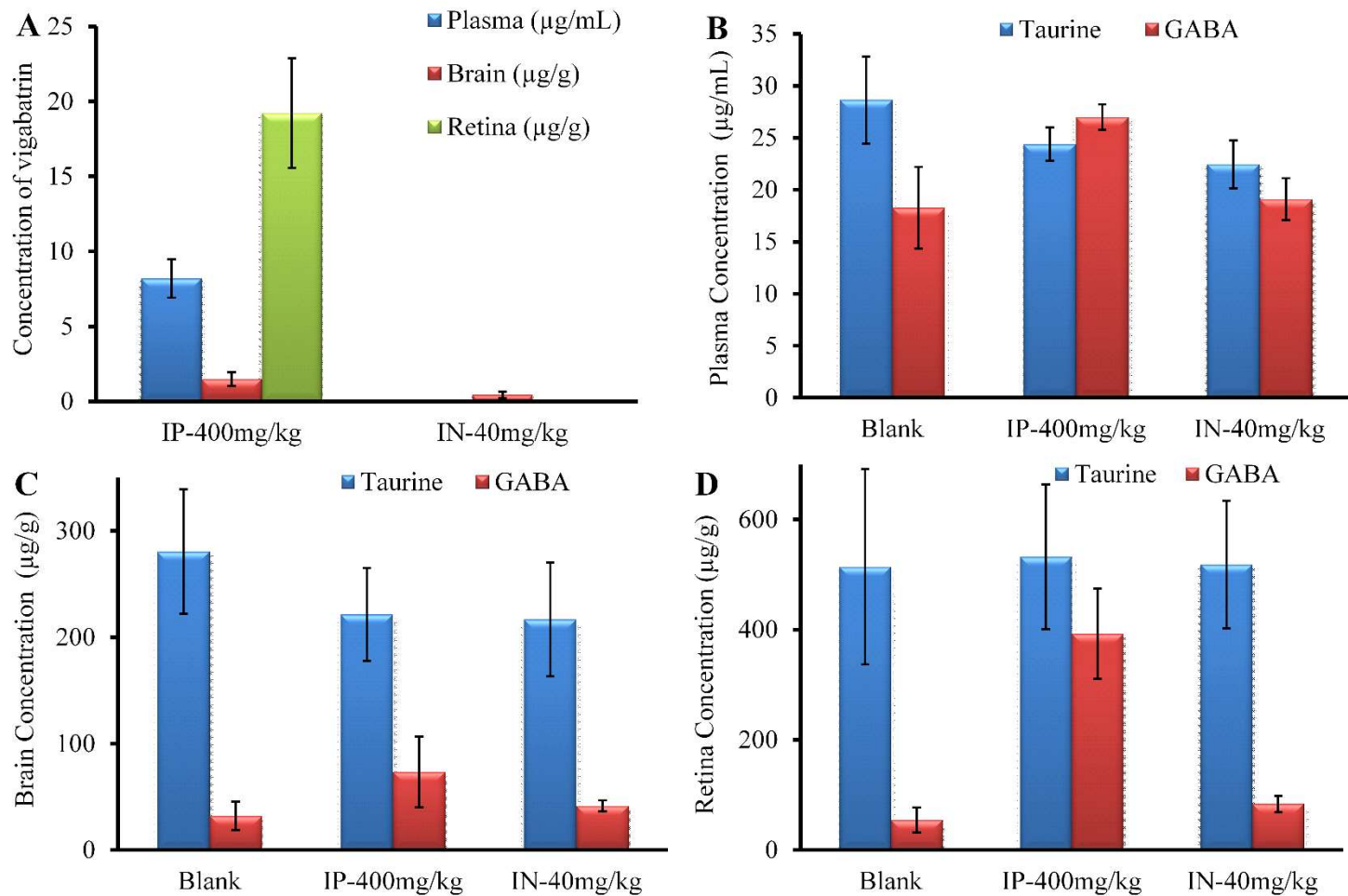


Figure.7 The concentrations of taurine, GABA and vigabatrin in rat plasma, retina and brain at 2 h after single intraperitoneal and intranasal dose of vigabatrin in *Sprague-Dawley* rats (mean ± SD) n=5.

3.6.1.2 Chronic Study

The chronic VGB intraperitoneal administration of 40 mg/kg for 28 days, have shown higher VGB concentrations in retina ($5.54 \pm 1.06 \mu\text{g/g}$) compared to plasma ($2.11 \pm 0.34 \mu\text{g/mL}$) and brain ($0.37 \pm 0.05 \mu\text{g/g}$). The concentration of VGB in retina was ~ 2.62 and 14.9 times higher compared to plasma and brain, respectively. The GABA levels in plasma ($18.0 \pm 5.25 \mu\text{g/mL}$), brain ($79.0 \pm 16.2 \mu\text{g/g}$) and retina ($179 \pm 30.4 \mu\text{g/g}$) were increased by ~ 3.15 , 2.33 and 3.70 folds, respectively on VGB treatment compared to control group. The taurine levels in plasma ($11.6 \pm 0.71 \mu\text{g/mL}$), brain ($66.3 \pm 11.8 \mu\text{g/g}$) and retina ($263 \pm 22.2 \mu\text{g/g}$) were decreased by ~ 1.54 , 2.28 and 2.51 folds, respectively on VGB treatment compared to control group.

The chronic VGB intranasal administration of 40 mg/kg for 28 days, have shown higher VGB concentrations in brain ($0.72 \pm 0.21 \mu\text{g/g}$) compared to plasma ($0.25 \pm 0.07 \mu\text{g/mL}$) and retina ($0.16 \pm 0.10 \mu\text{g/g}$). The concentration of VGB in brain was ~ 2.87 and 4.58 times higher compared to plasma and retina, respectively. The GABA levels in plasma ($9.49 \pm 1.00 \mu\text{g/mL}$), brain ($63.7 \pm 28.0 \mu\text{g/g}$) and retina ($55.5 \pm 6.77 \mu\text{g/g}$) were increased by ~ 1.65 , 1.88 and 1.14 folds, respectively on VGB treatment compared to control group. There was negligible change in taurine levels in plasma, brain and retina, respectively on intranasal VGB treatment compared to control group. The concentrations of VGB, GABA and taurine observed in plasma, brain and retinal homogenate after chronic administration were shown in Figure 8.

The retinal sections of intranasal, intraperitoneal and control group of animals were stained with H&E. The microscopic images of H&E stained retina are presented in Figure 9, labelled areas a, b, c and d represents rods and cones, outer nuclear, inner nuclear and ganglion cell layer, respectively. The negligible change in retinal histology of animals administered with chronic intranasal VGB compared to control group of animals. The retinal histological sections on chronic

intraperitoneal administration of VGB, demonstrates the retinal layers were disrupted, photoreceptors were disorganized and formation of vacuoles in photoreceptor region and inner retinal layer.

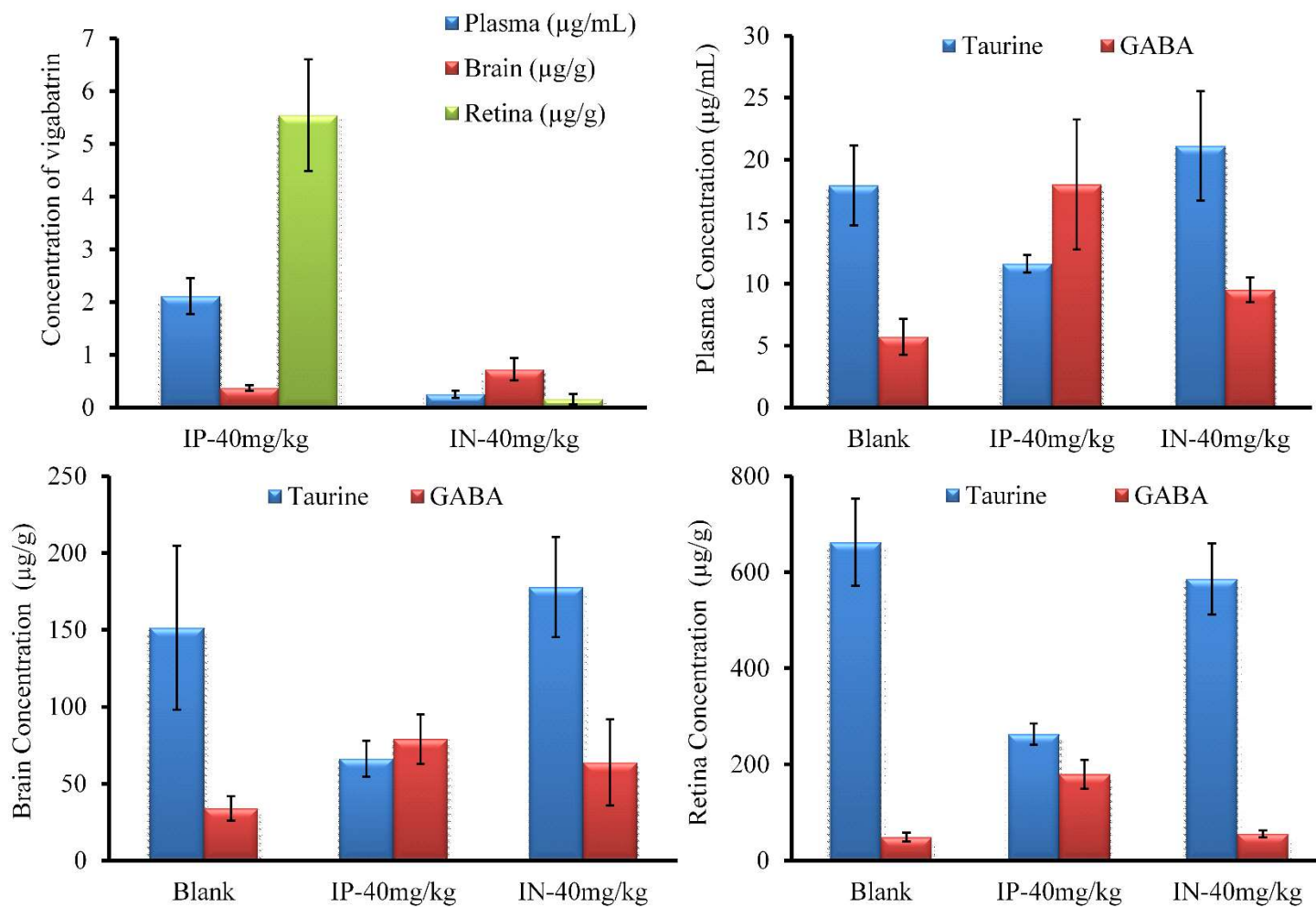


Figure.8 The concentrations of taurine, GABA and vigabatrin in rat plasma, retina and brain at 2 h after 28th day intraperitoneal and intranasal (chronic) dose of vigabatrin in *Sprague-Dawley* rats (mean \pm SD) n=5.

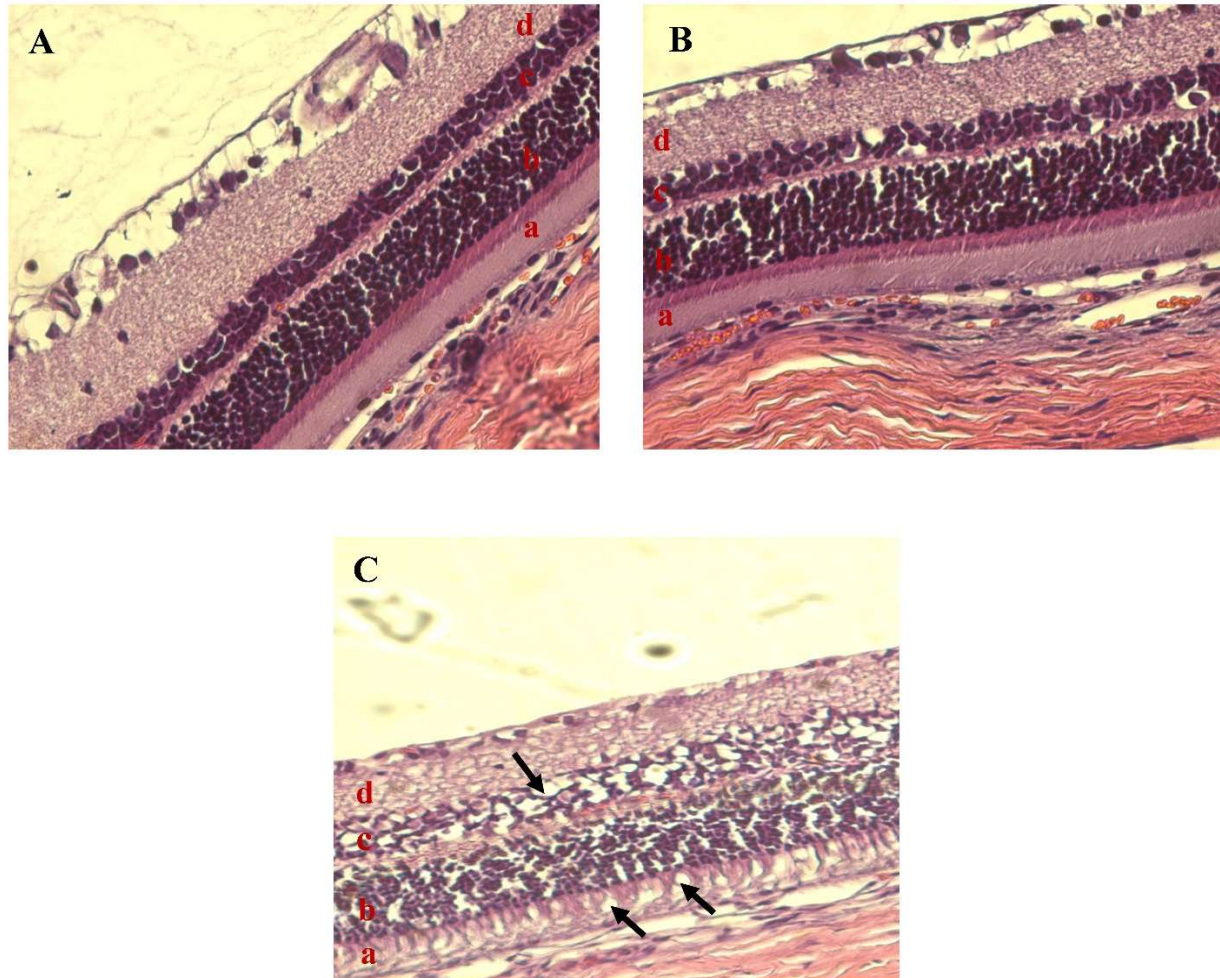


Figure.9 The microscopical image of retinal histology stained with H&E of control (A), intranasal (B) and intraperitoneal (C) group of *Sprague-Dawley* rats.

3.6.2 Vigabatrin antiepileptic activity on intranasal administration

The antiepileptic activity of VGB on intranasal and intraperitoneal administration are presented in Fig 10. The onset time of seizures has been delayed significantly after intraperitoneal and intranasal administration of VGB compared to PTZ control group. There were no seizures in control group of animals administered with saline and the seizure intensity severity score for animals treated with PTZ was 3.4. The seizure intensity of animals treated with intraperitoneal VGB (900 mg/kg) 6 h pre PTZ dose, intranasal VGB (40 mg/kg) 0.5 h pre PTZ dose, intranasal VGB (40 mg/kg) 1 h pre PTZ dose, intranasal VGB (40 mg/kg) 2 h pre PTZ dose and intranasal VGB (40 mg/kg) 4 h pre PTZ dose was decreased by 47.1, 23.5, 17.6, 29.4 and 29.4% compared to PTZ alone treated animals, respectively. The animals treated with intraperitoneal VGB (900 mg/kg) 6 h pre PTZ dose, intranasal VGB (40 mg/kg) 2 h pre PTZ dose, and intranasal VGB (40 mg/kg) 4 h pre PTZ dose, shown significant decrease in seizure intensity compared to PTZ alone treated animals. The animals dosed with 900 mg/kg of VGB intraperitoneally produced maximum antiepileptic activity compared to animals received 40 mg/kg of intranasal VGB dose. However, pharmacodynamic studies demonstrated smaller intranasal dose produced significant antiepileptic activity and duration of action of intranasal VGB was upto 4 h.

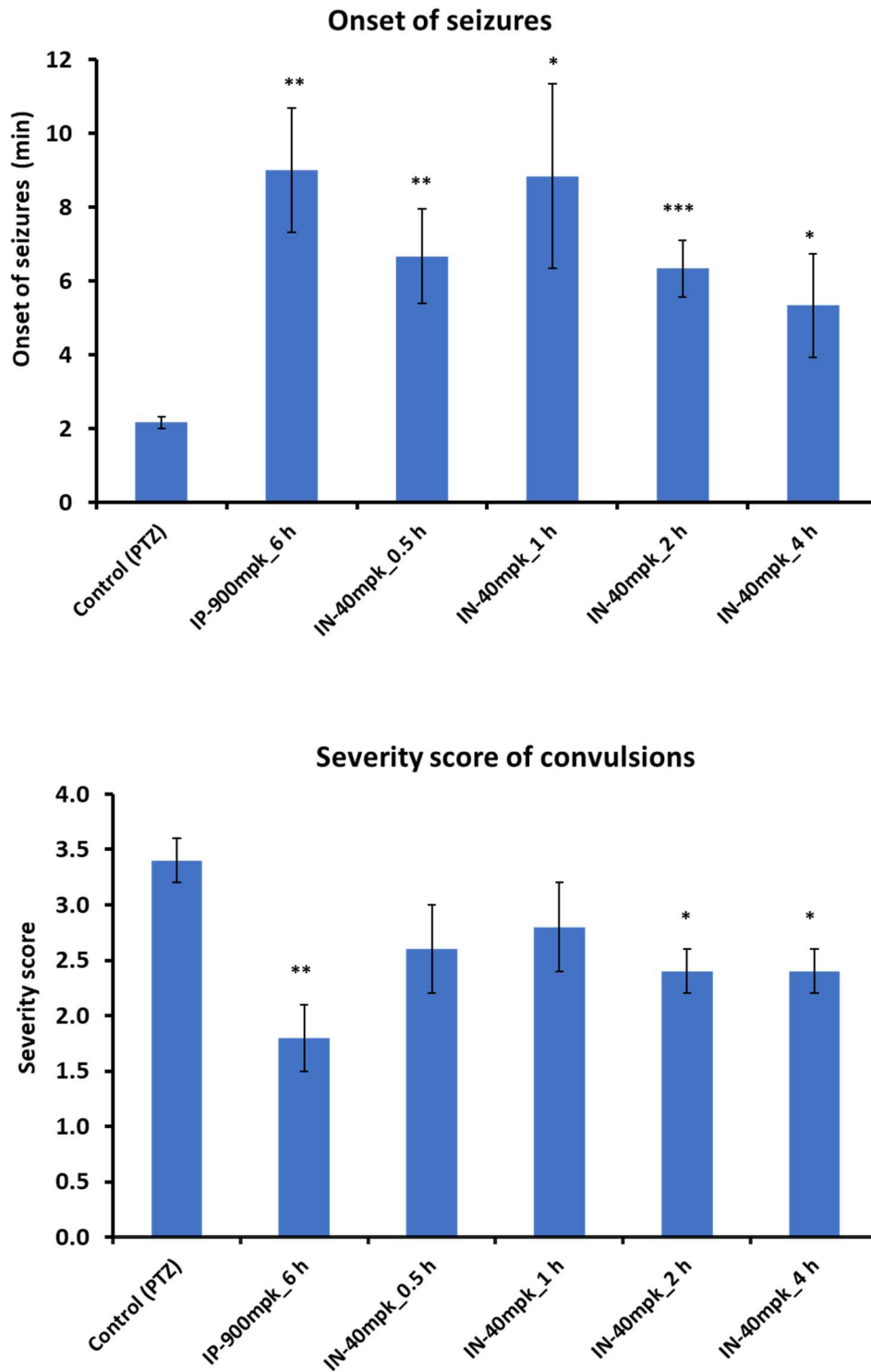


Figure.10 The antiepileptic activity; onset of seizures and severity score of convulsions on intraperitoneal and intranasal dose of VGB.

4. Conclusion

A highly sensitive, specific, and reproducible RP-HPLC method was developed and validated as per USFDA guidelines for simultaneous estimation of VGB, GABA and taurine. This study involves simple protein precipitation extraction method with adequate recovery and requires low sample volume. The NDA method was optimized to produce sensitive and stable derivatized product, this method of derivatization can be used to produce stable derivatized product of other primary amine and amino acid with minor modifications. The method was successfully applied to simultaneously determine the VGB, GABA and taurine concentration in human plasma, rat plasma, brain and retina. The modulatory effects of VGB on GABA and taurine on intraperitoneal and intranasal (acute and chronic administration) of VGB were determined. This HPLC method developed could be applied widely in various clinical and preclinical studies to investigate role of vigabatrin, taurine and GABA levels on vigabatrin induced ocular toxicity. The MBCP gel increased the permeation of VGB across the bovine olfactory mucosa. The chronic study established intranasal administration would be beneficial to increase the VGB levels in brain and decrease the retinal levels, thus VGB induced retinal toxicity can be alleviated. *In vivo* pharmacodynamic studies in epileptic SD rat model has shown intranasal administration of VGB can be potential approach for management of seizure at lower dose.

CHAPTER 3

Role of Taurine Transporter in the Retinal Uptake of Vigabatrin

1. Introduction

Vigabatrin is an anti-epileptic drug of choice for treatment of infantile spasms associated with tuberous sclerosis complex.⁵⁰ In treatment of other complex partial seizures, VGB is used as an adjunct therapy.⁵¹ VGB is γ -vinyl-aminobutyric acid, structural analog of inhibitory neurotransmitter γ -aminobutyric acid. VGB elicits therapeutic activity by suicidal inhibition of GABA-transaminase thereby preventing degradation of GABA and thus increasing their levels at synaptic cleft of neurons.⁵⁰ VGB is a low molecular weight, hydrophilic compound with 60-70% of oral bioavailability and only 10 % of absorbed VGB crosses the blood brain barrier.⁵² On chronic administration of VGB, adults and infants were diagnosed with peripheral atrophy of retinal nerve fiber layer and decreased electroretinogram amplitudes indicating damage to the retina.⁸ Retinal damage causes adverse secondary events leading to bilateral concentric constriction of the visual field and abnormal visual acuity in 30-40% of patients.^{3,8} Baseline visual field testing or electroretinography should be carried out before initiation of treatment and regularly thereafter to monitor the functions of retina.

VGB is approved by USFDA with black box warning for potential benefit, which outweigh the risk of causing permanent concentric visual field defects.⁵³ Preclinical studies of VGB chronic administration have demonstrated ocular toxicity is caused by VGB accumulation

in retina.^{5,6} Accumulated VGB increases GABA concentrations significantly higher in retina compared to brain^{5,14} and studies have reported VGB treatment in rodent models decrease taurine levels in the retina.^{11,13,14} The preclinical studies demonstrated taurine supplementation decreases ocular toxicity on VGB administration.^{12,13,54} Taurine is an antioxidant, plays a major role in neuroprotective activities and taurine deficiency causes retinal degeneration.^{10,55} The mechanism involved in retinal accumulation of VGB and retinal taurine depletion on VGB chronic administration is ambiguous.

The uptake of the drug from circulating blood to ocular tissues is via blood aqueous barrier and the blood retinal barrier. At retinal barrier, lipophilic drugs are transported through ABC transporters, and amino acid mimetic drugs via solute carrier nutrient transporters.⁵⁶ Taurine from circulating blood is transported into ocular tissues through TauT in RPE and inner BRB.⁵⁷ *In vitro* (CaCo2 and MDCK) and *in vivo* rat studies have demonstrated VGB is majorly transported by proton coupled amino acid transporter-1 (PAT1) across the intestinal barrier.⁵⁸⁻⁶⁰ Reported studies have shown PAT1 is involved in cellular influx of zwitterionic amino acids (glycine, proline and alanine), drugs (D-serine, betaine and D-cycloserine), an essential amino acid taurine and neurotransmitter GABA, and its analogues.⁶¹ *In vitro* studies in CaCo2, MDCK, and renal cells have reported taurine transporter (TauT/SLC6a6) is partially involved in uptake of VGB and VGB inhibits taurine cellular uptake.²⁰

The purpose of present study was to evaluate mechanism involved in VGB transport across the blood retinal barrier. The *in vitro* adult retinal pigment epithelium (ARPE-19) cell line studies and *in vivo* studies in Sprague Dawley (SD) rats were used to evaluate the role of TauT in VGB transport into retinal cells. It is crucial to explore the mechanism involved in VGB accumulation and subsequent taurine depletion to determine the cause of associated retinal toxicity. This study

will be beneficial to identify and select approaches to prevent or alleviate VGB induced retinal toxicity.

2. Materials and methods

ARPE-19 cells and Dulbecco's Modified Eagle Medium (DMEM)-F12 were purchased from American Type Culture Collection (Manassas, VA, USA). Fetal bovine serum was purchased from Atlanta Biologics (Flowery Branch, GA, USA). Guanidinoethyl sulfonate was purchased from Cayman Chemical Company (Ann Arbor, MI, USA). Vigabatrin was purchased from Santa Cruz Biotechnology Inc. (Dallas, TX, USA). Culture plates and flasks were purchased from Corning Inc. (Corning, NY, USA). Taurine, GABA and other chemicals were purchased from Sigma Aldrich (St Louis, MO, USA) and used without further purification.

2.1 ARPE-19 Cell culture

ARPE-19 cells used for uptake studies were between passages of 22 and 30. The ARPE-19 cells were maintained at 37 °C in a humidified atmosphere of 5% CO₂ and 90% relative humidity with culture media consisting of D-MEM/F-12 supplemented with 10% fetal bovine serum, penicillin (100 mg/ml) and streptomycin (100 mg/ml). The medium was replaced every other day in flask and when the cells reached 80-90% confluence, cells were detached using Trypsin-EDTA. Detached cells were plated at a density of 0.5 million cells/well in 24-well culture plates. On attaining cell confluence of 90–95% in 24–well plates, the media was aspirated. These cells were washed twice with Dulbecco's phosphate-buffered saline (DPBS) and used for cell uptake studies. All uptake studies were performed by incubating cells with drug containing uptake buffer⁶² at 37 °C for 30 min to get maximum uptake. At the end of 30 min incubation period, buffer

with drug was aspirated and washed with ice cold DPBS three times. After washing, the cells were precipitated by addition of ice-cold acetonitrile and plates were centrifuged at 4000 RPM to extract the intracellular drug. The supernatant was aspirated from the plates and subjected to HPLC analysis.

2.2 ARPE-19 cell uptake studies

The concentration dependent uptake of VGB, GABA and taurine by ARPE-19 cells was evaluated. The cells were incubated with uptake buffer containing different concentrations of VGB (50, 40, 30, 20, 10, 5, 2.5, and 1.25 mM), GABA (20, 10, 5, 2.5, 1.25, 0.625, and 0.312 mM), and taurine (200, 100, 50, 25, 12.5, 6.25, 3.12, and 0.15 μ M) for 30 min at 37 °C. At the end of 30 min incubation period cellular uptake was determined.

2.3 Effect of osmolarity and pH on uptake of VGB

The effect of osmolarity on VGB and taurine uptake were studied. The cells were preincubated for 16 h with hyperosmolar (400 mOsm) uptake buffer containing 50 mM sodium chloride.⁶³ After preincubation, hyperosmolar uptake buffer was aspirated and washed the cells with DPBS twice. These cells were incubated with uptake buffer containing VGB (50 mM) and taurine (0.2 mM) for 30 min at 37 °C. The effect of pH on uptake of VGB was evaluated by incubating the cells with uptake buffer of pH 5.5, 6.5 and 7.5 containing VGB (50 mM) and taurine (0.2 mM) for 30 min at 37 °C. At the end of 30 min incubation period cellular uptake was determined.

2.4 Effect of Guanidinoethyl sulfonate on uptake of VGB

The study was performed to identify the transporter involved in ARPE-19 cellular uptake of VGB. The cells were preincubated with uptake buffer containing different concentrations (50, 40, 30, 20, 10, 5 and 2.5 mM) of TauT inhibitor guanidinoethyl sulfonate (GES)^{64,65} for 30 min. To the preincubated cells VGB (50 mM), GABA (20mM), and taurine (200 μ M) was added and cells were incubated for 30 min at 37 °C. At the end of 30 min incubation period cellular uptake was determined.

2.5 Competitive inhibition of cellular uptake of TauT substrates in ARPE-19 cells

To study VGB interaction with TauT, the uptake experiments were conducted in presence of TauT endogenous substrates. The cells were preincubated with uptake buffer containing VGB, GABA and taurine for 30 min. To the cells preincubated with VGB (10 mM), different concentrations of GABA (20, 10, 5, 2.5, 1.25, 0.625, and 0.312 mM), and taurine (200, 100, 50, 25, 12.5, 6.25, 3.12, and 0.15 μ M) were added and incubated for 30 min to study the effect of VGB on uptake of GABA and taurine. To the cells preincubated with GABA (2 mM), different concentrations of VGB (50, 40, 30, 20, 10, 5, 2.5, and 1.25 mM), and taurine (200, 100, 50, 25, 12.5, 6.25, 3.12, and 0.15 μ M) were added and incubated for 30 min to study the effect of GABA on uptake of VGB and taurine. To the cells preincubated with taurine (50 μ M), different concentrations of VGB (50, 40, 30, 20, 10, 5, 2.5, and 1.25 mM), and GABA (20, 10, 5, 2.5, 1.25, 0.625, and 0.312 mM) were added and incubated for 30 min to study the effect of taurine on uptake of VGB and GABA. At the end of 30 min incubation period cellular uptake was determined.

2.6 Animal Studies

The Animal study was conducted as per study protocol approved by the institutional animal ethical committee at University of Mississippi, School of Pharmacy, Mississippi- 38677, USA. Twenty-four male SD rats of age 7–8 weeks were procured from Envigo and used for assessing the effect of chronic administration of GES and taurine on retinal levels of VGB. The animals were housed in a room, where temperature and humidity were controlled with 12 h light:12 h dark cycle. Animals were divided into four groups each containing 6 animals. The first group of animals were untreated, where they were dosed with normal saline to estimate the basal levels of taurine in retina. The second group of animals was dosed with normal saline for 10 days intravenously and on 10th day animals were dosed with 400 mg/kg of VGB by intraperitoneal route. The third group of animals were dosed with GES at 1 mg/kg intravenously for 10 days and on 10th day animals were dosed with 400 mg/kg of VGB by intraperitoneal route. The fourth group of animals were dosed with taurine at 100 mg/kg orally for 10 days and on 10th day animals were dosed with 400 mg/kg of VGB by intraperitoneal route. On 10th day, after 2 h of dosing animals of all groups were euthanized using Euthasol®, and eyes are enucleated and snap frozen. Retina was isolated at 4 °C and homogenized using phosphate buffered saline and stored at -70 ± 5 °C until bioanalysis.

2.7 Sample Preparation

The samples are analyzed simultaneously for VGB, GABA and taurine using method described in Chapter-2. The samples for analysis were derivatized using 2, 3-Naphthalene dicarboxaldehyde (NDA) derivatization method. Briefly, 20 µL of supernatant of *in vitro* uptake study samples/retinal homogenate were added to derivatizing agent containing 20 µL of potassium cyanide (4 mM) in water, 20 µL of NDA (2.5 mM) in methanol and 180 µL of dibasic potassium

phosphate buffer (pH 6.5). The reaction mixture was incubated at room temperature for 10 min and 20 μ L of 1% glacial acetic acid was added to terminate the reaction. Above reaction mixture was vortexed and 10 μ L of these samples were injected into HPLC.

2.8 HPLC Analysis

Waters HPLC system equipped with Waters 2475 fluorescence detector and Waters 1525 binary pump system was used for analysis. Zorbax Eclipse AAA column (150 \times 4.6 mm, 3.5 μ m; Agilent Technologies) was used as stationary phase, which was maintained at 25 ± 2 °C. The mobile phase consisted of methanol (70%): 10 mM dibasic potassium phosphate at pH 6.5 (30%) with flow rate of 1 ml/min. The VGB, GABA and taurine were analyzed using fluorescence detector at excitation and emission wavelength of 400 nm and 500 nm, respectively.

2.9 Statistical analysis

All study data are expressed as mean \pm S.D of sextuplicate values. The unpaired student t-test or one-way analysis of variance (ANOVA) were used for statistical comparisons of mean values. The data with P value <0.05 were considered as statistically significant. The K_m and V_{max} of substrates and IC_{50} values of inhibitors were calculated using GraphPad Prism version 6.0.

3. Results

3.1 ARPE-19 cell uptake studies

Uptake of VGB, GABA and taurine into ARPE-19 cells was evaluated by quantifying intracellular drug levels after 30 min incubation. ARPE-19 cells are outer blood retinal barrier cells and the entry of drug into cells is guarded by ABC and SLC transporters. The reported studies have proved that GABA and taurine uptake into retinal cells are TauT mediated.⁶⁶⁻⁶⁹ In this study, known substrates GABA and Taurine for TauT are used as positive control for uptake studies.

ARPE-19 cell line studies demonstrate the transport of the VGB, GABA and taurine into cells are concentration dependent. The cellular uptake study curve Figure 1. (A, B and C) displays saturable kinetics indicating VGB, GABA and taurine transport into cells are carrier mediated. The K_m value of VGB, GABA and taurine were calculated using Michaelis-Menten equation for translocation of these molecules into ARPE-19 cells and the K_m value of VGB, GABA and taurine was found to be 13.1 mM, 1.92 mM and 58.72 μ M, respectively.

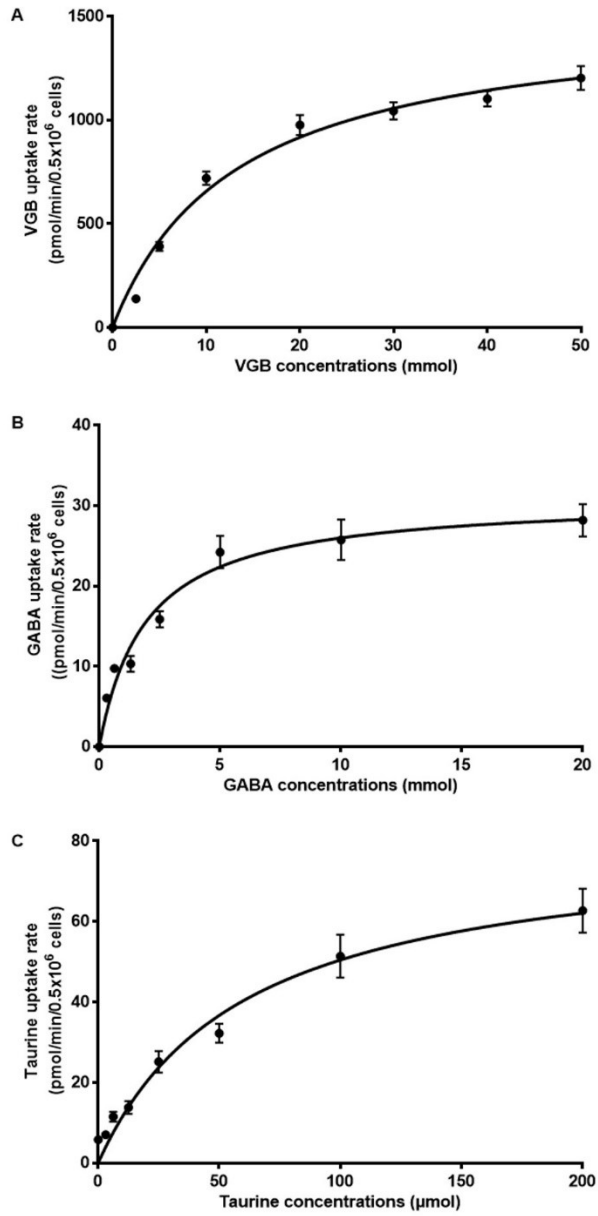


Figure 1. The ARPE-19 cell uptake of (A) VGB, (B) GABA and (C) Taurine at different concentrations (mean \pm SD) n=6.

3.2 Involvement of TauT in VGB uptake by ARPE-19 cells

The expression of TauT in ARPE-19 cells has been demonstrated in previous studies by immunohistochemical experiments,⁷⁰ by ARPE-19 TauT mRNA quantification⁶³ and *in-vitro* experiments were conducted to demonstrate presence of high affinity transport system in ARPE-19 cells.⁶⁸ TauT is Na⁺-Cl⁻ dependent transporter, their expression and/or functionality is dependent on the osmolarity, pH conditions, and presence of TauT substrates or inhibitors.^{57,63,71} In present study taurine was used as positive control as it has higher affinity to TauT and are specifically transported into human RPE cells by TauT.⁷²

3.2.1 Effect of osmolarity and pH on uptake of VGB

To evaluate TauT (Na⁺-Cl⁻ dependent transporter) role in VGB uptake, the cells were incubated in different pH and osmolarity conditions. The results in figure 2 (A and B) depicts uptake of VGB and taurine under hyperosmolar condition was increased significantly by 3.6 and 3.2-fold, respectively compared to iso-osmolar conditions at pH 7.4 (P<0.001, n=6). The results in figure 2C depicts VGB uptake into cells was decreased significantly by 5.8 and 2.6-fold at pH 5.5 and 6.5 compared to pH 7.4, respectively (P<0.001, n=6). The results in figure 2D depicts taurine uptake into cells was decreased significantly by 3.4 and 1.2-fold at pH 5.5 and 6.5 compared to pH 7.4, respectively (P<0.001, n=6). The TauT shows maximum activity at hyperosmolar condition and pH 7.4. At lower pH, VGB and taurine transport across the cell barrier is reduced.³³

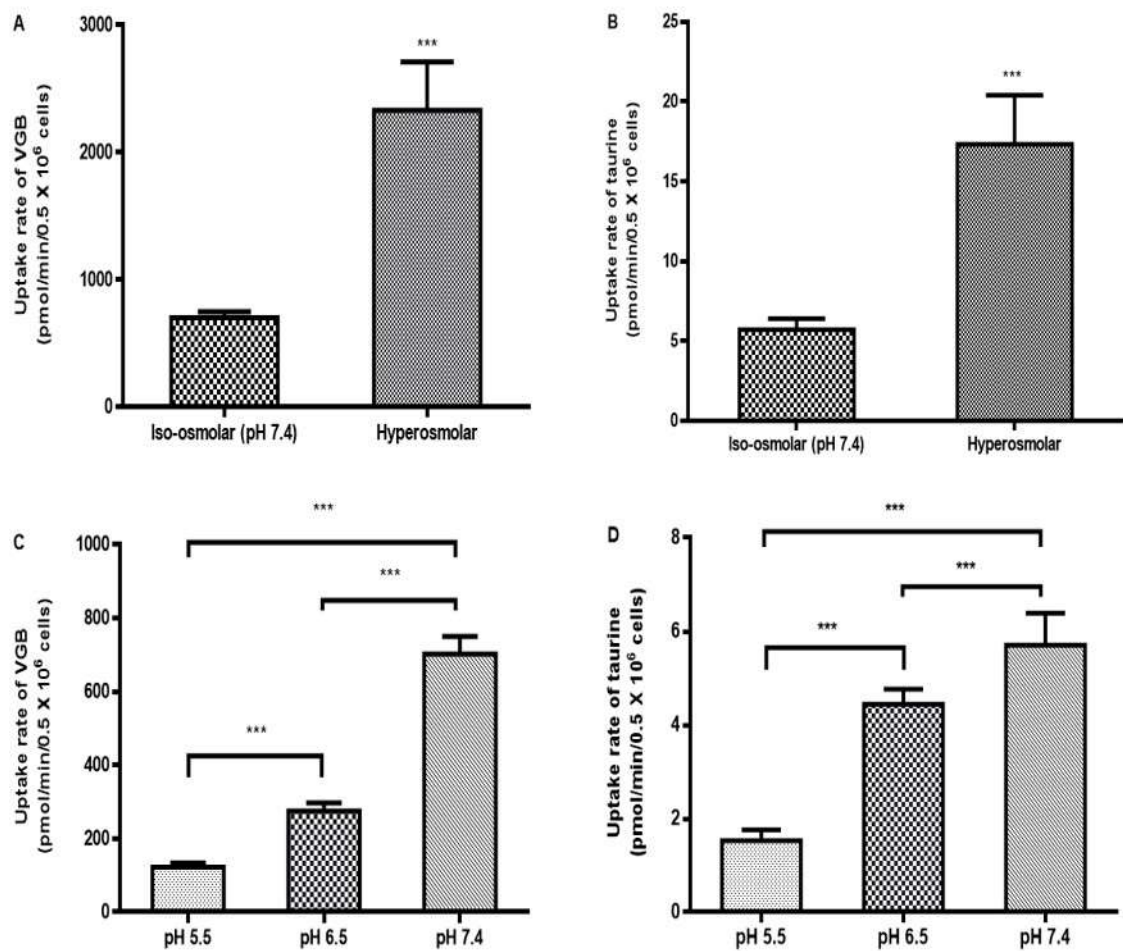


Figure 2. The effect of osmolarity and pH on uptake of (A, C) VGB and (B, D) taurine by ARPE-19 cells. (* $p < 0.05$, ** $p < 0.01$, and *** $p < 0.001$) (mean \pm SD) $n=6$.

3.2.2 Effect of Guanidinoethyl sulfonate on uptake of VGB

Preincubation of cells with GES, a TauT inhibitor decreased the cellular uptake of VGB, GABA and taurine (figure 3). The IC_{50} value of GES was 2.62, 3.48 and 7.49 mM for ARPE-19 cell uptake of VGB, GABA and taurine, respectively. Study results confirms TauT is involved in VGB uptake across ARPE-19 cell barrier.

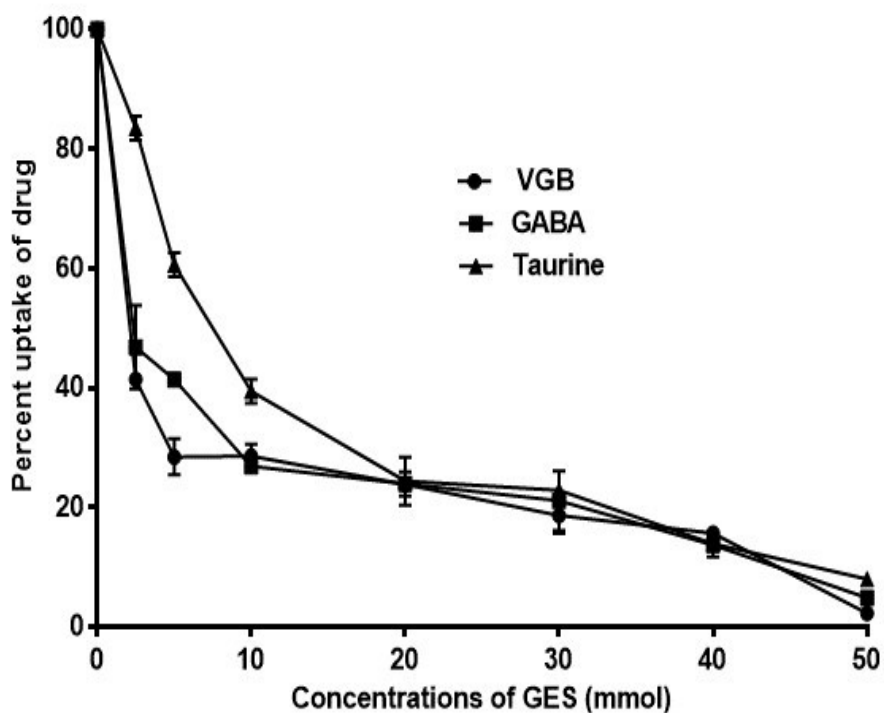


Figure 3. The effect of GES on uptake of VGB, GABA and taurine by ARPE-19 cells (mean \pm SD) n=

3.2.3 Competitive inhibition of cellular uptake of TauT substrates in ARPE-19 cells

Competitive inhibition of ARPE-19 cell uptake of VGB, GABA and taurine were analyzed using Lineweaver-Burk plot. The K_m of vigabatrin 13 mM was significantly increased by 4.86 and 2.10-fold in presence of taurine and GABA, respectively ($P < 0.01$, $n = 6$). The K_m of taurine 60 μM was significantly increased by 4.31 and 3.43-fold in presence of GABA and VGB, respectively ($P < 0.01$, $n = 6$). The K_m of GABA at 1.89 mM was significantly increased by 3.65 and 1.79-fold in presence of taurine and VGB, respectively ($P < 0.01$, $n = 6$). There were no significant changes in V_{max} of VGB, taurine and GABA in presence of each other. The Lineweaver-Burk Plot for uptake of VGB, taurine and GABA in presence of taurine and GABA, GABA and VGB, and taurine and VGB are presented in figure 4. These results indicate VGB is substrate of TauT and VGB competes with GABA, and taurine for ARPE-19 cellular uptake.

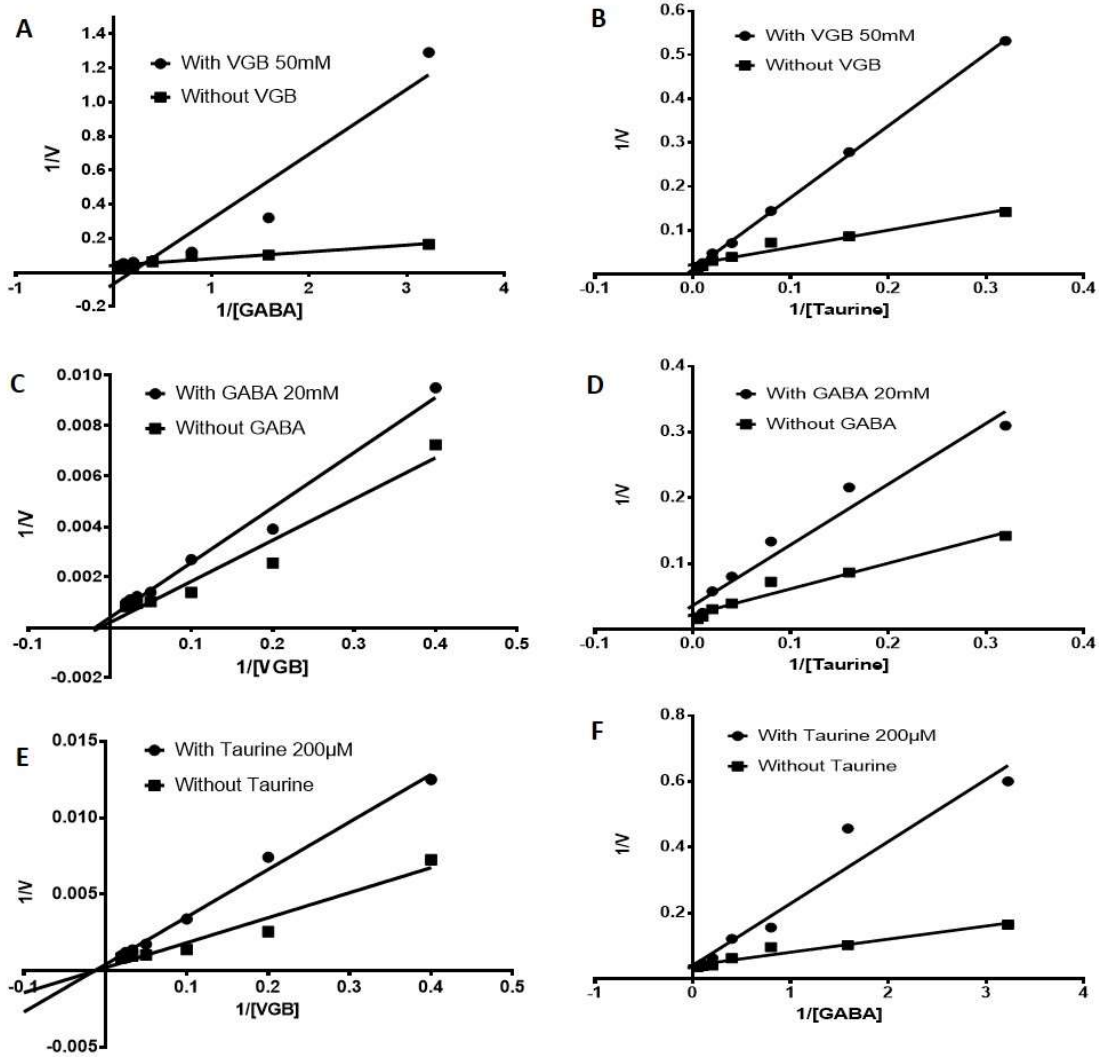


Figure 4. Competitive uptake inhibition (Lineweaver-Burk plot) of VGB, GABA and taurine in ARPE-19 cells. Effect of VGB on uptake of (A) GABA and (B) taurine. Effect of GABA on uptake of (C) VGB and (D) taurine. Effect of Taurine on uptake of (E) VGB and (F) GABA by ARPE-19 cells (mean \pm SD) n=6.

3.3 Animal Studies

In vivo studies in SD rats were performed to confirm TauT involvement in retinal exposure of VGB. On chronic administration of GES at 1 mg/kg, retinal levels of VGB (figure 5) decreased significantly by 1.5-fold ($P < 0.001$, $n = 6$) compared to animals administered with similar dose of VGB alone. On chronic administration of taurine at 100 mg/kg, retinal levels of VGB (figure 5) decreased significantly by 1.3-fold ($P < 0.01$, $n = 6$) compared to animals administered with single similar dose of VGB alone. This study results prove TauT plays a pivotal role in retinal exposure of VGB.

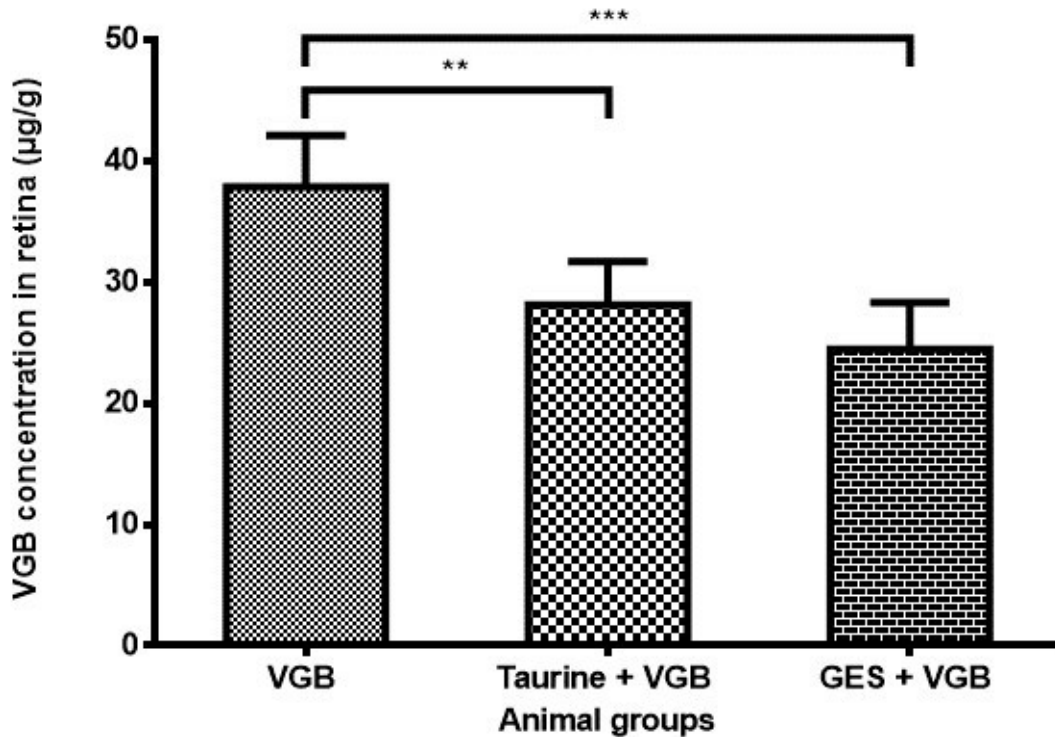


Figure 5. The effect of chronic administration of taurine and GES on retinal exposure of VGB on single dose of VGB 400 mg/kg body weight. (* $p < 0.05$, ** $p < 0.01$, and *** $p < 0.001$) (mean \pm SD) $n = 6$.

4. Discussion

Blood retinal barrier is composed of retinal pigment epithelium (RPE), these cells form tight junctions at lateral surfaces of retina and prevents the inner retinal layer from systemic exposure. RPE plays a major role in supplying nutrients to retina and maintaining ocular homeostasis.⁷³ ARPE-19 is a spontaneously arising retinal pigment epithelium cell line derived from eyes of a male 19-year-old human. RPE-19 cell lines express variety of ABC and SLC transporters and hence used as a potential *in vitro* model for assessing drug and nutrient transport across blood retinal barrier.^{67,74,75} SLC6A6/TauT is a Na⁺-Cl⁻ dependent high affinity taurine transporter expressed in ARPE-19 cells, which is involved in transport of taurine.⁷² Taurine is an abundant amino acid present in retina and plays a crucial role in osmoregulation and neuromodulator effect.⁵⁵ TauT is expressed in brain, retina, liver, intestine and renal tissues. Though TauT is expressed in different tissues, its activity is greater at BRB and transportability of taurine across BRB is 30 times greater than blood brain barrier.⁵⁷

Previous *in vitro* studies using CaCo2 and MDCK studies have proven VGB transport across the cells are mediated by SLC (PAT-1 and partially by TauT).⁷⁶ In the present study, uptake of VGB into ARPE-19 cell was saturable and concentration dependent indicating carrier mediated process was involved in VGB translocation into retinal cells. GABA and taurine are known substrates of TauT in retinal cells and the Km values in present APRE-19 cell line studies are 1.92 mM and 58.72 μM, respectively.

In vitro taurine uptake was inhibited by 30 mM of VGB in MDCK and Caco-2 cell lines, which indicates interaction of VGB with TauT.⁷⁷ We hypothesized that VGB transport across the retinal barrier might also involve TauT. In hyperosmolar conditions taurine levels increase in RPE cells to maintain cell volume homeostasis.⁷⁸ *In vitro* studies have shown ARPE-19 cells cultured

in hyperosmolar conditions increased TauT activity, which maximized the taurine uptake.⁶³ In present study, the effect of hyperosmolarity on VGB uptake into ARPE-19 cells was assessed. VGB uptake was significantly increased compared to iso-osmolar condition. At lower pH, TauT activity has been reported to be lesser than physiological pH conditions.⁷¹ In agreement with the earlier report, the present study demonstrated the decreased uptake of VGB at pH 5.5 in ARPE-19 cells. Whereas, at physiological pH 7.4 the cell uptake of VGB was concentration dependent and saturable. These studies indicate the involvement of TauT in VGB uptake into ARPE-19 cells. Studies reported have shown GABA and GABA mimetics competitively inhibits taurine uptake in retinal and other cell lines,⁷⁶ indicating interaction of TauT in transport of GABA and GABA mimetics. The competitive inhibition study results of GABA and taurine was in accordance with the previous published reports in retinal cell lines, where GABA and taurine were competitively inhibiting the uptake of each other into cells.⁹ The kinetic analysis using Lineweaver-Burk plot demonstrated a increase in the Km of VGB in presence of GABA and taurine with unchanged Vmax, which proves the competitive inhibition in presence of TauT substrates in ARPE-19 cells. The competitive inhibition of VGB, GABA and taurine indicate increased levels of VGB at site of retinal barrier will decrease the uptake of taurine, and vice versa.

On chronic administration of GES in rats, GES produces taurine depletion in retina and other tissues by interacting with its carrier-mediated transport.^{64,65,79} *In vitro* and *In vivo* study results demonstrated VGB uptake into ARPE-19 cells (figure 3) and retinal tissues (figure 5) was inhibited by GES, indicating the involvement of TauT in VGB retinal uptake. On chronic administration of taurine in rats decreased the levels of VGB into retinal tissues (figure 5), demonstrating competitive inhibition of VGB retinal uptake by taurine. Previous studies have reported chronic supplementation of taurine decreased the VGB related ocular toxicity in rats.¹¹

Apparently, these findings from *in vitro* and *in vivo* studies indicate the VGB transport and accumulation into retina is predominantly governed by TauT. The subsequent retinal toxicity is associated with taurine depletion from retina on chronic administration of VGB^{6,13,14} is due to competitive inhibition of taurine retinal uptake by VGB. Further preclinical studies are required to optimize the dose and duration of taurine supplementation to alleviate the VGB induced retinal toxicity.

5. Conclusion

In vitro ARPE-19 cell line and *in vivo* rat studies demonstrate VGB uptake into retinal cells involves TauT. The TauT mediated uptake of VGB was modulated by GABA, taurine and TauT inhibitor. These studies explain mechanism involved in VGB accumulation and subsequent retinal toxicity. The supplementation of taurine will alleviate VGB treatment associated visual complications in infantile spasms, however further preclinical and clinical studies are required to optimize the taurine dosage regimen.

CHAPTER 4

Cytoprotective Effects of Silymarin on Antiepileptic Drug Induced Retinal Toxicity

1. Introduction

Most of the antiepileptic drugs at therapeutic dose cause visual disturbances and retinal neuronal toxicity on chronic treatment^{80,81}. The mechanism of antiepileptic drugs involves modulation of GABA and glutaminergic transmission. An increase in non-synaptic GABA responses and glutamate induced oxidative stress in retinal neuronal tissue produces visual complications and retinal electrophysiological changes. Anti-epileptic drugs, modulating GABAergic system such as vigabatrin, gabapentin, topiramate and tiagabine were selected and all these produces clinical adverse ocular events. Antiepileptic drugs toxicity in retinal cell lines were studied.

Neuroprotective and antioxidant adjuvants would be beneficial for suppressing antiepileptic drug induced retinal toxicity. The extract of *Silybum marianum* comprises of flavonolignan and flavanol mixtures collectively termed as silymarin⁸². Taxifolin, silychristin, silydianin, silybin and isosilybin are the major constituents of extract. Silymarin is used traditional as antidote for amatoxin poisoning and to treat chronic liver disorders (hepatitis and cirrhosis). Silymarin constituents are extensively studied (both *in vitro* and *in vivo*) to evaluate its potential in treatment or management of cancer, hypocholesterolemia and chronic liver diseases⁸³. The therapeutic activity of silymarin is attributed to their antioxidant activity⁸⁴. Silymarin extracts are

one of the most widely used herbal supplements in United States, as no severe adverse events reported on their consumption.

The objective of present study was to evaluate the effects of antiepileptic drug VGB, gabapentin, topiramate and tiagabine on retinal neuronal and retinal epithelial cells. To investigate the potential cytoprotective effect of silymarin and taurine on antiepileptic drug induced retinal toxicity and to establish the probable mechanism of silymarin cytoprotective effect.

2. Methods and Materials

ARPE-19 cells and Dulbecco's Modified Eagle Medium (DMEM)-F12 were purchased from American Type Culture Collection (USA). R28 cells were purchased from Kerabfast, Inc (USA). Bovine calf serum was purchased from GE Healthcare life sciences (USA). Fetal bovine serum (FBS) was purchased from Atlanta Biologics (USA). JC-1 assay kit and Hoechst stain were purchased from Cayman chemical. Viagabtrin and gabapentin was purchased from Santa Cruz Biotech. (USA). Topiramate, hydrogen pyroxide, tiagabine, MTT reagent, Silybin (Silibinin), Silymarin extract and DCHDA reagent were purchased from Sigma-Aldrich (USA). Isosilybin and silychristin was purchased from Tractus Company Limited (England). Silydianin was purchased from ChromaDex Inc. (USA). Taxifolin was purchased from Enzo Life Sciences Inc. (USA). DNA tunnel and LDH assay kit were purchased from Promega Inc. (USA). Culture plates and flasks were obtained from Costar (Corning, USA). All other chemicals were purchased from Sigma Chemical Company (USA) and used without further purification.

2.1 Retinal Cell culture

Retinal cell toxicity of antiepileptic drugs was determined using adult retinal pigmental epithelial (ARPE-19) cells and retinal neuronal (R28) cells.

2.1.1 ARPE-19 cell culture

ARPE-19 cells are adult retinal pigmental epithelial cells. The cells between passages of 22 and 30 were used for uptake studies. The ARPE-19 cells were maintained at 37 °C in a humidified atmosphere of 5% CO₂ and 90% relative humidity with culture media that consisted of D-MEM/F-12 supplemented with 10% fetal bovine serum, penicillin (100 µg/mL) and streptomycin (100 µg/mL).

2.1.2 R28 cell culture

R28 cells are immortal postnatal day 6 rat retinal neuronal cells with characteristics of glial and neuronal cell markers. R28 cells were cultured in Dulbecco's modified Eagle's medium supplemented with 10% bovine calf serum, 3% sodium bicarbonate solution (7.5% stock solution), 1% MEM non-essential amino acids 10X, 1% MEM vitamins 10X, 1% L-glutamine (200mM stock solution) with gentamicin (100 µg/mL) and incubated at 37 °C in 5% CO₂.

In both cell culture studies, media was replaced every other day in flask and when the cells reached 80-90% confluence, cells were detached using Trypsin-EDTA. Detached cells were plated at a density of 0.1 million cells/well on 96-well culture plates and used for studies.

2.2 Cell Viability Assay

Cell viability assays were performed by exposing each well of ARPE-19 and R28 cells to different concentrations of VGB (40, 20, 10, 5, 2.5, 1 and 0.5 mM), gabapentin (40, 20, 10, 5, 2.5, 1 and 0.5 mM), topiramate (50, 25, 12.5, 6.25, 3.62, 1.81 and 0.9 μ M), tiagabine (10, 5, 2.5, 1, 0.5 and 0.25 mM) and hydrogen peroxide (1, 0.5, 0.25, 0.1, 0.05 and 0.025 mM) in six replicates to determine the IC₅₀ (concentration required to kill 50% of total cells incubated). After incubation period of 24 h, cell viability in each well was quantified by using 3-(4,5-dimethylthiazol-2-yl)-2,5-diphenyltetrazolium bromide (MTT) reagent. 20 μ L of MTT reagent solution (5 mg/mL) was added to each well and incubated at 37 °C for 4h. After incubation period, the MTT solution was removed and the purple formazan crystals formed were dissolved by adding 100 μ L of DMSO in each well. Absorbance was determined at 570 nm using a Microplate Reader.

2.3 Nuclear condensation and DNA fragmentation assay

Nuclear condensation and DNA fragmentation are the morphological and biochemical characteristics of apoptosis. The effect of VGB and gabapentin exposure on nuclear condensation of R28 and ARPE-19 cells was evaluated using Hoechst 33258 stain. On R28 and ARPE-19 cells attaining 80-90% confluence, the R28 and ARPE-19 cells were exposed to vigabatrin and gabapentin at 20mM concentration in serum free media for 24 h at 37 °C. After incubation period the media was aspirated and washed cells with PBS. The cells were treated with Hoechst's stain and incubated in dark for 10 min at room temperature. The staining solution was removed, and cells were washed with PBS two times. The bright field and fluorescence microscopy images using DAPI filter were captured using Olympus microscope equipped with camera.

The effect of vigabatrin and gabapentin exposure on DNA of R28 and ARPE cells were detected using Dead End™ Fluorometric TUNEL System. The ARPE-19 and R28 cells were exposed to different concentrations of VBG (20, 10, 5, 2.5, 1 and 0.5 mM) and gabapentin (20, 10, 5, 2.5, 1 and 0.5 mM) for 24 h at 37 °C in 5% CO₂ in six replicates to determine the concentration dependent effect on DNA fragmentation. After incubation period, the cells were washed with PBS two times and processed to detect DNA fragmentation induced by vigabatrin and gabapentin. The DNA fragmentation in cells were detected by employing the method described by Promega (Dead End™ Fluorometric TUNEL System kit supplier). Briefly, the cells were fixed in 96 well plate using freshly prepared 4% methanol free formaldehyde solution in PBS for 25 min at 4 °C. The cells were washed with PBS three times and cells were permeabilized by treating with 0.2% Triton® X-100 solution in PBS for 5 min. These cells were washed with PBS three times and incubated for 10 min at room temperature with equilibration buffer. The Terminal Deoxynucleotidyl Transferase, recombinant enzyme (rTdT) was added to each well and incubated for 60 min at 37 °C. The reaction was terminated by addition of 2X SSC solution and incubating for 15 min at room temperature. The cells were washed with PBS for 3 times to remove the unincorporated fluorescein-12-dUTP and cells were stained with Hoechst's stain as mentioned above to visualize the nuclei. The cells were visualized to detect the fragmented DNA with Olympus fluorescence microscope using DAPI and GFP filters equipped with camera.

2.4 Mitochondrial membrane potential assay

Mitochondrial membrane integrity is an important parameter of mitochondrial function and indicates the cell health. 5,5',6,6'-tetrachloro-1,1',3,3'-tetraethylbenzimidazolylcarbocyanine iodide (JC-1) is a cytofluorimetric lipophilic cationic dye used to evaluate the difference in mitochondrial membrane potential. JC-1 enters the mitochondria of healthy cells and forms aggregates with emission of red fluorescence. In unhealthy cells, JC-1 remain in monomeric form with emission of green fluorescence. This study was performed to evaluate the early apoptosis induced by vigabatrin and gabapentin using JC-1 mitochondrial membrane potential detection kit. The ARPE-19 and R28 cells were exposed to different concentrations of VBG (50, 25, 12.5, 6.25, 3.62, 1.81 and 0.9 mM) and gabapentin (50, 25, 12.5, 6.25, 3.62, 1.81 and 0.9 mM) in six replicates to determine the concentration dependent effect on mitochondrial membrane potential of cells. After incubation period of 24 h, the cells were washed with DPBS two times and treated with JC-1 reagent for 30 min at 37° C in 5% CO₂. Cells were washed and measured on a fluorescence multi well plate reader at two different set of wavelengths at excitation/emission 540/570 nm (red fluorescence for healthy cells) and 485/535 nm (green fluorescence for unhealthy/apoptotic cells). The cells were pretreated with silymarin and taurine, to study their effect on VGB and gabapentin induced mitochondrial membrane potential changes.

2.5 Detection of Reactive oxygen species generation

The ROS generation by antiepileptics and hydrogen peroxide was estimated in ARPE19 and R-28 cells by using the fluorescent dye 2,7- dichlorodihydrofluorescein diacetate (DCFDA). DCFDA hydrolyses in presence of reactive oxygen species and produces fluorescent dichlorodihydrofluorescein DCF. The amount of DCF produced is proportional to the amount of

ROS present. On cells attaining the 80-90% confluence, cells were washed with Dulbecco's phosphate buffered saline (DPBS) and incubated with 0.5 mM of DCFDA in DPBS for 1 h at 37 °C. R28 Cells were washed with DPBS and incubated with 25 mM VGB, 15 mM gabapentin and 0.1 hydrogen peroxide in serum free media for 24 h at 37°C. ARPE-19 Cells were washed with DPBS and incubated with 25 mM VGB, 50 mM gabapentin and 0.3 hydrogen peroxide in serum free media for 24 h at 37°C. Cells were washed and measured on a fluorescence multi well plate reader setting the wavelength at excitation 485 nm, and emission 530 nm. The effect of silymarin and taurine on ROS generated by VBG, gabapentin and hydrogen peroxide were evaluated. The ARPE-19 and R28 cells (pretreated with DCFDA for 60 min) were treated to VGB, gabapentin and hydrogen peroxide in presence of taxifolin (100 µM), silychristin (100 µM), silydianin (100 µM), silybin (100 µM), isosilybin (100 µM) and taurine (10 mM).

2.6 Cytoprotective effect

Cytoprotective effect of silymarin and taurine were evaluated by exposing each well of ARPE and R28 cells to different concentrations of taxifolin, silychristin, silydianin, silybin, isosilybin (200, 100, 50, 25, 10 and 5 µM) and taurine (20, 10, 5, 2.5, 1 and 0.5 mM) along with IC₅₀ concentrations of VGB, gabapentin and hydrogen peroxide in six replicates. After incubation period of 24 h, cell viability in each well was quantified by using MTT reagent and absorbance was determined at 570 nm using a Microplate Reader.

2.7 Statistical Analysis

Data from *in vitro* cell line studies were subjected to statistical analysis by ANOVA (Tukey's Multiple Comparison Test for comparing between pairs of data) using the GraphPad Prism version 3.00 statistics program (GraphPad Software, Inc., San Diego, CA). P values less than 0.05 were considered statistically significant.

3. Results and discussion

3.1 Cell Viability Assay

The viability of R28 and ARPE-19 cells on exposure to VGB, gabapentin, tiagabine, topiramate and hydrogen peroxide (positive control) was assessed using the MTT reagent solution. The percentage viability of R28 cells after 24 h exposure of VGB (40 mM), gabapentin (40 mM), tiagabine (50 μ M), topiramate (10 mM) and hydrogen peroxide (0.25 mM) was 48.0, 4.04, 73.7, 79.7 and 2.05 %, respectively (Figure 1). At 24 h of exposure to VGB, gabapentin and hydrogen peroxide the viability of R28 cells were decreased with increasing concentrations and the IC₅₀ was 37.5, 13.7 and 0.10 mM, respectively.

The percentage viability of ARPE-19 cell on 24 h exposure of VGB (50 mM), gabapentin (50 mM), tiagabine (50 μ M), topiramate (10 mM) and hydrogen peroxide (0.5 mM) was 47.7, 67.9, 73.7, 80.2 and 9.49 %, respectively (Figure 2). At 24 h of exposure to VGB, gabapentin and hydrogen peroxide the viability of ARPE-19 cells were decreased with increasing concentrations and the IC₅₀ was 27.5, 73.5 and 0.31 mM, respectively. The VGB, gabapentin was found to be toxic for both cell lines in concentration dependent manner compared to topiramate and tiagabine. VGB and gabapentin were further studied to determine mechanism of retinal cell toxicity.

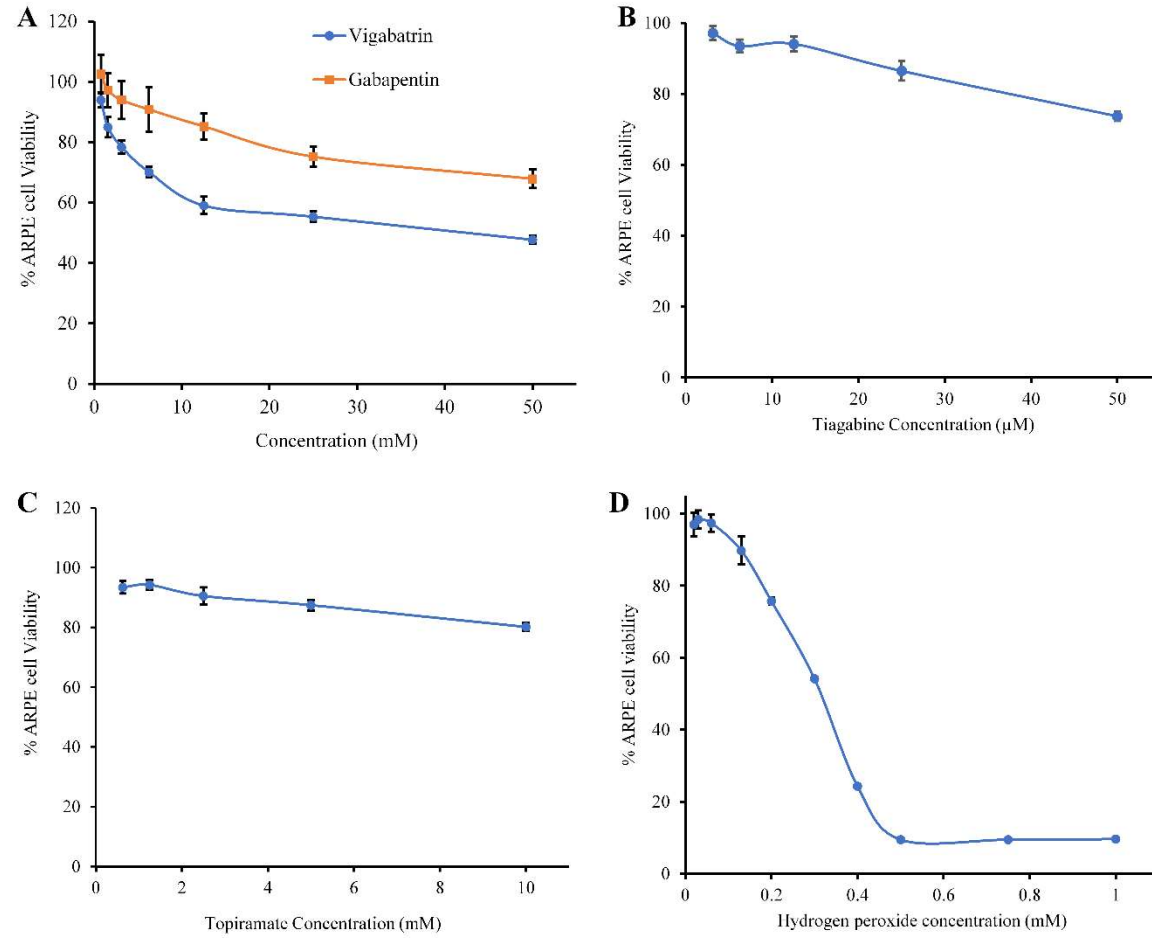


Figure 1. Effect of varying concentrations of vigabatrin(A), gabapentin(A), tiagabine(B), topiramate(C) and hydrogen peroxide(D) exposure on viability of R28 cells (mean \pm SD) n=6.

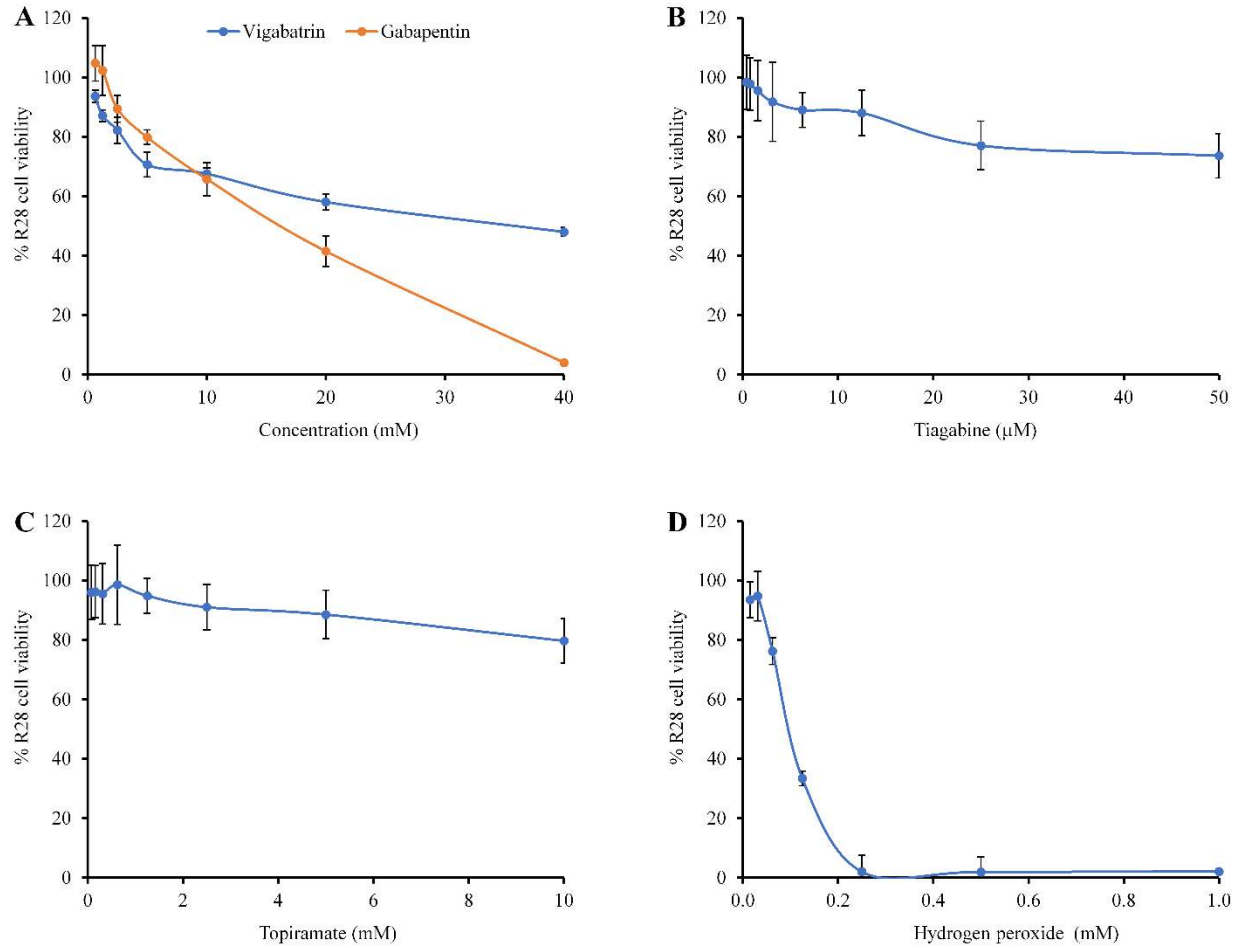


Figure 2. Effect of varying concentrations of vigabatrin(A), gabapentin(A), tiagabine(B), topiramate(C) and hydrogen peroxide(D) exposure on viability of ARPE-19 cells (mean \pm SD) n=6.

3.2 Nuclear condensation and DNA fragmentation assay

Apoptosis is programmed cell death with biochemical features including loss of membrane asymmetry, membrane blebbing, increase in caspase activity, decrease in mitochondrial membrane potential, chromosome condensation (pyknosis), DNA fragmentation (karyohexis), DNA laddering and the eventual engulfment of the cell by phagosomes⁸⁵.

The condensation of cell nuclei was captured by fluorescence microscope, blue fluorescent Hoechst 33258 is a cell permeable nucleic acid dye used to identify condensed nuclei by staining⁸⁶. The morphological observation in the cell nuclei of R28 and ARPE-19 cells after 24 h treatment with or without vigabatrin and gabapentin showed significant morphological alterations when compared to untreated control. ARPE-19 and R28 cells nuclear condensation was showed in figure 3 and 4, respectively. As observed in figures 3 A and B, the control or untreated cells appeared to be intact oval shape and the nuclei were stained with a less bright blue fluorescence (due to the Hoechst 33258 dye). Cells treated with VGB and gabapentin exhibited typical features of apoptosis such as chromatin condensation. The condensed or fragmented chromatin were emitting fluorescence in cells depicting vigabatrin (Figure 3 C and D) and gabapentin (Figure 3 E and F) induced cell apoptosis. The cells treated with taxifolin, silychristin, silydianin, silybin, isosilybin and taurine along with VGB and gabapentin had no condensed nuclei indicating the drugs prevented apoptosis and decreased cell toxicity.

The DeadEnd™ Fluorometric TUNEL (Terminal deoxynucleotidyl transferase dUTP) System was used for specific detection of R28 and ARPE-19 apoptotic cells. The fragmentation of DNA is an important event in apoptosis of cell. The DeadEnd™ Fluorometric TUNEL System incorporates fluorescein-12-dUridine triphosphate at 3'-OH DNA end of fragmented DNA of apoptotic cells using the Terminal Deoxynucleotidyl Transferase recombinant enzyme⁸⁷. The cells

treated with VGB and gabapentin increased the TUNEL-positive cells proportional to the concentration of VGB and gabapentin compared to untreated cells. The apoptotic cells were differentiated from late stages of necrotic cell death, by merging the Hoechst stain and labelled with TUNEL system. The nuclear Hoechst's stain accurately discriminated apoptotic cells from cells that are in late-stage necrosis (Figure 5 and 6). The cells pretreated with taxifolin, silychristin, silydianin, silybin and isosilybin depicted cells with nuclear condensation and fragmented DNA were decreased compared to cells treated with VGB and gabapentin alone.

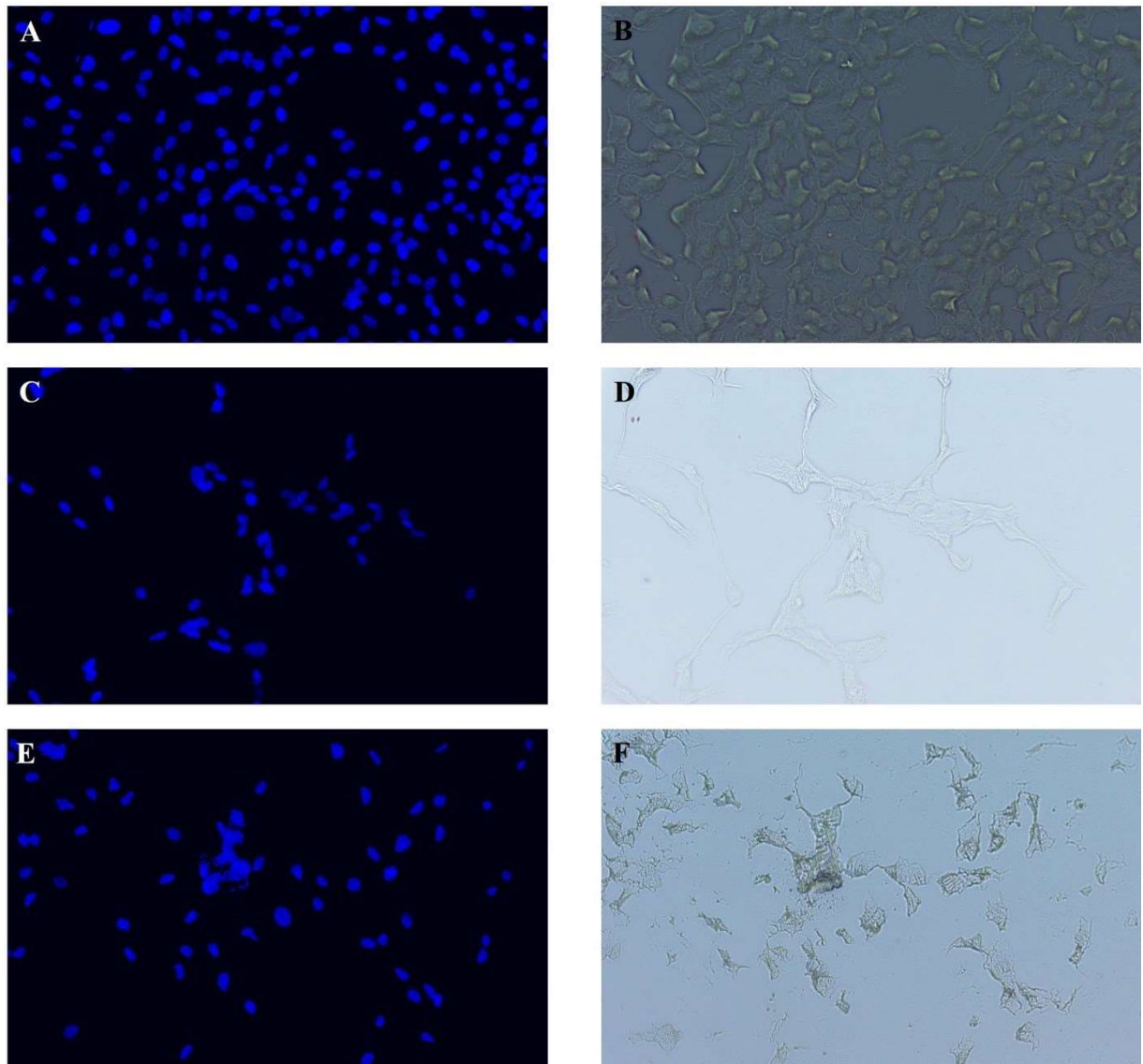


Figure 3. Representative DAPI and bright field fluorescence images show morphological changes of ARPE-19 cells detected with staining of Hoechst 33258. The images of cells untreated (A&B), treated with 25 mM vigabatrin (C&D) and 50 mM Gabapentin (E&F) for 24 h and imaged by fluorescence microscope (magnification 10X).

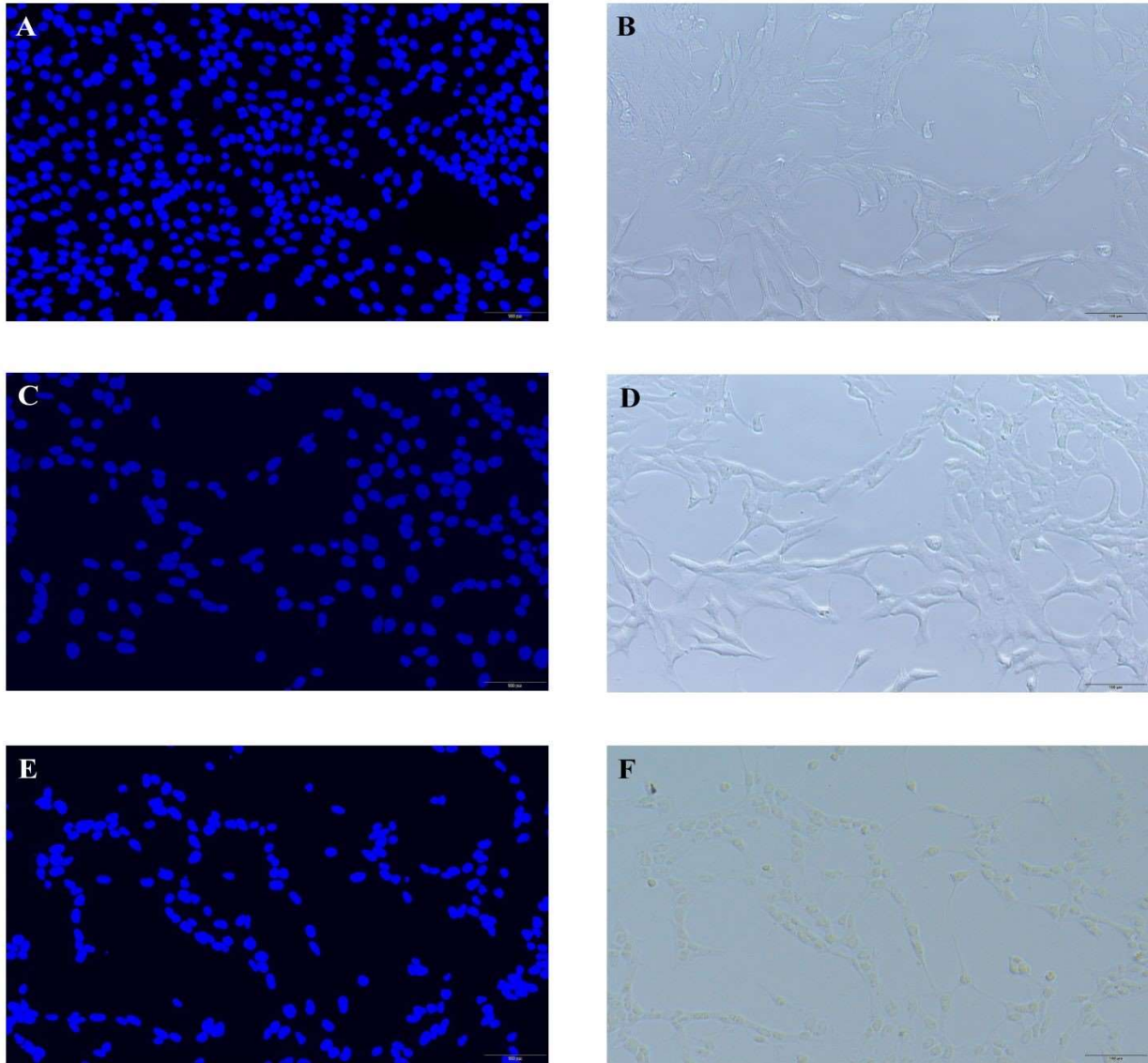


Figure 4. Representative DAPI and bright field fluorescence images show morphological changes of R28 cells detected with staining of Hoechst 33258. The images of cells untreated (A&B), treated with 25 mM vigabatrin (C&D) and 15 mM Gabapentin (E&F) for 24 h and imaged by fluorescence microscope (magnification 10X).

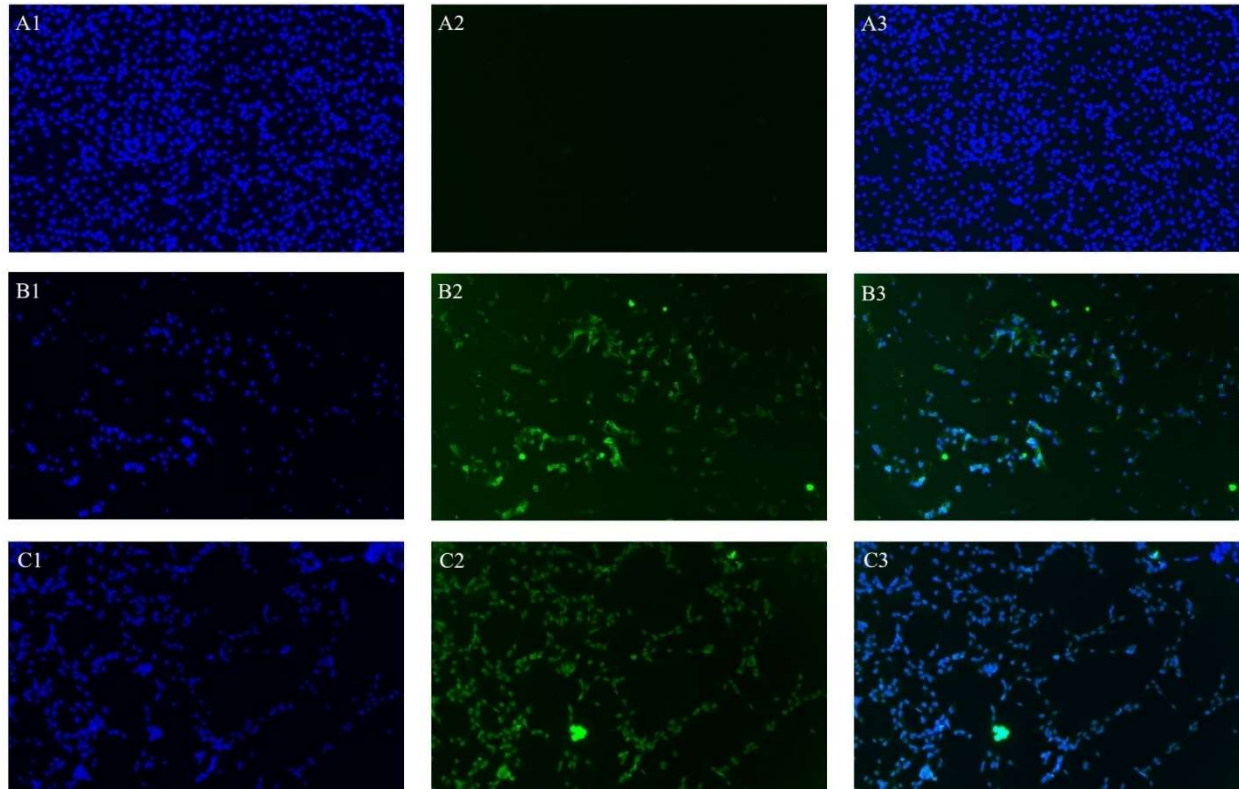


Figure 5. Representative DAPI and GFP fluorescence images show morphological changes of ARPE-19 cells detected by staining with Dead end TUNEL system and Hoechst 33258. The images of untreated cells (A1-A3), treated with vigabatrin (B1-B3) and Gabapentin (C1-C3) for 24 h and imaged by fluorescence microscope (magnification10X).

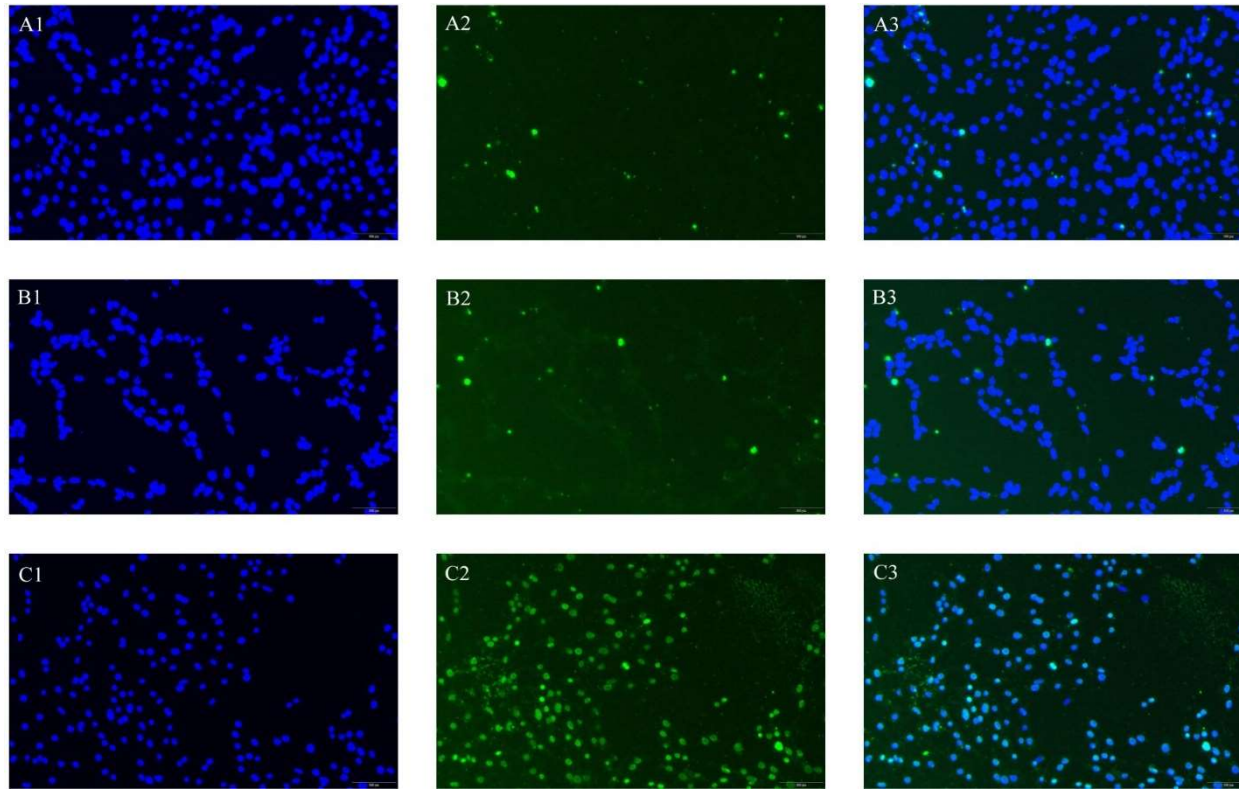


Figure 6. Representative DAPI and GFP fluorescence images show morphological changes of R28 cells detected by staining with Dead end TUNEL system stain and Hoechst 33258. The images of untreated cells (A1-A3), treated with vigabatrin (B1-B3) and Gabapentin (C1-C3) for 24 h and imaged by fluorescence microscope (magnification 10X).

3.3 Mitochondrial membrane potential assay

During normal cell conditions mitochondria maintains electrochemical proton gradient across their membrane. The mitochondria are electronegative, membrane potential facilitates the entry of cations and thus accumulation of cations in mitochondria favors synthesis of ATP. During the apoptosis of cells, mitochondrial membrane is compromised and there is formation of pore leading to decrease in membrane potential⁸⁸. Hence, this mitochondrial membrane potential is used as an indicator of cell health and to detect the apoptotic cells.

JC-1 dye is a cationic, lipophilic dye have a potential to enter healthy mitochondria and form an aggregate to produce red-fluorescence, which can be analyzed at excitation and emission wavelength of 540 and 570nm, respectively. In apoptotic cells, there is decrease in mitochondrial membrane potential and JC-1 stains remain in cytosol in their monomeric form producing green-fluorescence, which can be analyzed at excitation and emission wavelength of 480 and 530nm, respectively. The ratio of J-aggregates to J-monomers in ARPE-19 cells treated with VGB and gabapentin were inversely proportional to the concentration of VGB and gabapentin treated to cells (Figure. 7). The ratio of J-aggregates to J-monomers in cells pretreated with taxifolin (50 μ M), silychristin (50 μ M), silydianin (100 μ M), silybin (50 μ M), isosilybin (50 μ M) and taurine (10 mM) were increased in presence of VGB and gabapentin (Table. 2). These study results demonstrate silymarin and taurine protects the cells from apoptosis induced by VGB and gabapentin. In R28 cells, negligible changes in the ratio of J-aggregates to J-monomers cells were observed when treated with VGB and gabapentin (Figure. 8). Negligible changes in mitochondrial potential could be due to R28 cell death caused by necrotic pathway.

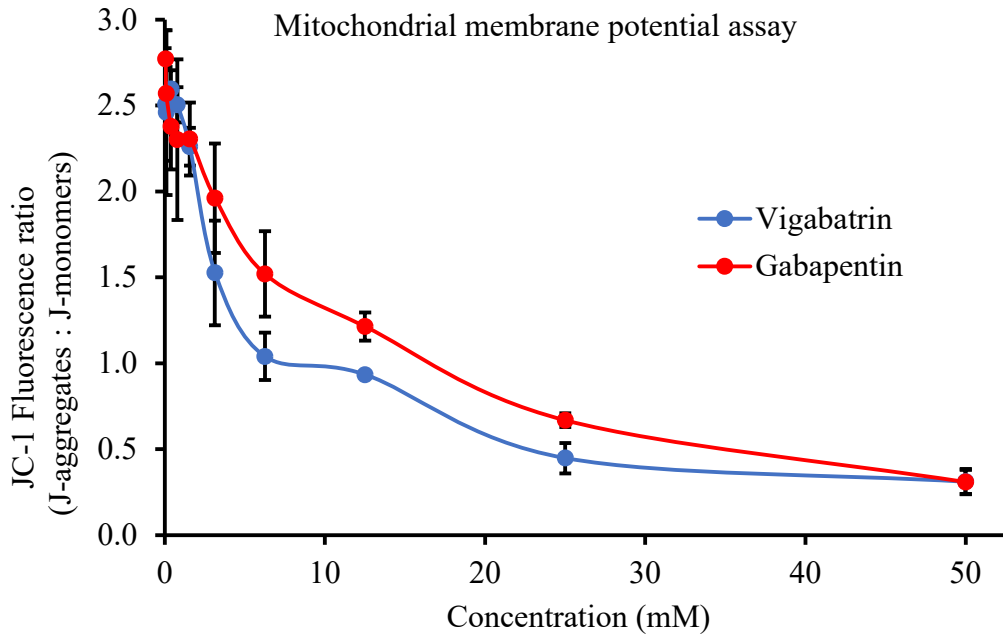


Figure 7. Concentration dependent effect of vigabatrin and gabapentin on ratio of J-aggregates to J-monomers in ARPE-19 cells (mean \pm SD) n=6.

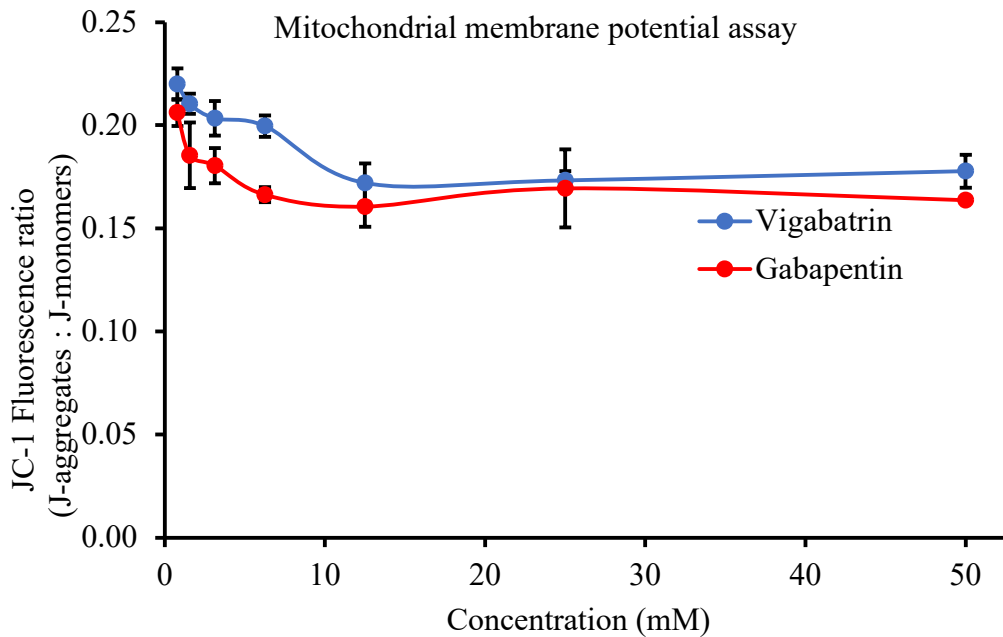


Figure 8. Concentration dependent effect of vigabatrin and gabapentin on ratio of J-aggregates to J-monomers in R28 cells (mean \pm SD) n=6.

Table 2. Effect of silymarin and taurine on changes in ratio of J-aggregates to J-monomers in ARPE-19 cells produced by vigabatrin and gabapentin (mean \pm SD) n=6.

Drug treatment	Ratio of J-aggregates to J-monomers in ARPE-19 cells	
	Vigabatrin (25 mM)	Gabapentin (25 mM)
Taxifolin (50 μ M)	1.49 \pm 0.19	1.25 \pm 0.08
Silychristin (50 μ M)	1.79 \pm 0.08	1.33 \pm 0.21
Silydianin (100 μ M)	1.38 \pm 0.13	1.14 \pm 0.17
Silybin (50 μ M)	1.88 \pm 0.07	1.58 \pm 0.29
Isosilybin (50 μ M)	1.61 \pm 0.11	1.80 \pm 0.31
Taurine (10 mM)	1.15 \pm 0.06	0.83 \pm 0.10
No pretreatment	0.44 \pm 0.09	0.67 \pm 0.04
Blank	2.51 \pm 0.32	2.77 \pm 0.17

3.4 Detection of Reactive oxygen species generation

The amount of reactive oxygen species produced by R28 and ARPE-19 cells on exposure to VGB, gabapentin and hydrogen peroxide was estimated using the oxidant-sensing fluorescent probe 2',7'-dichlorodihydrofluorescein diacetate (DCFH-DA). DCFH-DA is a lipophilic dye converted to its nonfluorescent polar derivative DCFH by esterase present in cells and these derivative gets oxidized to highly fluorescent DCF by intracellular ROS and other peroxides⁸⁹.

The ROS in ARPE-19 and R28 cells treated with hydrogen peroxide at 0.3- and 0.1-mM concentration, respectively was considered as 100 %. The ROS in ARPE-19 cells treated with vigabatrin (25 mM) and gabapentin (50 mM) was 92.4 % and 73 %, respectively. The vigabatrin induced ROS in ARPE-19 cells pretreated with silymarin and taurine were decreased significantly as shown in Figure 9, in following order, taxifolin > silydianin > silybin > silychristin > isosilybin > taurine. The ROS in R28 cells treated with vigabatrin (25 mM) and gabapentin (15 mM) was

83.1 % and 73 %, respectively. The vigabatrin induced ROS in R28 cells pretreated with silymarin and taurine were decreased significantly as shown in Figure 10, in following order, taxifolin > silybin > silychristin > isosilybin > silydianin > taurine. The antioxidants silymarin protected R28 cells from ROS highly efficiently compared to taurine.

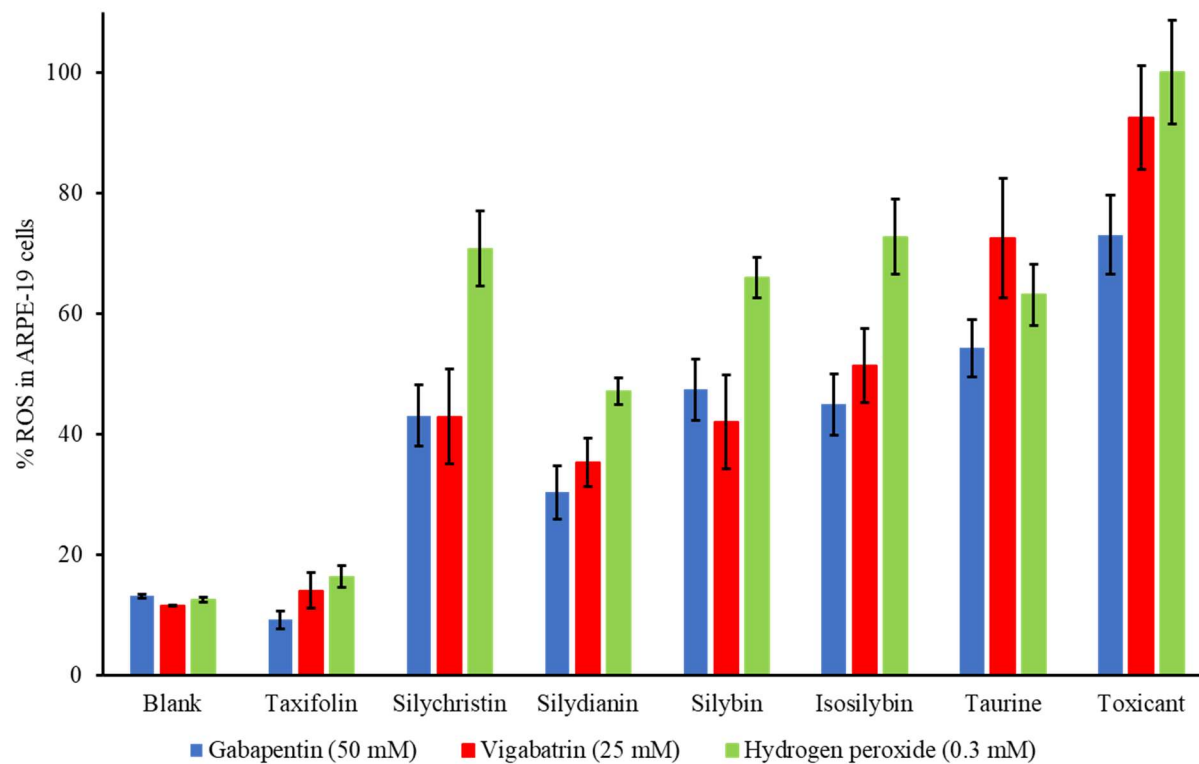


Figure 9. Effect of taxifolin (100 μ M), silychristin (100 μ M), silydianin (100 μ M), silybin (100 μ M), isosilybin (100 μ M) and taurine (10 mM) on ROS generated by gabapentin (25 mM), vigabatrin (50 mM) and hydrogen peroxide (0.3 mM) exposure in ARPE-19 cells (mean \pm SD) n=6.

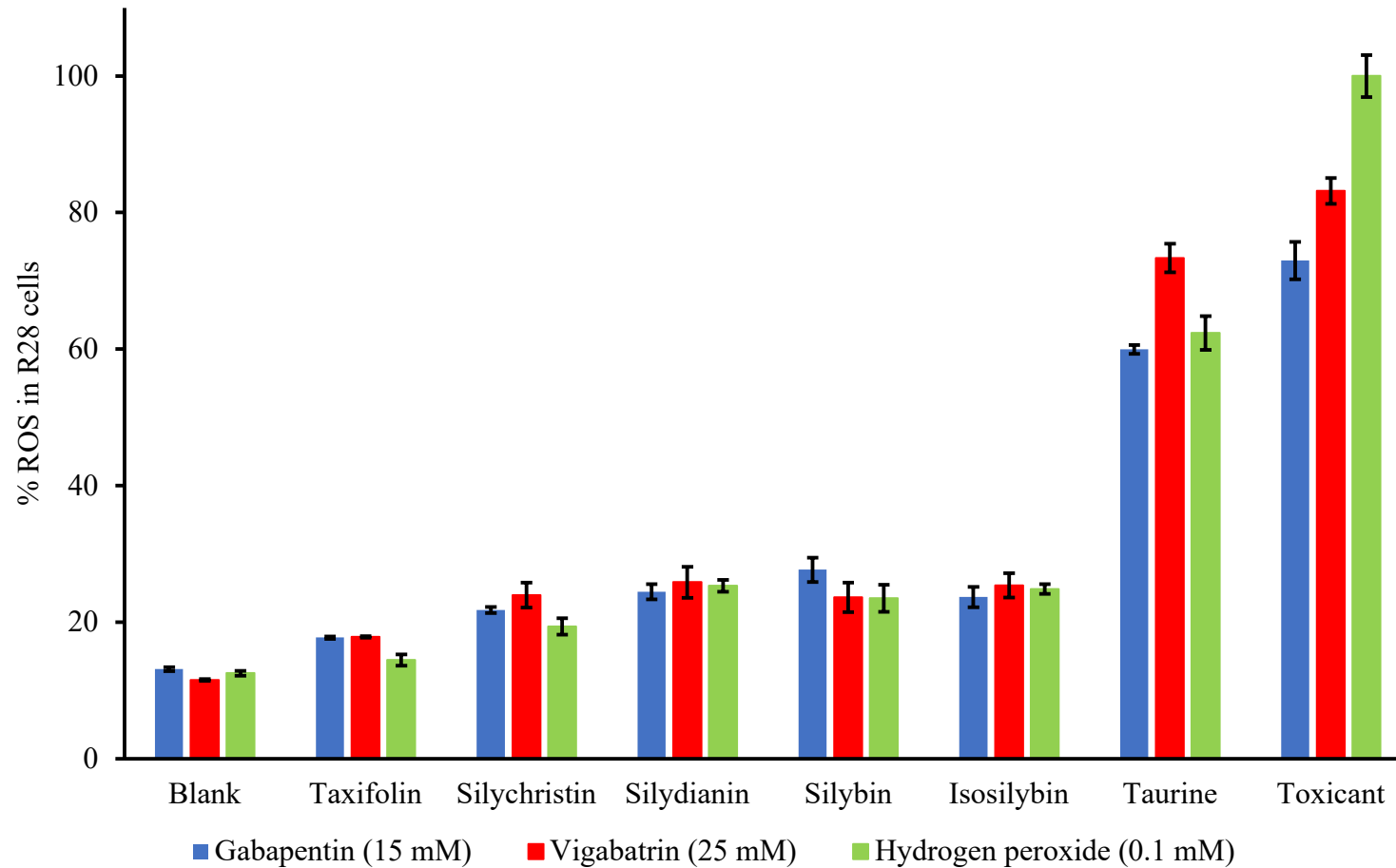


Figure 10. Effect of taxifolin (100 μ M), silychristin (100 μ M), silydianin (100 μ M), silybin (100 μ M), isosilybin (100 μ M) and taurine (10 mM) on ROS generated by gabapentin (15 mM), vigabatrin (25 mM) and hydrogen peroxide (0.3 mM) exposure in R28 cells (mean \pm SD) n=6.

3.5 Cytoprotective effect

The cytoprotective effect of different concentrations of silymarin and taurine on VGB, gabapentin and hydrogen peroxide induced R28 and ARPE-19 cellular toxicity were evaluated. The R28 cells exposed to 25 mM of VGB for 24 hours produced cytotoxicity of $53.2 \pm 0.93\%$ (cell viability of 46.8 %). Pretreatment of cells with taxifolin (50 μM), silychristin (100 μM), silydianin (100 μM), silybin (25 μM), isosilybin (50 μM) and taurine (5 mM) increased the cell viability to 92.9 ± 10.7 , 105 ± 3.60 , 65.0 ± 8.72 , 104 ± 1.97 , 101 ± 4.26 and $95.0 \pm 10.3\%$, respectively in presence of 25 mM vigabatrin (Figure 11A and 11D).

The R28 cells exposed to 15 mM of gabapentin for 24 hours produced cytotoxicity of $46.5 \pm 1.23\%$ (cell viability of 53.5 %). Pretreatment of cells with taxifolin (50 μM), silychristin (25 μM), silydianin (100 μM), silybin (100 μM), isosilybin (100 μM) and taurine (2.5 mM) increased the cell viability to 99.8 ± 5.18 , 92.0 ± 3.79 , 79.8 ± 4.38 , 91.1 ± 7.68 , 88.7 ± 4.19 and $99.5 \pm 5.14\%$, respectively in presence of 15 mM gabapentin (Figure 11B and 11D).

The R28 cells exposed to 0.1 mM of hydrogen peroxide for 24 hours produced cytotoxicity of $68.2 \pm 7.56\%$ (cell viability of 31.8 %). Pretreatment of cells with taxifolin (100 μM), silychristin (100 μM), silydianin (100 μM), silybin (100 μM), isosilybin (100 μM) and taurine (10 mM) increased the cell viability to 72.8 ± 5.81 , 76.3 ± 3.60 , 56.8 ± 5.72 , 75.7 ± 4.23 , 75.9 ± 4.75 and $93.2 \pm 6.69\%$, respectively in presence of 0.1 mM hydrogen peroxide (Figure 11C and 11D).

The ARPE-19 cells exposed to 25 mM of vigabatrin for 24 hours produced cytotoxicity of $47.7 \pm 12.7\%$ (cell viability of 52.3 %). Pretreatment of cells with taxifolin (25 μM), silychristin (25 μM), silydianin (100 μM), silybin (100 μM), isosilybin (50 μM) and taurine (5 mM) increased the cell viability to 93.9 ± 1.32 , 93.2 ± 0.67 , 81.7 ± 2.35 , 86.9 ± 1.57 , 99.9 ± 9.85 and $93.4 \pm 1.50\%$, respectively in presence of 25 mM vigabatrin (Fig. 12A and 12D).

The ARPE-19 cells exposed to 50 mM of gabapentin for 24 hours produced cytotoxicity of $51.6 \pm 8.72\%$ (cell viability of 49.4 %). Pretreatment of cells with taxifolin (25 μM), silychristin (50 μM), silydianin (100 μM), silybin (50 μM), isosilybin (100 μM) and taurine (10 mM) increased the cell viability to 95.1 ± 9.51 , 98.1 ± 8.89 , 101 ± 21.1 , 90.0 ± 9.98 , 99.4 ± 7.66 and $86.2 \pm 4.72\%$, respectively in presence of 50 mM gabapentin (Fig. 12B and 12D).

The ARPE-19 cells exposed to 0.3 mM of hydrogen peroxide for 24 hours produced cytotoxicity of $49.6 \pm 7.56\%$ (cell viability of 50.4 %). Pretreatment of cells with taxifolin (100 μM), silychristin (50 μM), silydianin (100 μM), silybin (25 μM), isosilybin (25 μM) and taurine (10 mM) increased the cell viability to 80.8 ± 7.51 , 104 ± 10.7 , 70.5 ± 1.56 , 106 ± 7.80 , 104 ± 9.03 and $93.0 \pm 3.01\%$, respectively in presence of 0.3 mM hydrogen peroxide (Fig. 12C and 12D).

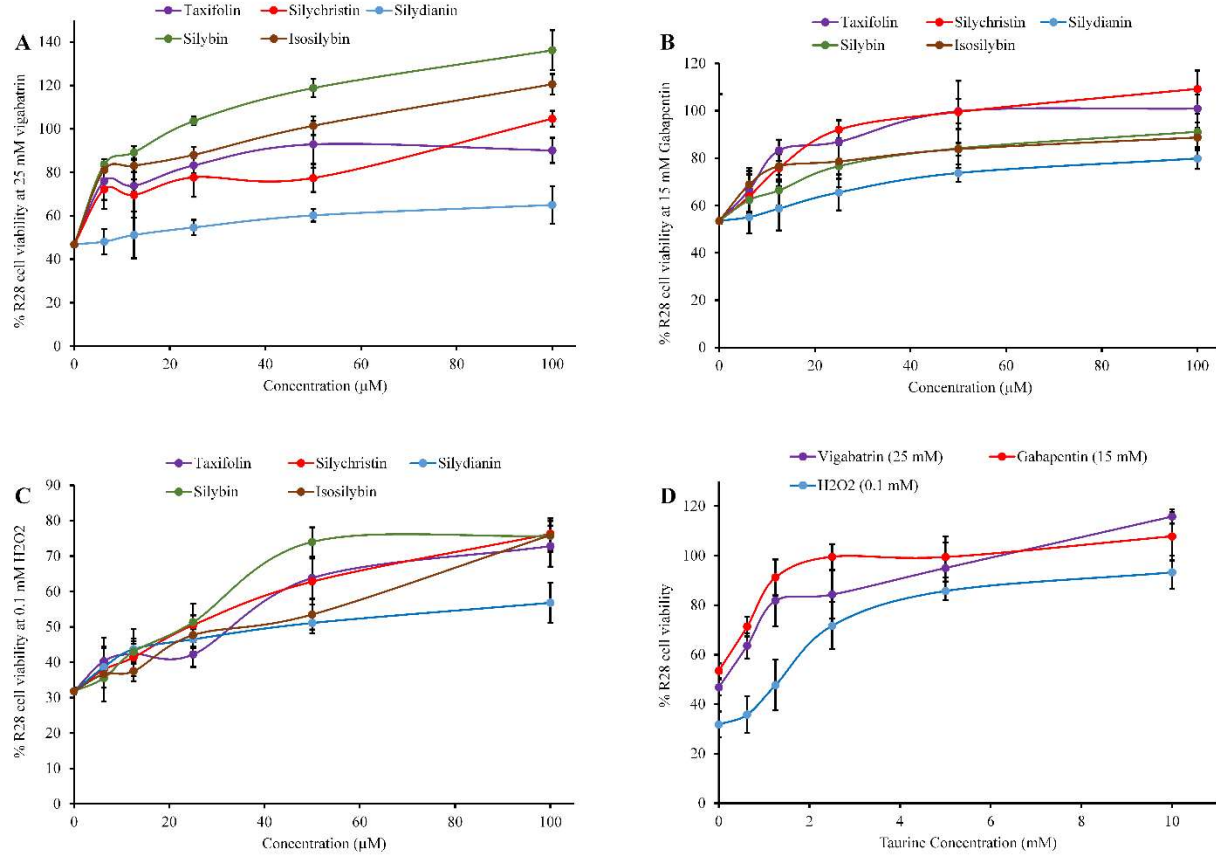


Figure 11. The cytoprotective effect of different concentrations of silymarin (A, B and C) and taurine (D) on vigabatrin, gabapentin and hydrogen peroxide produced R28 cellular toxicity (mean ± SD) n=6.

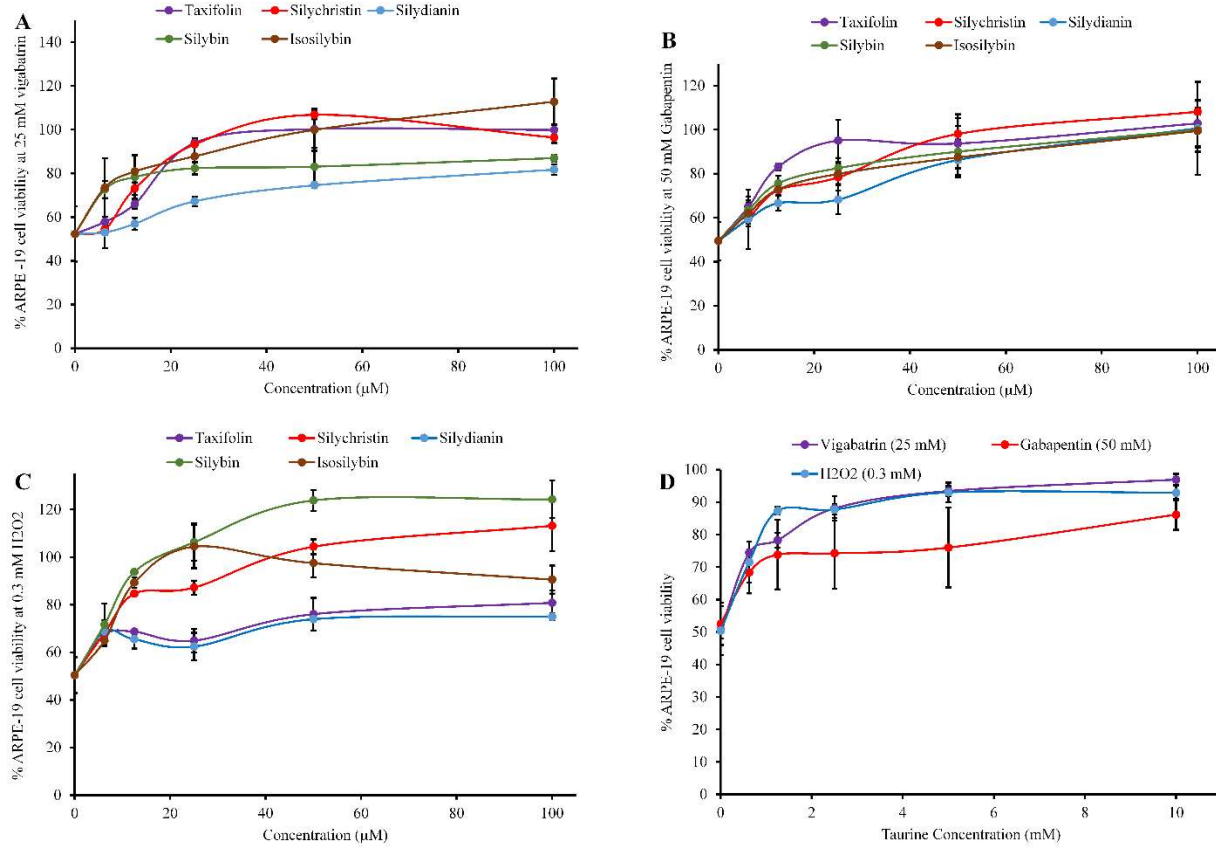


Figure 12. The cytoprotective effect of different concentrations of silymarin (A, B and C) and taurine (D) on vigabatrin, gabapentin and hydrogen peroxide produced ARPE-19 cellular toxicity (mean ± SD) n=6.

4. Conclusions

The results indicate vigabatrin and gabapentin are toxic for retinal neuronal and pigment epithelial cells in concentration dependent manner compared to topiramate and tiagabine. The mechanism of cell death on exposure to VGB and gabapentin to retinal neuronal and epithelial cells are different. In ARPE-19 cells, VGB and gabapentin has shown clear chromatin condensation, DNA fragmentation and decrease membrane potential leading to apoptotic cell death as major path. In R28 cells, the decrease in membrane potential was not clear and thus indicating oxidative pathway as major cause leading to direct necrosis. The study results speculate major reason for VGB, and gabapentin induced retinal cell toxicity was ROS generation. Silymarin and taurine constituents decreased VGB and gabapentin induced cell toxicity. The mechanism of cytoprotective action of silymarin and taurine are due to decrease in ROS in R28 and ARPE cells. The silymarin and taurine can be used as supplement or adjuvant in the treatment of seizure to prevent the ocular adverse events caused by chronic use of antiepileptic agents.

BIBLIOGRAPHY

1. Wong M, Trevathan E. Infantile spasms. *Pediatr Neurol*. 2001;24:89–98.
2. Susana C, Elizabeth T. Vigabatrin in Infantile Spasms. *Epilepsy*. 2009;82–4.
3. Pellock JM, Hrachovy R, Shinnar S, Baram TZ, Bettis D, Dlugos DJ, et al. Infantile spasms: A U.S. consensus report. *Epilepsia*. 2010;51(10):2175–89.
4. Erturk S, Aktas ES, Atmaca S. Determination of vigabatrin in human plasma and urine by high-performance liquid chromatography with fluorescence detection. *J Chromatogr B Biomed Sci Appl*. 2001;760:207–12.
5. Sills GJ, Butler E, Forrest G, Ratnaraj N, Patsalos PN, Brodie MJ. Vigabatrin, but not gabapentin or topiramate, produces concentration-related effects on enzymes and intermediates of the GABA shunt in rat brain and retina. *Epilepsia*. 2003;44(7):886–92.
6. Heim MK, Gidal BE. Vigabatrin-associated retinal damage - potential biochemical mechanisms. *Acta Neurol Scand*. 2012;126:219–28.
7. Butler WH, Ford GP, Newberne ' JW. A Study of the Effects of Vigabatrin on the Central Nervous System and Retina of Sprague Dawley and Lister-Hooded Rats*. 1987;15(2):143–8.
8. Comaish IF, Gorman C, Brimlow GM, Barber C, Orr GM, Galloway NR. The effects of vigabatrin on electrophysiology and visual fields in epileptics: A controlled study with a discussion of possible mechanisms. *Doc Ophthalmol*. 2002;104:195–212.
9. Sivakami S, Ganapathy V, Leibach FH, Miyamoto Y. The γ -aminobutyric acid transporter and its interaction with taurine in the apical membrane of the bovine retinal pigment epithelium. *Biochem J*. 1992;283:391–7.

10. Harris R, Shen W. Review Taurine A “very essential” amino acid. *Mol Vis*. 2012;18:2673–86.
11. Jammoul F, Dégardin J, Pain D, Gondouin P, Simonutti M, Dubus E, et al. Taurine deficiency damages photoreceptors and retinal ganglion cells in vigabatrin-treated neonatal rats. *Mol Cell Neurosci*. 2010;43(4):414–21.
12. Froger N, Cadetti L, Lorach H, Martins J, Bemelmans AP, Dubus E, et al. Taurine Provides Neuroprotection against Retinal Ganglion Cell Degeneration. *PLoS One*. 2012;7(10):1–11.
13. Jammoul F, Wang Q, Nabbout R, Coriat C, Duboc A, Simonutti M, et al. Taurine deficiency Is a cause of vigabatrin-induced retinal phototoxicity. *Ann Neurol*. 2009;65(1):98–107.
14. Tao Y, Yang J, Ma Z, Yan Z, Liu C, Ma J, et al. The Vigabatrin Induced Retinal Toxicity is Associated with Photopic Exposure and Taurine Deficiency: An in Vivo Study. *Cell Physiol Biochem*. 2016;40:831–46.
15. A Study of the Structure and Function of the Retina in Adult Patients with Refractory Complex Partial Seizures Treated with Vigabatrin (Sabril®). [Internet]. 2017 [cited 2017 Jul 7]. Available from: <https://clinicaltrials.gov/ct2/show/NCT01278173>.
16. Acceptability Study of a New Paediatric Form of Vigabatrin in Infants and Children with Infantile Spasms or Pharmacoresistant Partial Epilepsy (SoluWest). [Internet]. 2017 [cited 2017 Jul 17]. Available from: <https://clinicaltrials.gov/ct2/show/NCT02220114>
17. Pardeshi CV, Belgamwar VS. Direct nose to brain drug delivery via integrated nerve pathways bypassing the blood-brain barrier: An excellent platform for brain targeting. *Expert Opin Drug Deliv*. 2013;10(7):957–72.
18. Khan AR, Liu M, Khan MW, Zhai G. Progress in brain targeting drug delivery system by nasal route. *J Control Release* [Internet]. 2017;268(November):364–89. Available from:

<https://doi.org/10.1016/j.jconrel.2017.09.001>

19. Manda P, Hargett JK, Vaka SRK, Repka MA, Murthy SN. Delivery of cefotaxime to the brain via intranasal administration. *Drug Dev Ind Pharm.* 2011;37(11):1306–10.
20. Vermeij TAC, Edelbroek PM. Simultaneous high-performance liquid chromatographic analysis of pregabalin, gabapentin and vigabatrin in human serum by precolumn derivatization with o-phthalaldehyde and fluorescence detection. *J Chromatogr B Anal Technol Biomed Life Sci.* 2004;810(2):297–303.
21. Al-Majed AA. A derivatization reagent for vigabatrin and gabapentin in HPLC with fluorescence detection. *J Liq Chromatogr Relat Technol.* 2005;28(19):3119–29.
22. Chollet DF, Goumaz L, Juliano C, Anderegg G. Fast isocratic high-performance liquid chromatographic assay method for the simultaneous determination of gabapentin and vigabatrin in human serum. *J Chromatogr B.* 2000;746:311–4.
23. Mercolini L, Mandrioli R, Amore M, Raggi MA. Simultaneous HPLC-F analysis of three recent antiepileptic drugs in human plasma. *J Pharm Biomed Anal.* 2010;53:62–7.
24. Applicationr B, Pharmaceuticals MD. Note Quantitative analysis of vigabatrin in plasma and urine by reversed-phase high-performance liquid chromatography. *J Chromatogr B Biomed Sci Appl.* 1985;341:232–8.
25. WANG X, CHI D, SU G, LI L, LiHua S. Determination of taurine in Biological samples by High-Performance Liquid Chromatography Using 4-Fluoro-7-Nitribenzofurazan as a Derivatizing Agent. *Biomed Environ Sci.* 2011. p. 537–42.
26. L?? Y, Zhang H, Meng X, Wang L, Guo X. A validated HPLC method for the determination of GABA by pre-column derivatization with 2,4-dinitrofluorodinitrobenzene and its application to plant GAD activity study. *Anal Lett.* 2010;43(17):2663–71.

27. Zandy SL, Doherty JM, Wibisono ND, Gonzales RA. High sensitivity HPLC method for analysis of in vivo extracellular GABA using optimized fluorescence parameters for o-phthalaldehyde (OPA)/sulfite derivatives. *J Chromatogr B Anal Technol Biomed Life Sci* [Internet]. 2017;1055–1056:1–7. Available from: <http://dx.doi.org/10.1016/j.jchromb.2017.04.003>
28. de Freitas Silva DM, Ferraz VP, Ribeiro ÂM. Improved high-performance liquid chromatographic method for GABA and glutamate determination in regions of the rodent brain. *J Neurosci Methods*. 2009;177(2):289–93.
29. Monge-Acuña AA, Fornaguera-Trías J. A high performance liquid chromatography method with electrochemical detection of gamma-aminobutyric acid, glutamate and glutamine in rat brain homogenates. *J Neurosci Methods*. 2009;183(2):176–81.
30. Hayat A, Jahangir TM, Khuhawar MY, Alamgir M, Hussain Z, Haq FU, et al. HPLC determination of gamma amino butyric acid (GABA) and some biogenic amines (BAs) in controlled, germinated, and fermented brown rice by pre-column derivatization. *J Cereal Sci*. 2015;64:56–62.
31. Khuhawar MY, Rajper AD, Kazi MA. Liquid chromatographic determination of gamma-aminobutyric acid in cerebrospinal fluid using 2-hydroxynaphthaldehyde as derivatizing reagent. *J Chromatogr B* [Internet]. 2003;788:413–8. Available from: www.elsevier.com
32. Clarke G, O'Mahony S, Malone G, Dinan TG. An isocratic high performance liquid chromatography method for the determination of GABA and glutamate in discrete regions of the rodent brain. *J Neurosci Methods*. 2007;160(2):223–30.
33. Benturquia N, Parrot S, Sauvinet V, Renaud B, Denoroy L. Simultaneous determination of vigabatrin and amino acid neurotransmitters in brain microdialysates by capillary

- electrophoresis with laser-induced fluorescence detection. *J Chromatogr B Anal Technol Biomed Life Sci.* 2004;806(2):237–44.
34. Löscher W, Fassbender CP, Gram L, Gramer M, Hörstermann D, Zahner B, et al. Determination of GABA and vigabatrin in human plasma by a rapid and simple HPLC method: correlation between clinical response to vigabatrin and increase in plasma GABA. *Epilepsy Res.* 1993;14(3):245–55.
35. Chen X, You J, Suo Y, Fan B. Sensitive determination of taurine, γ -aminobutyric acid and ornithine in Wolfberry Fruit and Cortex Lycii by HPLC with fluorescence detection and online mass spectrometry identification. *J Chromatogr Sci.* 2015;53(4):492–7.
36. Piepponen TP, Skujins A. Rapid and sensitive step gradient assays of glutamate, glycine, taurine and γ -aminobutyric acid by high-performance liquid chromatography-fluorescence detection with o-phthalaldehyde-mercaptoethanol derivatization with an emphasis on microdialysis sample. *J Chromatogr B Biomed Sci Appl.* 2001;757(2):277–83.
37. Perucho J, Gonzalo-Gobernado R, Bazan E, Casarejos MJ, Jimenez-Escrig A, Asensio MJ, et al. Optimal excitation and emission wavelengths to analyze amino acids and optimize neurotransmitters quantification using precolumn OPA-derivatization by HPLC. *Amino Acids.* 2015;47:963–73.
38. Frank MP, Powers RW. Simple and rapid quantitative high-performance liquid chromatographic analysis of plasma amino acids. *J Chromatogr B Anal Technol Biomed Life Sci.* 2007;852:646–9.
39. García Alvarez-Coque MC, Medina Hernández MJ, Villanueva Camañas RM, Mongay Fernández C. Formation and instability of o-phthalaldehyde derivatives of amino acids. *Analytical Biochemistry.* 1989. p. 1–7.

40. De Montigny P, Stobaugh F, Givens RS, Carlson RG, Srinivasachar K, Sternson A, et al. Naphthalene-2,3-dicarboxaldehyde/Cyanide Ion: A Rationally Designed Fluorogenic Reagent for Primary Amines. *Anal Chem.* 1987;59:1096–101.
41. Nussbaum MA, Przedwiecki JE, Staerk DU, Lunte SM, Riley CM. Electrochemical Characteristics of Amino Acids and Peptides Derivatized with Naphthalene-2,3-dicarboxaldehyde: pH Effects and Differences in Oxidation Potentials. 1992;64:1259–63.
42. Ich. ICH Topic Q2 (R1) Validation of Analytical Procedures : Text and Methodology. *Int Conf Harmon.* 2005;1994(November 1996):17.
43. Richardson D, Ortori CA, Chapman V, Kendall DA, Barrett DA. Quantitative profiling of endocannabinoids and related compounds in rat brain using liquid chromatography-tandem electrospray ionization mass spectrometry. *Anal Biochem.* 2007;360:216–26.
44. Aderibigbe BA. In situ-based gels for nose to brain delivery for the treatment of neurological diseases. *Pharmaceutics.* 2018;10(2).
45. Garripelli VK, Kim J, Namgung R, Kim WJ, Repka MA, Jo S. *Acta Biomaterialia* A novel thermosensitive polymer with pH-dependent degradation for drug delivery. *Acta Biomater* [Internet]. 2010;6(2):477–85. Available from: <http://dx.doi.org/10.1016/j.actbio.2009.07.005>
46. Schmidt MC, Simmen D, Hilbe M, Boderke P, Ditzinger G, Sandow J, et al. Validation of excised bovine nasal mucosa as in vitro model to study drug transport and metabolic pathways in nasal epithelium. *J Pharm Sci.* 2000;89(3):396–407.
47. Pediatric Focused Safety Review: Sabril® (vigabatrin). [Internet]. 2017 [cited 2017 Jul 17]. Available from: <https://www.fda.gov/downloads/AdvisoryCommittees/CommitteesMeetingMaterials/Pedi>

atricAdvisoryCommittee/UCM495248.pdf

48. Jang WS, In CS, Chang GS. Interpretation of Animal Dose and Human Equivalent. *J Korean Orient Med.* 2010;31:1–7.
49. Haugvicová R, Kubová H, Mareš P. Does Vigabatrin Possess an Anticonvulsant Action Against Pentylenetetrazol-Induced Seizures in Developing Rats ? 2002;363–70.
50. Pesaturo KA, Spooner LM, Belliveau P. Vigabatrin for infantile spasms. *Pharmacotherapy.* 2011;31(3):298–311.
51. Waterhouse EJ, Mims KN, Gowda SN. Treatment of refractory complex partial seizures: Role of vigabatrin. *Neuropsychiatr Dis Treat.* 2009;5(1):505–15.
52. Nøhr MK, Frølund S, Holm R, Nielsen CU. Pharmacokinetic aspects of the anti-epileptic drug substance vigabatrin: Focus on transporter interactions. *Ther Deliv.* 2014;5(8):927–42.
53. Reference ID : 2886665, FDA Approved Labeling for NDA 020427, WARNING : VISION LOSS Distribution Program for SABRIL Magnetic Resonance Imaging (MRI) Abnormalities Suicidal Behavior and Ideation Withdrawal of Antiepileptic Drugs (AEDs) Adverse Reaction. 2009.
54. Patent T. European Patent Application. EP Pat 0879946A2 [Internet]. 1998;1(19):1–14. Available from: <http://info.sipcc.net/files/patent/fulltext/EP/200605/EP2099194A1/EP2099194A1.PDF>
55. Amoreaux WL'. The roles of taurine in the retina. In: *Transworld Research Network.* 2012. p. 215–54.
56. Kubo Y, Akanuma S, Hosoya K. Ac ce pt us cr t. *Expert Opin Drug Metab Toxicol* [Internet]. 2018;0(0). Available from: <https://doi.org/10.1080/17425255.2018.1472764>

57. Tomi M, Terayama T, Isobe T, Egami F, Morito A, Kurachi M, et al. Function and regulation of taurine transport at the inner blood-retinal barrier. *Microvasc Res.* 2007;73:100–6.
58. Nøhr MK, Thale ZI, Brodin B, Hansen SH, Holm R, Nielsen CU. Intestinal absorption of the antiepileptic drug substance vigabatrin is altered by infant formula in vitro and in vivo. *Pharmacol Res Perspect.* 2014;2(2):1–11.
59. Emily L Abbot; Danielle S Grenade; David J. Kennedy; Kelly M. Gatfield; David T. Thwaites. Vigabatrin transport across the human intestinal epithelial. *Br J Pharmacol.* 2006;147:298–306.
60. Nøhr MK, Juul R V., Thale ZI, Holm R, Kreilgaard M, Nielsen CU. Is oral absorption of vigabatrin carrier-mediated? *Eur J Pharm Sci.* 2015;69:10–8.
61. Thwaites DT, Anderson CMH. The SLC36 family of proton-coupled amino acid transporters and their potential role in drug transport. *Br J Pharmacol.* 2011;164(7):1802–16.
62. Majumdar S, Gunda S, Pal D, Mitra AK. Functional activity of a monocarboxylate transporter, MCT1, in the human retinal pigmented epithelium cell line, ARPE-19. *Mol Pharm.* 2005;2(2):109–17.
63. El-Sherbeny A, Naggar H, Miyauchi S, Shamsul Ola M, Maddox DM, Martin PM, et al. Osmoregulation of taurine transporter function and expression in retinal pigment epithelial, ganglion, and Müller cells. *Invest Ophthalmol Vis Sci.* 2004;45(2):694–701.
64. Ryan J. Huxtable, Anders Lehmann, Mats Sandberg SS. Mori A., Cohen B.D., Koide H. (eds) *Guanidines 2.* Springer, Boston, MA. In: *Guidelines 2.* 1989. p. 189–90.
65. Frosini M, Sesti C, Dragoni S, Valoti M, Palmi M, Dixon HBF, et al. Interactions of taurine

- and structurally related analogues with the GABAergic system and taurine binding sites of rabbit brain. *Br J Pharmacol.* 2003;138(6):1163–71.
66. Tomi M, Tajima A, Tachikawa M, Hosoya K ichi. Function of taurine transporter (Slc6a6/TauT) as a GABA transporting protein and its relevance to GABA transport in rat retinal capillary endothelial cells. *Biochim Biophys Acta - Biomembr.* 2008;1778:2138–42.
 67. Kubo Y, Akanuma S-I, Hosoya K-I. Impact of SLC6A Transporters in Physiological Taurine Transport at the Blood-Retinal Barrier and in the Liver. Vol. 39, *Biol. Pharm. Bull.* 1903.
 68. Monte D, Miyamoto Y, Arbor A. Properties of taurine transport in a human retinal pigment epithelial cell line. *Curr Eye Res.* 1993;12(1):29–36.
 69. Yahara T, Tachikawa M, Akanuma S, Kubo Y, Hosoya K. Amino Acid Residues Involved in the Substrate Specificity of TauT/SLC6A6 for Taurine and γ -Aminobutyric Acid. *Biol Pharm Bull.* 2014;37(5):817–25.
 70. Bridges CC, Shamsul Ola M, Prasad PD, El-sherbeny A, Ganapathy V, Smith SB, et al. Regulation of taurine transporter expression by NO in cultured human retinal pigment epithelial cells. *Am J Physiol Cell Physiol* [Internet]. 2001;281:C1825–36. Available from: www.ajpcell.org
 71. Anderson CMH, Howard A, Walters JRF, Ganapathy V, Thwaites DT. Taurine uptake across the human intestinal brush-border membrane is via two transporters: H⁺-coupled PAT1 (SLC36A1) and Na⁺- and Cl⁻-dependent TauT (SLC6A6). *J Physiol.* 2009;587(4):731–44.
 72. Hillenkamp J, Hussain AA, Jackson TL, Cunningham JR, Marshall J. Taurine Uptake by Human Retinal Pigment Epithelium: Implications for the Transport of Small Solutes

- between the Choroid and the Outer Retina. *Invest Ophthalmol Vis Sci.* 2004;45(12):4529–34.
73. Strauss O. The Retinal Pigment Epithelium in Visual Function. *Physiol Rev* [Internet]. 2005;85(3):845–81. Available from: <http://www.physiology.org/doi/10.1152/physrev.00021.2004>
74. Pelkonen L, Sato K, Reinisalo M, Kidron H, Tachikawa M, Watanabe M, et al. LC-MS/MS Based Quantitation of ABC and SLC Transporter Proteins in Plasma Membranes of Cultured Primary Human Retinal Pigment Epithelium Cells and Immortalized ARPE19 Cell Line. *Mol Pharm.* 2017;14(3):605–13.
75. Pow D V. Amino acids and their transporters in the retina. *Neurochem Int.* 2001;38:463–84.
76. Rasmussen RN, Lagunas C, Plum J, Holm R, Nielsen CU. Interaction of GABA-mimetics with the taurine transporter (TauT, Slc6a6) in hyperosmotic treated Caco-2, LLC-PK1 and rat renal SKPT cells. *Eur J Pharm Sci.* 2016;82:138–46.
77. Plum J, Nøhr MK, Hansen SH, Holm R, Nielsen CU. The anti-epileptic drug substance vigabatrin inhibits taurine transport in intestinal and renal cell culture models. *Int J Pharm.* 2014;473:395–7.
78. Yokoyama T, Lin L, Chakrapani B, Reddy VN. Hypertonic Stress Increases NaK ATPase , Taurine , and Myoinositol in Human Lens and Retinal Pigment Epithelial Cultures. *Investig Ophthalmol Vis Sci.* 1993;34(8):2512–7.
79. Huxtable RJ. Effect of Guanidinoethane Sulfonate on Taurine Uptake by Rat Retina. *J Neurosci Res.* 1984;186(11):179–86.
80. Hilton EJR, Hosking SL, Betts T. The effect of antiepileptic drugs on visual performance.

- Seizure. 2004;1311(03):187–90.
81. Verrotti A, Manco R, Matricardi S, Franzoni E, Chiarelli F. Antiepileptic Drugs and Visual Function. *Pediatr Neurol*. 2007;353–60.
 82. Arampatzis DA, Karkanis AC, Tsiropoulos NG. Silymarin content and antioxidant activity of seeds of wild *Silybum marianum* populations growing in Greece. *Ann Appl Biol*. 2019;174(1):61–73.
 83. Serçe A, Toptanci BÇ, Tanrikut SE, Altas S, Kizil G, Kizil S, et al. Assessment of the antioxidant activity of silybum marianum seed extract and its protective effect against DNA oxidation, protein damage and lipid peroxidation. *Food Technol Biotechnol*. 2016;54(4):455–61.
 84. Surai PF. Silymarin as a natural antioxidant: An overview of the current evidence and perspectives. *Antioxidants*. 2015;4(1):204–47.
 85. Banfalvi G. Methods to detect apoptotic cell death. *Apoptosis*. 2017;22(2):306–23.
 86. Atale N, Gupta S, Yadav UCS, Rani V. Cell-death assessment by fluorescent and nonfluorescent cytosolic and nuclear staining techniques. Vol. 255, *Journal of Microscopy*. 2014. p. 7–19.
 87. Crowley LC, Marfell BJ, Waterhouse NJ. Detection of DNA fragmentation in apoptotic cells by TUNEL. *Cold Spring Harb Protoc*. 2016;2016(10):900–5.
 88. Ly JD, Grubb DR, Lawen A. The mitochondrial membrane potential ($\delta\psi_m$) in apoptosis; an update. Vol. 8, *Apoptosis*. 2003. p. 115–28.
 89. Eruslanov E, Sergei K. Identification of ROS Using Oxidized DCFDA and Flow-Cytometry. *Methods Mol Biol*. 594:155–62.

VITA

ANITHA POLICE

PhD Candidate

University of Mississippi

Profile

- Doctoral research focused on exploring retinal drug transport mechanism and novel drug delivery approaches to alleviate drug induced retinal toxicity.
- Over 8 years of experience in pharmaceutical industry and academic research encompassing *in-vitro*, *ex-vivo*, *in-vivo* and bioanalytical skills.
- Expertise in designing *in-vitro* ADME assays, preclinical formulation development and pharmacokinetic studies of new chemical entities (NCE's) to facilitate lead candidate selection and optimization.

Educational Qualifications

PhD in Pharmaceutical sciences GPA 3.88 (scale of 4)	University of Mississippi, Department of Pharmaceutics and Drug delivery, Mississippi, US	2016 – Present
Master of pharmacy (Pharmacology)	Kakatiya University, Warangal, India	2008 – 2010

Research Experience

- **Graduate Research assistant** (Jan 2016 to Present)
University of Mississippi, MS
 - Alleviated vigabatrin induced retinal toxicity by nose to brain drug delivery.
 - Explored role of transporters in vigabatrin retinal accumulation.
 - Developed assay to evaluate *in-vitro* skin intrinsic clearance of drugs using human skin models.
 - Developed novel anandamide topical formulation for alleviating peripheral neuropathic pain.
- **Drug metabolism Intern** (June 2019 -Aug 2019)
Pharmacyclics, Sunnyvale, CA
 - Evaluated species difference in the drug clearance pathway mechanisms.

- **Drug metabolism Intern** **(June 2018 -Aug 2018)**
Pharmacyclics, Sunnyvale, CA
- Established methods to predict human and rat *in-vivo* clearance of covalent Bruton's tyrosine kinase inhibitors using ADME properties.
 - Implemented microsomal binding assay to facilitate clearance prediction.
 - Evaluated hepatocyte clearance, CYP-inhibition assays, blood binding, and protein binding assays to accelerate targeted covalent inhibitor drug discovery research.
 - Interpreted ADME data of targeted covalent inhibitors.

- **Research Associate** **(Feb 2011 - Jan 2016)**
DMPK department in Jubilant Biosys, India.
- Contributed for **IND filing of EN3356** (Endo pharmaceuticals collaboration-2013) a novel CYP17A inhibitor for the treatment of metastatic castration resistant prostate cancer.
 - Implemented CYP450 enzymes kinetic assays for determination of Km, Ki and Kinact.
 - Expertise in designing and interpretation of *in-vitro* ADME assays and *in-vivo* preclinical pharmacokinetic, tissue distribution, ocular pharmacokinetic and mass balance studies for drug discovery programs.
 - Presented DMPK data in cross functional team meetings.
 - Developed and validated HPLC and LC-MS/MS bioanalytical methods for generic compounds and NCE's as per the regulatory guidelines.

Technical expertise

- Evaluation of physicochemical properties of NCE's.
- Metabolic stability studies in microsomes, S9 fractions and hepatocytes.
- High throughput CYP450 inhibition assays.
- Protein binding assays (EQD).
- Caco2 and MDR1-MDCK permeability assays.
- Cell based drug transport kinetic assays.
- Cell based assays in retinal pigmental epithelial, neuronal and human epidermal keratinocytes.
- Metabolite profiling of NCE's.
- PO, IP, IM, SC, IV and intranasal dosing in preclinical species.
- CSF collection from cisterna magna in rats.
- Subconjunctival and intravitreal (ocular) pharmacokinetics in rats and rabbits.
- *In-vitro* skin permeation studies.
- Formulation development for oral, topical and intranasal drug delivery.

Instrumentation expertise

- LC-MS/MS (Waters Xevo TQD, X500 QTOF Sciex, API-4000, API-5500 and Thermo).
- HPLC (Shimadzu), Waters alliance 2996 and Waters Acuity UPLC.

Software Proficiency

- Graph pad prism, Phoenix (Pharmacokinetic calculations), Analyst (AB Sciex), SciexOS (Sciex QTOF), Mass lynx (Waters), LC solutions (Shimadzu) and Empower (Waters HPLC).

Awards and Recognition

- Received **first place for poster** entitled ‘Anandamide Topical Delivery for Management of Pain’ in 8th annual research symposium 2018 at University of Mississippi.
- Received **Graduate Student Council Research Grant** for 2017 funded by Graduate Student Council of The University of Mississippi for project entitled ‘Topical anandamide gel for pain management’.
- Received **travelship award from American Association of Pharmaceutical Sciences** Annual Meeting and Exposition 2017 in San Diego, CA.
- Initiated as an active member of Chi chapter at University of Mississippi in 2017 for “**Rho Chi Honor Society**” for outstanding academic excellence.
- Recognized and awarded as **Emerging associate-2013** by Jubilant Biosys, for significant contribution and execution of *in-vitro* ADME assays.
- Recognized and awarded as **Best Team Player** by Jubilant Biosys for integrated discovery projects for the year 2012 (Endo pharmaceuticals), 2013 (Norgine) and 2014 (Mnemosyne).

Publications

- **Anitha Police**, Vijay Kumar Shankar, S. Narasimha Murthy. RP-HPLC Method for Simultaneous Estimation of Vigabatrin, Gamma-Aminobutyric Acid and Taurine in Biological Samples. Journal of chromatography B, 2018, 1076:44-53.
- Huy Dao, Prit Lakhani, **Anitha Police**, Venkataraman Kallakunta, Sankar Srinivas Ajjarapu, Kai-Wei Wu, Pranav Ponkshe, Michael A. Repka, and S. Narasimha Murthy. Microbial Stability of Pharmaceutical and Cosmetic Products. AAPS PharmSciTech, 2018, 19(1):60-78.
- Ravi Kanth Bhamidipati, Sandip Guav, **Anitha police**, Zainuddin Mohd, Sriram Rajagopal, Ramesh Mullangi. The human pharmacokinetics of odanacatib, a novel cathepsin K inhibitor, predicted by interspecies scaling: a retrospective analysis. International Journal of Pharmacokinetics, 2017, 2(1); 47-55.
- Vinod A B, **Anitha Police**, Rakesh Hiremath, Anusha Raj, Suresh P Sulochana, Devaraj V C, Zainuddin Mohd, Ravi Kanth Bhamidipati, Ramesh Mullangi. Preclinical assessment of ulixertinib, a novel ERK1/2 inhibitor. ADMET and DMPK, 2017, 5(4): 212-23.
- Suresh PS, **Anitha Police**, Rajnish Kumar, Mohd Zainuddin, Purushottam Dewang, Ragahava Reddy Kethiri, Sriram Rajagopal and Ramesh Mullangi. Simultaneous Determination of Abiraterone and Its Novel Active Metabolite, D4A by LC-MS/MS in Mice Plasma and Its Application to a Pharmacokinetic Study. Journal of Research Analytica, 2016; 2(1); 25-33.
- Mohd Zainuddin, A B Vinod, Sandip Dhondiram Gurav, **Anitha Police**, Avinash Kumar, Chandan Mithra, Purushottam Dewang, Raghava Reddy Kethiri, Ramesh Mullangi. Preclinical assessment of Orteronel(®), a CYP17A1 enzyme inhibitor in rats. European Journal of Drug Metabolism and Pharmacokinetics, 2016, 41(1): 1-7.
- Suresh PS, Rajnish Kumar, **Anitha Police**, Mohd Zainuddin and Ramesh Mullangi. Simultaneous Quantitation of Rifampicin and Piperine in Rat Plasma by a Selective and Sensitive Liquid

Chromatography-Tandem Mass Spectrometric Method and Its Pharmacokinetic Application. Journal of Research Analytica, 2015; 1(1); 31-8.

- **Anitha Police**, Sandip Gurav, Vinay Dhiman, Mohd Zainuddin, Ravikanth Bhamidipati, Sriram Rajagopal, Ramesh Mullangi. Development and validation of a RP-HPLC method for the quantitation of odanacatib in rat and human plasma and its application to a pharmacokinetic study. Biomedical Chromatography, 2015, 29(11): 1664-69.
- Sandip Gurav, **Anitha Police**, Mohd Zainuddin, Ravindra Ramachandra Punde, Purushottam Dewang, Chandregowda V, Raghava Reddy Kethiri, Sriram Rajagopal, Ramesh Mullangi. Development and validation of an enantioselective LC-MS/MS method to quantify enantiomers of (\pm)-TAK-700 in rat plasma: lack of in vivo inversion of (+)-TAK-700 (Orteronel) to its antipode. Biomedical Chromatography, 2013, 27: 164-71.
- Kuldeep Sharma, **Anitha Police**, Avinash Kumar, Gopal V Pawar, Sanjeev Giri, Sriram Rajagopal, Ramesh Mullangi. Development and validation of an LC-MS/MS-ESI method for the determination of lorglumide, a CCK-1 antagonist in mouse plasma: application to a pharmacokinetic study. Biomedical Chromatography, 2012, 26(7):833-38.
- Sandip Gurav, **Anitha Police**, Mohd Zainuddin, Junaid Hassan Farooqui, Krishna Reddy G, Raghava Reddy Kethiri, Sriram Rajagopal, Ramesh Mullangi. Development and validation of a highly sensitive LC-ESI-MS/MS method for the determination of Orteronel® (TAK-700) in rat plasma: application to a pharmacokinetic study. Bioanalysis, 2012; 4(12):1471-80.

Publications under communication

- **Anitha Police**, Vijay Kumar Shankar, S. Narasimha Murthy. Role of Taurine Transporter in Retinal Uptake of Vigabatrin.
- **Anitha Police**, Vijay Shankar, Pankaj Pandey, Robert Doerksen, S. N. Murthy. Development and Evaluation of novel anandamide topical formulation for peripheral neuropathic pain.
- Vijay Kumar Shankar, **Anitha Police**, Pankaj Pandey, Zachary Cuny, Robert J. Doerksen, S. Narasimha Murthy. Optimization of Sulfobutyl-Ether- β -Cyclodextrins Levels in Oral Formulation to Enhance Progesterone Bioavailability.
- Vijay Kumar Shankar, **Anitha Police**, Pankaj Pandey, Zachary Cuny, Robert J. Doerksen, S. Narasimha Murthy. Oral bioavailability enhancement of silymarin constituents using SBE- β -CD.

Posters Presented

- Presented poster in 43rd Annual Conference of Indian Pharmacological Society conducted by National Institute of Nutrition, Hyderabad 2010, entitled “Effect of Nicardipine on the pharmacokinetics and pharmacodynamics of Pioglitazone in normal and diabetic rats”.
- Presented poster in AAPS conference 2016, Denver; titled “RP-HPLC method for simultaneous determination of vigabatrin, GABA and taurine in different biological tissues”.
- Presented poster in annual neuroscience research day conference at UMMC 2017 entitled “Nose to brain drug delivery approach for alleviating retinal neuronal toxicity of vigabatrin”.
- Posters presented at AAPS annual conference, San Diego, CA., 2017
 - Approaches to Alleviate Antiepileptic Drug Induced *In-vitro* Retinal Neuronal Toxicity.
 - Thermo Sensitive Gel for Intranasal Delivery of Vigabatrin.
 - Anandamide topical delivery for management of pain.

- Presented poster entitled ‘Anandamide Topical Delivery for Management of Pain’ on March 20th, 2018 in research day 8th annual research symposium at University of Mississippi.
- Posters presented at AAPS annual conference, Washington DC, 2018
 - Role of Taurine Transporter in Retinal Uptake of Vigabatrin.
 - Inhibition of Anandamide Metabolism in *In-Vitro* Human Skin Model.
 - Effect of anti-oxidants on vigabatrin induced retinal cell toxicity.